Secretary: D H Napper
School of Chemistry
University of Sydney
NSW 2006
Australia

IPCG

INTERNATIONAL POLYMER COLLOIDS GROUP

JULY 1995

VOLUME 26 NUMBER 1

NEWSLETTER

INDEX

FROM THE EDITOR'S DESK

Due to the illness of Mrs Jean Proctor, the reminder cards were late going out to members. Jean's many friends in IPCG hope that her recovery has now been complete.

Three contributions arrived too late for the November 1994 Newsletter and have been held over to this one. I apologise to the members concerned but I usually set a production deadline determined by when more than a week passes after the receipt of what I think might be the last contribution. This time I have allowed two weeks...

Dr Gregor Ley will be retiring from BASF at the end of the year. We all thank him for his many contributions to the subject over many years and wish him a long and happy retirement.

GENERAL MEETING OF IPCG

A General Meeting of the IPCG accompanied the very successful Gordon Conference held recently at Tilton NH. Minutes (thanks to the good graces of my colleague Bob Gilbert) are included in this Newsletter.

UK POLYMER COLLOIDS FORUM

The third in the very successful series of Polymer Colloids Forum will be held at Keele University, 19-20 September 1995. Pete Lovell is our contact (e-mail: pal@umist.ac.uk; fax: (0) 161 200 3586)

NEXT NEWSLETTER

Contributions should be sent to me by AIR MAIL to be received by 30 November, 1995.

D H Napper
Editor

IPCG meeting July 6 1995.
Tilton School, New Hampshire.

Present: Theo van de Ven (Chair), Don Sundberg (Vice-Chair), Bob Fitch, Ton German, Bob Gilbert (minutes secretary), Pete Sperry, Koichi Takamura, Rudi Müller-Mall, Klaus Tauer, Bob Rowell, Mohamed El-Aasser, Masayashi Okubo, Ron Ottewill, Pete Lovell, Julian Waters, Irja Piirma, Jose Asua, Mamoru Nomura, Jacques Joosten, Dave Bassett, JunghYun Kim, Christian Pichot, Irv Krieger, Sunil Jayasuriya, Françoise Candau, Do-Ik Lee, Joaquim Delgado, Bob Pelton.

1. Date of next Gordon Conference: first choice of week starting June 29 1997, Tilton.

2. NATO Advanced Studies Institute meeting in Spain. June 23-July 5 1996.Veenue is hotel in Pyrenees, 50 km from San Sebastian, close to French border. Airports: Biarritz and San Sebastian are equidistant from venue. Official answer for NATO ASI will be known in February. Organizing/program committee: El-Aasser, Bassett, Tauer, Asua, Ottewill. The program will comprise invited review talks, covering more than just author's own work. Output will be a book. Number of attendees is limited to slightly more than 100, because of the limitations of the lecture room. The scheduled lectures etc. will be 9 am-5 pm, with free evenings, although perhaps there might be some swapping of these. There will be contributed posters. NATO rules say only 15 speakers, but might be stretched to 25.

3. Meetings for 1997. Tilton GRC. Nomura gave details of 7th Iketani Conference: International Symposium on Advanced Technology of Fine Particles, Oct 14-17 1997, at Yokahama. Enthusiastic and unanimous support that this meeting be co-sponsored by IPCG, and Vice-Chair from IPCG. Details to be published in IPCG Newsletter.

4. Meetings for 1998. Gilbert proposed that there be an IPCG-backed Polymer Colloids component to the 1998 IUPAC Macromolecular conference ("Macro 98) to be held at the Gold Coast (near Brisbane, Australia) July 12-17 1998; Gilbert and Napper are Co-Chairs of this conference, for which the number of attendees is expected to be about 1000. The topics of this meeting will be co-chaired by an Australian and an overseas person, and it was proposed and accepted that Gilbert or Napper should be the local co-chair, and Perry the overseas co-chair, with primary responsibility for the scientific program (through the Macro 98 Scientific Subcommittee, chaired by Graeme George of the Queensland University of Technology). A satellite meeting was proposed on "Advances in Polymer Colloids", to review the progress since the last such meeting at Wingspread (1986) and to look to the future. This would be held at Boomerang Beach, 300 km north of Sydney, a venue which has often been used for meetings of this size Some objectives will be the changing world order in polymer colloids and polymer colloids in the Pacific Rim. Joosten nominated a Co-Chair, he and Gilbert to prepare proposal for consideration at next IPCG meeting.

5. In the year 2000, there will be an ACS Colloid Symposium at Lehigh, 2nd week June. Polymer colloids and interfaces will be main theme. IPCG sponsoring endorsed.

6. Distant future meetings. 25th (Silver Anniversary) in year 2002 (actually 27 years), as European Gordon Conference. Tauer to chair.

7. Newsletter. Napper to be asked if he wants some financial assistance. Vote of thanks to Napper, Sperry, Pichot.

8. New membership: Following were unanimously elected: DiSimone, Ger Koper (Leiden), Steve Downing (ICI), John Padget (Zeneca), Chee-Chong Ho (Malaysia). Waters reigns as ICI but comes on as personal member. Napper to check membership activity of any Rhône-Poulenc member, otherwise Frederic Leising will be invited.

Napper to check if Uschold (DuPont) has been active, otherwise invite Steve Major. Proposed emeritus membership, this was accepted.

9. Van de Ven was thanked with acclamation.

Actions:
Napper to put details of Yokahama meeting in Newsletter.
Joosten, Gilbert to put up proposal for "Future Directions in Polymer Colloids" meeting, Australia, 1998.
Tauer to initiate proposal for European Gordon Conference.
Napper to write letters of invitation to new members.

First circular and call for papers

Third Meeting
of the
UK Polymer Colloids Forum

19-20 September 1995, Keele University

The UK Polymer Colloids Forum was set up under MacroGroupUK in the Autumn of 1993. It is the intention of the forum to promote the level of academic activity in the UK in the field of polymer colloids, most especially in the area of synthetic aspects and emulsion polymerisation. An Inaugural meeting was held to ascertain the level of support from both academia and industry, and was very well received by both.

One of the major functions of the Forum is to arrange regular meetings at which advances and progress in the field Polymer Colloids, both scientific and technological, can be discussed freely by industry and academia. The inaugural and second meetings of the UK PCF in achieving this aim were very successful. The third meeting in this series is announced below.

Call for Papers and Further Information

Position papers, technological papers, and experimental and theoretical research papers on any topic relevant to the field of Polymer Colloids are invited for presentation. Papers from UK academics and industrial scientists will be particularly welcome.

If you wish to offer a paper for inclusion in the meeting and/or receive the second circular giving details of the programme and registration information, please return the form below by 24 March 1995.

Third Meeting of the UK Polymer Colloids Forum

Keele University, United Kingdom, 19-20 September 1995

☐ I wish to receive the second circular giving programme details and registration information.

☐ I wish to offer the following paper(s) for inclusion in the programme and enclose 200-300 word abstract(s) of the paper(s).

Paper title(s) ....

....

....

Preferred method of presentation ☐ oral ☐ poster

Please complete in CAPITAL LETTERS:

Surname .... Initials .... Prof/Dr/Mr/Mrs/Miss

Address for correspondence ....

....

....

Tel .... Fax ....

Name(s) of accompanying person(s) ....

Return by 24 March 1995 to: Dr. P A Reynolds, Bristol Colloid Centre, School of Chemistry University of Bristol, Cantock's Close, Bristol BS8 1TS, UK

CONFERENCES

CONFERENCE	LOCATION	DATE/CONTACT
	1995	
210th ACS National Meeting	Chicago	20-25 August
3rd UK Polymer Colloids Forum	Keele	19-20 September (Lovell)
1995 Industrial Symposium on Surface Chemistry	Oslo	8-9 November
Lyklema Retirement Symposium	Wageningen	26-29 November
4th Pacific Polymer Conference	Kauai, Hawaii	12-16 December
	1996	
211th ACS National Meeting	New Orleans	24-29 March
Colloidal Aspects of Complex Fluids	Cambridge	26-28 March
Smart Colloids	Bristol	(?) April (Ottewill)
70th Annual Colloid & Surface Science Symposium	Potsdam, NY	16-19 June
NATO ASI	Spain	23 June- 5 July

ON THE STABILITY OF EMULSIFIER-FREE ALKYL METHACRYLATE LATEXES SIGNIFICANTLY DIFFERED IN WATER SOLUBILITY

T.R.Aslamazova
Russian Academy of Sciences
Leninskij prospect 31, 117915 Moscow
Institute of Physical Chemistry of, Russia

In this contribution, the role of the structural component of the disjoining pressure and the relationship of electrostatic and structural factors in the stability of emulsifier-free alkyl methacrylate latexes with a contact angle of the particle surface of 26° and 90° was studied.

Variation in the polymer surface hydrophobicity was achieved by the variation in the concentration ratio of the copolymerizing monomers that differ significantly in their solubility in water. The solubility of methyl acrylate (MA), butyl acrylate (BA) in water is equal to 5.6 and 0.32 % (30°) respectively and is a measure of their polarity.

The study was performed with model latexes obtained by emulsifier-free polymerization of alkyl methacrylates - MA and BA - at different ratios β (M_2/M_1+M_2, where M_2 - is the more hydrophobic monomer). Latex concentration 15%. Initiator - potassium persulfate.

Figure 1 presents the dependence of the coagulum concentration m_c/m_0 (where m_c, m_0 - is the weight of coagulum and initial monomer) and ζ-potential on ratio β. As seen, on the addition of a more hydrophobic monomer and an increase in its concentration in the monomer mixture up to 20% (β=0,2), the latex stability increased (m_c/m_0) up to the concentrations of M_2=80% followed by the gradual growth of the coagulum. The ζ-potential of the particles increased over the whole range of β; this growth slowed down at the concentration of hydrophobic monomer above 30%.

In order to find out the reason for the decrease of the latexes at the concentration of hydrophobic monomer over 80%, the role of the structural component of the disjoining pressure in the destabilization of the dispersion was studied.

Figure 2 (curve 1) shows the contact angles θ of latex films against the monomeric composition β of latexes. The increase in the θ values can be seen with of the hydrophobic monomer concentration, which is sharper than that at the final part of the curves. Therefore, the two characteristic regions of the change in contact angles can be distinguished: θ= 26°-65° (0<β<0.8) and θ=65° - 90° (0.8<β<1.0). The presence of these regions may be associated with the fact that structural forces are stronger for hydrophobic surfaces with contact angles over 65° and a coefficient of structural forces is much higher than for slightly hydrophobic surfaces with contact angles under 65°.

The quantative evaluation of the role of the structural component of the disjoining pressure in the stability of emulsifier-free latexes with a particle surface hydrophobicity varying within the range of contact angles from 26° to 90° is based on the treatment of the coagulation of polymer dispersions in the nearest potential well using technigues and calculations discussed in Newletters, 1994, V. 24, N2, p.1;V.25, N2, p.1.The formula for the estimation of the structural coefficient K in experiments *i* and *l* :

$$K_i = K_l r_i / r_l + \{kT[ln(C_{pi}/C_{pl}) - 3ln(r_i/r_l) + ln(m_{ci}/m_{cl})] + \Delta V_e\} / \{r_l \exp(-H^{max}/H_s)\},$$

where r - radius, C_p - concentration of particles, *k* - Boltzmann constant, T-absolute temperature, V_e - electrostatic component of energy, H^{max}, H_s - distance between particles at V^{max} and when energy decreases at e times.

The mean value of r and C_p are 117nm and $1.0.10^{-12}$ cm^{-3} respectively. The experiment with the minimum value of the coagulum concentration (m_{cl}/m_{ol}) was taken as a standard. The value of $K=40.10^{-6}$ dyne was used as K_l obtained [1]. For the calculations, it was assumed that T=343*K*, H_s = 1 nm, H^{max} = 3.8 ÷ 6.9 nm.

Figure 2 shows the dependence of the structural energy coefficient K on the monomer ratio β, indicating the increase in the K values with an increase in the content of hydrophobic polymer in the latex composition. One can see the region of the delayed rise in the coefficient K corresponding to the ratio β varying from 0.2 to 0.8 and to the region of the maximum stability observed. The increase of the structural forces at the concentrations of the more hydrophobic monomer higher than 80% is indicative of the significant growth of the hydrophobic attractive forces in the case of highly hydrophobic polymers. This explains the loss of the stability of the latex particles even at rather high values of ζ-potential.

Much lower values of K in the region of β values corresponding to the initial part of curve 1 indicate the smaller destabilizing influence of the structural forces that may be manifested in the stabilization of the particles. However low values of their ζ-potential do not provide stability, thus resulting in the coagulum growth at the initial part of the $m_c/m_o = f(\beta)$ dependence.

The results obtained show that the region of maximum stability is caused by the overall effect of change in the electrostatic and structural factors of the stabilization of the latex particles under variation in the hydrophobic-hydrophilic characteristic of their surface.

Reference: 1. Eliseeva V.I., Aslamazova T.R., Rabinovich Y.I. et al., Kolloidn.Zh., 1991, vol.53, no.1, p.21 and 69.

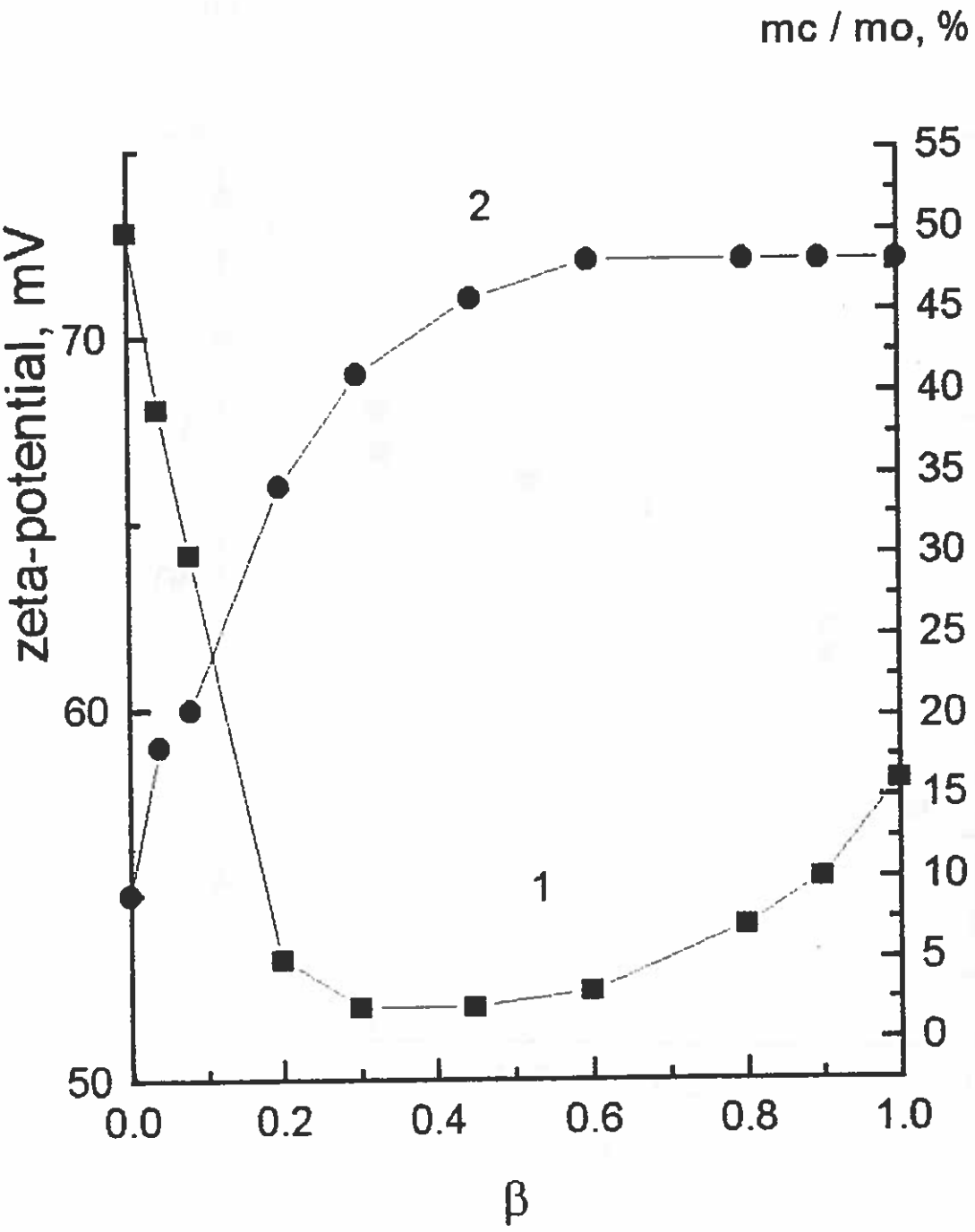

Fig.1. Dependences of coagulum concentration (1) and zeta-potential of particles (2) upon monomers ratio β.

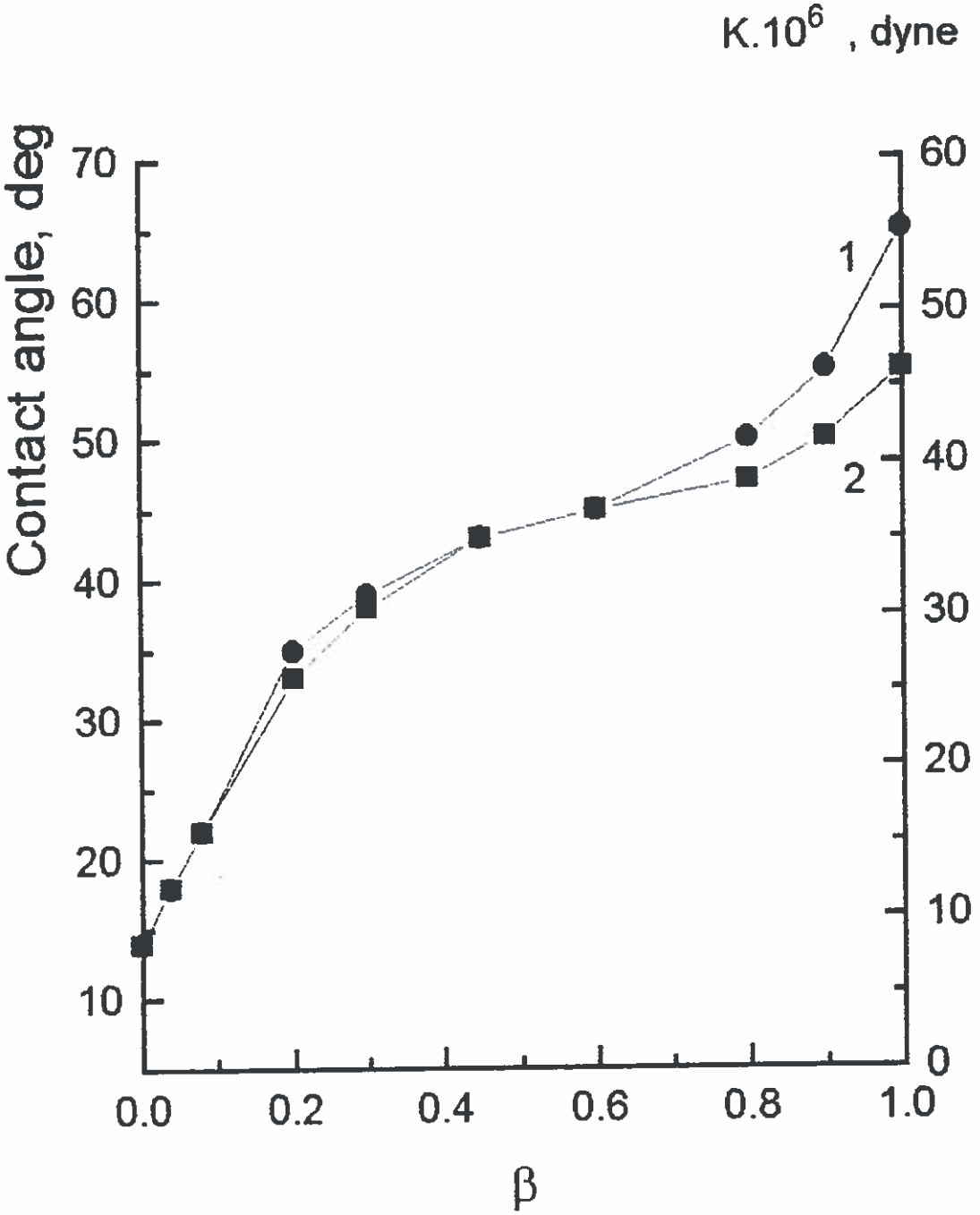

Fig.2. Dependences of contact angle for latex film surface (1) and coefficient of structural forces of particcles interaction (2) upon monomers ratio β.

INTERNATIONAL POLYMER COLLOIDS GROUP NEWSLETTER

Contribution from the Grupo de Ingeniería Química, Facultad de Ciencias Químicas, Universidad del País Vasco, Apdo. 1072, 20080 San Sebastián, Spain.

Reported by José M. Asua

MODELLING GELATION AND SOL MWD IN EMULSION POLYMERIZATION

Gurutze Arzamendi and José M. Asua

A mathematical model for the computation of the molecular weight distribution (MWD) of the sol, the gel fraction and the gel point in emulsion polymerization systems was developed. The model accounts for the compartmentalization of the free radicals in the reaction system and for the changes in the environment where the chain was growing. An improved numerical fractionation technique that allows a better description of the MWD of the sol was used. A parametric sensitivity analysis was carried out and a comparison between the batch and the semicontinuous processes is presented.

DISPERSION POLYMERIZATION IN POLAR SOLVENTS

José M. Sáenz and José M. Asua

The effect of the nitrogen purge, monomer purification, type of agitation and presence of co-stabilizer on the particle size distribution (PSD) was investigated in the dispersion polymerization of styrene in ethanol and in the dispersion copolymerization of styrene and butyl acrylate in a water-ethanol mixture. Purging with nitrogen and, to a lesser extent, monomer purification were of paramount importance to achieve monodispersity. The type of agitation had a weak effect on the PSD, whereas the presence of co-stabilizer had no effect on the PSD.

DISPERSION COPOLYMERIZATION OF STYRENE AND BUTYL ACRYLATE IN POLAR SOLVENTS

José M. Sáenz and José M. Asua

Monodisperse copolymer particles from 0.8 to 2.6 μm in diameter were obtained by unseeded batch dispersion copolymerization of styrene and butyl acrylate in an ethanol-water medium. A two level factorial design was initially carried out including the following variables: stabilizer type, stabilizer concentration, initiator concentration, polarity of the dispersion medium, initial monomer concentration and temperature. Once the region of experimental conditions in which monodisperse latexes can be prepared was identified, further effort was devoted to analyze the effect of other variables. It was found that an increase in the purge with nitrogen was essential in order to obtain monodispersity. The particle size increased with increasing initial monomer concentration and ethanol-water weight ratio, and decreasing stabilizer concentration. A minimum quantity of emulsifier was necessary to avoid coalescence of particles and to obtain monodisperse particles.

COPOLYMER COMPOSITION CONTROL IN UNSEEDED EMULSION POLYMERIZATION USING CALORIMETRIC DATA

Luis M. Gugliotta , José R. Leiza, Michel Arotçarena, Philip D. Armitage and José M. Asua

A method to determine the minimum time monomer addition policy for composition control in unseeded emulsion polymerization systems based on calorimetric measurements was developed. The iterative approach requires a series of semicontinuous emulsion copolymerizations to be carried out under semistarved conditions. Only the values of the reactivity ratios and the heat of homopolymerization of each monomer involved are required to apply the approach. The method, that was checked in the vinyl acetate-butyl acrylate emulsion copolymerization, converged in four steps even when technical grade monomers were used.

START-UP PROCEDURES IN THE EMULSION COPOLYMERIZATION OF VINYL ESTERS IN A CONTINUOUS LOOP REACTOR

Carlos Abad, José C. de la Cal and José M. Asua

Different start-up strategies for the 55 wt % solids content redox initiated emulsion copolymerization of vinyl acetate and veova 10 in a continuous loop reactor were studied to determine the optimal start-up procedure in terms of smoothness of the operation and minimum out of specification product. These strategies included different initial charges and temperature profiles. The evolutions of the monomer conversion, particle size, number of polymer particles and molecular weight distribution during the start-up were analyzed and the effect of the start-up procedure on the steady state values of these variables determined.

MIXING EFFECTS IN THE EMULSION COPOLYMERIZATION OF VINYL ACETATE AND VEOVA 10 IN A CONTINUOUS LOOP REACTOR

Carlos Abad, José C. de la Cal, and José M. Asua

The effect of the state of the micromixing on the performance of a continuous loop reactor during the redox initiated emulsion polymerization of vinyl acetate and veova 10 was investigated. Mixedness was improved by preemulsifiying the feed and by means of the adequate choice of the feeding point. The conditions under which monomer mass transfer did not control the polymerization were determined. The interaction between monomer mass transfer and a high radical generation rate was discussed.

EMULSION POLYMERIZATION IN A LOOP REACTOR: EFFECT OF THE OPERATION CONDITIONS.

Carlos Abad, José C. de la Cal, and José M. Asua

The effect of several operation conditions (space time, emulsifier concentration, temperature and initiator concentration) on the performance of a continuous loop reactor during the redox initiated emulsion copolymerization of vinyl acetate and veova10 was investigated. The study was carried out under industrial like conditions, namely, high solids content latexes (55wt%) and high conversions (≈90%). It was found that high performance latexes can be produced at high polymerization rates in the loop reactor by starting the process at high temperature, initiator concentration and space time, and reducing these

parameters afterwards.

DEVELOPMENT OF PARTICLE MORPHOLOGY IN EMULSION POLYMERIZATION. II.- CLUSTER DYNAMICS IN REACTING SYSTEMS.

Luis J. González-Ortiz and José M. Asua.

A mathematical model for the development of particle morphology in emulsion polymerization has been developed. The polymer particles are considered to be a biphasic system comprising clusters of polymer 1 dispersed in a matrix of polymer 2. The model accounts for both polymerization and cluster migration. Polymerization of monomer 1 occurs in both the polymer matrix and in the clusters. The polymer 1 formed in the matrix diffuses instantaneously into the clusters. The clusters migrate toward the equilibrium morphology to minimize the free energy of the system. The driving forces for the motion of the clusters are the van der Waals interaction forces between the clusters and the aqueous phase, and those between the clusters themselves. The effect of polymer matrix viscosity on the cluster motion is included. Illustrative simulations and comparison with experimental date are presented.

EMULSION POLYMERIZATION: PARTICLE GROWTH KINETICS

Lourdes López de Arbina, María J. Barandiaran, Luis M. Gugliotta and José M. Asua

An attempt to develop a predictive and manageable mathematical model for particle growth in emulsion homopolymerization was carried out by fitting the time evolution of the conversion in the chemically initiated seeded emulsion polymerization of styrene carried out under a wide range of experimental conditions with models of different complexity. Model discrimination based on the best fitting of the experimental data was carried out. The dependence of the radical entry and exit rate parameters on the particle size was used to elucidate between the different mechanisms proposed for these processes.

POLYMER COLLOID GROUP NEWSLETTER

Contribution from the Institut Charles Sadron (CRM-EAHP)
6, Rue Boussingault, 67083 Strasbourg Cédex, France.

by

Françoise CANDAU

RECENT DEVELOPMENTS IN ASSOCIATING POLYMERS PREPARED BY MICELLAR POLYMERIZATION (I. Lacik, J. Selb, F. Candau)

(Preprint for the Symposium on "Associating Polymers", Loen, Norway, June 25-29, 1995)

Over the past years, extensive studies have been focused on water-soluble polymers modified with low amounts of a hydrophobic monomer (1-3 mol%) for their use as rheology modifiers in a number of applications including enhanced oil recovery or latex paints. In aqueous solution above a critical polymer concentration, the hydrophobic groups associate intermolecularly and thereby produce a greater viscosity than for the analog without the hydrophobe. Depending on the method of synthesis, the hydrophobes can be distributed anywhere in the copolymer, for example at each end of the backbone or within the chain as pendant groups in a random or blocky fashion.

Copolymers based on acrylamide have certainly been among those most investigated. Their preparation may be difficult because of the insolubility of the hydrophobic monomer in water, and a few methods have been devised to overcome this problem. An ingenious approach was that developed by Evani,[1] and Valint et al.[2] In this process, the hydrophobic monomer is solubilized within surfactant micelles whereas the hydrophilic monomer is dissolved in the aqueous continuous medium (Fig.1a). This one-step micellar copolymerization route was found to give hydrophobically modified water-soluble polymers (HMWSP) which could be adequately used as aqueous viscosifiers. Another route devised to prepare associating polymers is to replace the surfactant and the hydrophobe by a polymerizable surfactant, such as hexadecyldimethylvinylbenzylammonium chloride, N16 (Fig.1b).[3]

An intriguing question which was addressed by several groups and partly solved, was how the initial monomer segregation in the reaction mixture affects the copolymer microstructure. The high local concentration of the hydrophobes in the micelles should favor their incorporation in the copolymer as blocks rather than isolated units. In our laboratory, we clearly established that the thickening properties

of hydrophobically modified polyacrylamides were directly related to the molecular structure, the longer the hydrophobic blocks, the greater the thickening efficiency at a constant level. The length of the blocks could be monitored by adjusting the hydrophobe-to-surfactant ratio in the synthesis.[4]

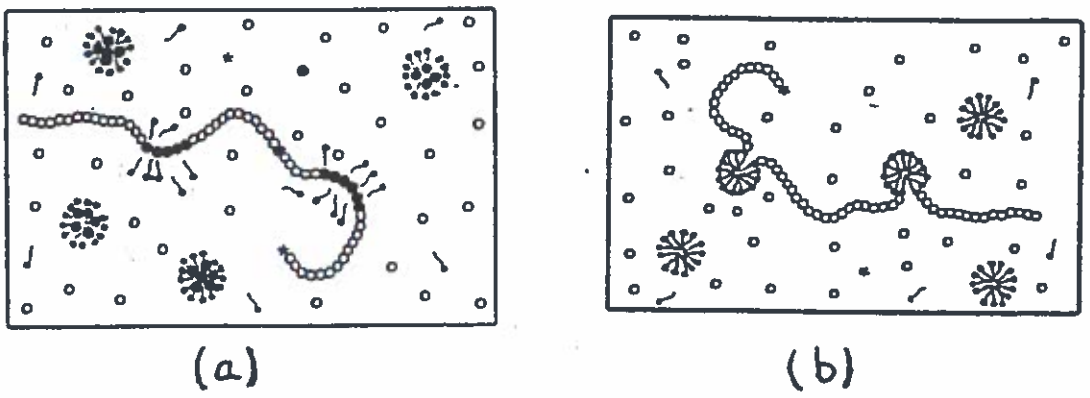

Figure 1. Schematic representation of the micellar copolymerization medium
○ : acrylamide; ● : hydrophobic monomer; —● : surfactant; ✱ : initiator

Another problem to face in this micellar polymerization process is the compositional heterogeneity of the high conversion samples. Kinetic studies[5] performed on the micellar copolymerization of various monomer pairs - acrylic acid/ styrene (AA-S), acrylic acid/ethylphenylacrylamide (AA,eΦAM), acrylamide/ styrene (AM-S) and acrylamide-N16 (AM-N16) - have shown that the reaction mechanism of this particular process is essentially governed by the two following parameters : (i) the values of the reactivity ratios of the monomers as for any copolymerization reaction ; (ii) the micellar effect which originates from the high monomer concentration within the micelles, the residence time of the active end of the growing radical in the micelle and the rate of hydrophobic monomer exchange between micelles. The latter effect should lead to an enhanced apparent reactivity for the hydrophobic monomer solubilized within the micelles.

When the hydrophobic monomer is more reactive than the hydrophilic monomer (AA-S, AM-S and AM-N16 cases), the two above effects reinforce each other to yield copolymers with a strong compositional heterogeneity. When both monomers have a similar reactivity (AM-eΦAM case), the micellar effect is essentially responsible for the positive increase of the rate of hydrophobe incorporation in the copolymer. The copolymer heterogeneity is therefore reduced with respect to the former case. When the hydrophobic monomer is the less reactive (AA-eΦAM case), the two effects vary in opposite direction. This case is most interesting since the lowered hydrophobe incorporation can be balanced by the

micellar effect through optimization of the hydrophobe/surfactant ratio in the synthesis.

The rheological properties of HMWSP prepared by micellar copolymerization are directly related to their structural compositional heterogeneity. AA-S copolymers obtained at full conversion do not exhibit associative properties : the hydrophobically modified copolymer chains are diluted within a continuous medium made of pure homopolyacrylic acid. On the contrary, a good thickening ability is obtained with a AA-S sample obtained in the early stages of the reaction owing to a greater compositional homogeneity. AA-eΦAM copolymers characterized by a quasi-invariance of their average composition with conversion should also present some interesting rheological properties and experiments are presently underway.

Finally, it should be noted that the balance between the hydrophobicity of the associating sequences and the hydrophilic character of the backbone is critical. The appropriate conditions for the production of effective thickeners lie between the two limiting cases where the HMWSP exhibit no associative behavior (hydrophobe content too low or too small hydrophobic groups, backbone too highly charged), or phase separate (hydrophobe content too high, backbone too hydrophobic as is the case for acrylic acid). The conclusions recently reached in this field should help in defining the very narrow gap existing between these two limits.

REFERENCES

1. Evani, S., US Patent 4 432 881, 1984.
2. Valint, P.L. Jr.; Bock, J.; Schulz, D.N. *Polym. Mater. Sci. Eng.* **57**, 482, 1987 .
3. D. Renoux, Ph.D. Thesis, University of Strasbourg, 1995.
4. Biggs, S.; Hill, A.; Selb, J. and Candau, F. *J. Phys. Chem.* **96**, 1505, 1992.
5. Lacik, I.; Selb, J. and Candau, F. *Polymer* (in press), 1995.

Dynamic aspects of bridging flocculation

Y. Adachi, M.A. Cohen Stuart, R. Fokkink
Dept. Physical and Colloid Chemistry, Wageningen Agricultural University

Some dynamic aspects of bridging flocculation were studied in turbulent flow by means of a standardized mixing procedure[1]. Polyelethylene oxide (MW ≈ 5. 10^6) and salt (KCl) were added to dilute dispersions of polystyrene latex and the number concentration of flocs was monitored as a function of time, using a single particle optical sizing technique [2].
We found an initial rapid flocculation, which stopped rather abruptly after a while (fig.1).

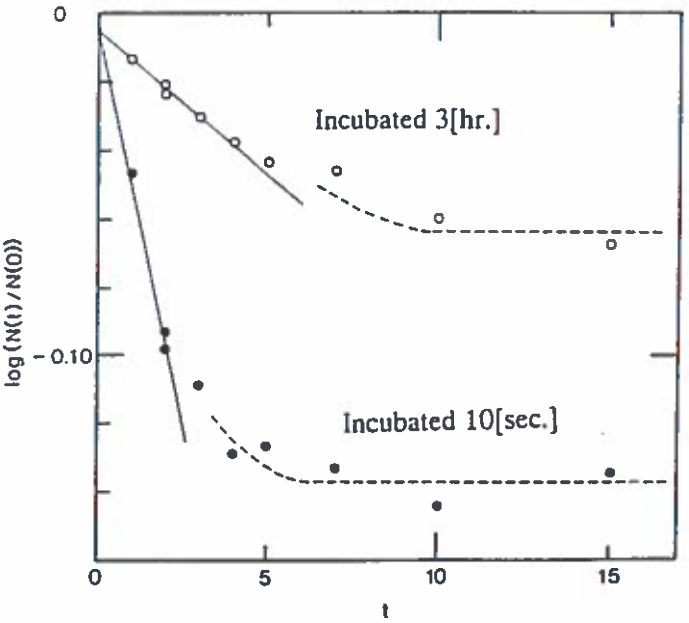

Fig. 1. Normalized umber of aggragates as a function of time (= no. of mixing steps) for flocculation of PS latex (555 nm diameter) with PEO. The experiment was carried out with PEO mixed with a KCl solution, either shortly before the experiment (10sec) or after prolonged storage (3 hr).

The rate of flocculation in the initial stage was substantially (several times) higher than that of rapid coagulation induced by salt only. This enhancement must be due to an increase in the effective collision radius of the particles upon adsorption of the polymer. Using this idea, the effective thickness of the adsorbed layer in the initial stage of the flocculation process can be assessed. The value so obtained should not depend on the size of the bare particle, which was indeed verified. However, this thickness is much larger than what is measured for latex particles covered with an equilibrated layer

of PEO, which indicates that the polymer is still in a transient, swollen state during flocculation. Since the time between two subsequent collisions of polymer molecules with a given particle is, under the conditions chosen, of the order of one second, this indicates that the lifetime of this transient state is at least one second.

It was found that the thickness in the transient state was dependent on the way the polyethylene oxide solution was made up and kept prior to the experiment. With freshly prepared PEO solutions we obtained thicknesses of about 615 nm, which is much more than the radius of gyration of the free PEO coil in solution. When the PEO solution is mixed with KCl, however, and stored for 3 hours prior to its use in a flocculation experiment, we found an effective layer thickness of about 250 nm, which is roughly equal to the coil radius. Apparently, the PEO in pure water is present in the form of aggregates, as was confirmed recently by Van de Ven et al [3], but in KCl solution the aggregates disappear.

References.

1. Y. Adachi, M.A. Cohen Stuart, and R. Fokkink; J. Colloid Interface Sci. **165** (1994) 310-317.

2. E.G.M. Pelssers, M.A. Cohen Stuart, G.J. Fleer; J. Colloid Interface Sci. **137** (1990) 350.

3. M. Polverari, T.G.M. van de Ven; J. Solution Chem. to be published (1994).

Contribution by M.A. Cohen Stuart

Dept. of Physical and Colloid Chemistry

Wageningen University

The Netherlands

Initial Rates of Flocculation of Polystyrene Latex with Polyelectrolyte: Effect of Ionic Strength

The rate of flocculation of polymer latices immediately after the addition of polyelectrolyte was measured by applying the standardized procedure of colloid mixing. It was found that the rate of flocculation in the initial stage is remarkably enhanced by the addition of polyelectrolyte and that the extent of this enhancement decreases with an increase in the ionic strength. The conformation of polyelectrolyte in the solution is considered to have a direct influence on this result.

The flocculation of colloidal dispersions is a common operation in many industrial processes and in water and waste water treatment. Usually, this process is initiated by the addition of a small amount of polymer into the colloidal dispersion mixed by turbulent agitation. However, the inevitably complex situation of the turbulent flow makes quantitative analysis of the mechanism of flocculation difficult. Recently, we showed a way to characterize the mixing flow condition in terms of collision processes between colloidal particles (1). This method allows us to analyze the temporal evolution of flocculation within times as short as 1 s from the start. By this method, we found a remarkable enhancement of the rate of flocculation of polystyrene latex upon the addition of poly(ethylene oxide), which was used as a bridging agent (2). The enhancement was ascribed to the increase in the effective collision radius due to the attachment of polymer molecules onto the surface of the colloidal particles. Since the values that we found for this increase in size correlated with the size of the polymer molecules in solution rather than with the equilibrium hydrodynamic thickness of the adsorbed layer (which can be measured separately by photon correlation spectroscopy), we concluded that the flocculation rate reflects the conformation of the dissolved polymer. Apparently, a nonequilibrium process is quite important during the formation of flocs, and probably a similar behavior will be observed in another important version of flocculation, i.e., the charge neutralization of a colloid by an oppositely charged polyelectrolyte.

Normally, a polyelectrolyte chain takes a swollen conformation in the solution due to electrostatic repulsions between segments of like charge. If we increase the ionic strength of the solution, the electrostatic interaction will be screened and, as a consequence, the swollen polyelectrolyte will shrink. When the charge is completely screened, the polyelectrolyte will behave like a homopolymer. It is generally accepted that highly charged polymers adsorb in a flat conformation onto an oppositely charged surface (3) and that they induce flocculation by way of charged neutralization (4–6). However, very little is known about the dynamics of the process. If the conformation of a free polymer chain has a direct influence on the kinetics of flocculation (as we observed for the bridging flocculation with homopolymer), a smaller rate of flocculation is expected to occur when a less swollen polymer is used, i.e., at higher ionic strength. In contrast the equilibrium thickness of adsorption is expected to increase upon increasing the ionic strength of the bulk solution because the adsorbing conformation will approach that of homopolymer, which typically consists of long loops and tails. In this case, the rate of flocculation is expected to increase with an increase in ionic strength.

In order to clarify which process takes place, we measured the rate of flocculation of negatively charged polystyrene latex with positively charged polyelectrolyte while varying the ionic strength of the solution. Application of the standardized mixing procedure allows us to evaluate the flow conditions in terms of the collision process between the colloidal particles. In our experiment, a standard emulsifier-free polystyrene latex particle with a diameter of 555 nm was flocculated with a cationic polymer of trimethylaminoethyl methacrylate. According to the supplier, its molecular weight is approximately 5.6 million and the content of charged monomers is 100%. The study of the same system has been reported by several groups (4–6), revealing that this system constitutes a typical example of flocculation by charge neutralization. That is, the optimum dosage of flocculant corresponds to the condition when the charge of the colloidal is apparently eliminated by the adsorption of the oppositely charged polymer. The concentration of the polyelectrolyte in the final mixture was adjusted to 0.26 ppm. The relative viscosity of the polyelectrolyte solution at KCl = 5×10^{-4} *M* was measured and found to be less than 1.002. This result guarantees that the effect of viscosity change on the kinetics of flocculation is negligibly small.

The experimental results are shown in Fig. 1. We plot $\log(N(t)/N(0))$ as a function of the number of mixing steps, in accordance with the first-order kinetics expected for the initial flocculation rate. From the slope, we obtain the effective collision radius (1, 2). As a reference, the result of the rapid coagulation, i.e., coagulation induced only by salt in the absence of electrostatic repulsion taken from (1, 2), is indicated. As can be seen, the rate of flocculation by polyelectrolyte in the initial stage is remarkably enhanced. At $t = 10$, however, flocculation stops abruptly as the particles

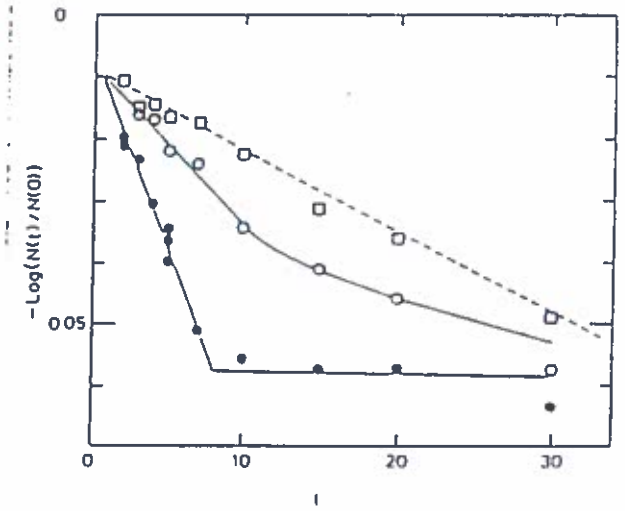

FIG. 1. Total number concentration of clusters $N(t)$ as a function of the number of mixing steps. One mixing was carried out in 1.36 s. The initial number concentration of polystyrene latex particle was 1.55×10^{9} 1/cm³. The concentration of polyelectrolyte was 0.26 ppm. The concentrations of KCl were (●) 5.85×10^{-5} *M*, (○) 5.85×10^{-3} *M*, and (□) 5.85×10^{-2} *M*, respectively. The dashed line is the result of rapid coagulation, i.e., coagulation induced only by salt in the absence of electrostatic repulsive forces, and was taken from (2).

0021-9797/95 $6.00

become protected by a fully developed polymer sheath. The largest rate of flocculation which was observed for KCl = 5.85×10^{-4} *M* is approximately six times larger than the rate of rapid coagulation by salt. If we ascribe this enhancement to the increase in collision radius due to the attached polymer layer as was done previously (2), the value of the layer thickness is estimated to be approximately 150 nm. Since the degree of enhancement clearly decreases by increasing the ionic strength of the solution, we are forced to conclude that it is the conformation of the polymer dissolved in the solution that determines this enhancement.

In most of the literature, the collision efficiency of bridging flocculation has been discussed simply in terms of the fraction of the surface covered with polymer (7, 8). Our result clearly reveals the importance of the transient conformation of the adsorbing polymer which should be taken in to account when analyzing the nonequilibrium flocculation. Attached polymer protruding far into the solution leads to a collision efficiency (with respect to bare particles) which is larger than unity. Mores systematic research for this regime should further elucidate the bridging mechanism.

ACKNOWLEDGMENTS

Kounan Kagaku Co. Ltd., is acknowledged for providing the flocculation used in the experiment. Y.A. expresses his thanks to the Netherlands International Agricultural Center for a fellowship. This work is partly funded by a Grant-in-Aid for Scientific Research (05453050) from the Japanese Ministry of Education.

REFERENCES

1. Adachi, Y., Cohen Stuart, M. A., and Fokkink, F., *J. Colloid Interface Sci.* 165, 310 (1994).
2. Adachi, Y., Cohen Stuart, M. A., and Fokkink, R., *J. Colloid Interface Sci.* 165, (1994) 346.
3. Dahlgren, M. A., Claresson, and Cludelert, *Nord. Pulp Paper Res. J.* 8, 1 (1993).
4. Gregory, J., *J. Colloid Interface Sci.* 42, 448 (1973).
5. Higashitani, K., and Kubota, T., *Powder Technol.* 51, 61 (1987).
6. Eriksson, L., Alm, B., and Stenius, P., *Colloids Surf. A* 70, 47 (1993).
7. Smellie, R. H., and La Mer, V. K., *J. Colloid Sci.* 23, 589 (1958).
8. Hogg, R., *J. Colloid Interface Sci.* 102, 232 (1984).

Y. ADACHI*[1]
M. A. COHEN STUART†
R. FOKKINK†

*Institute of Agricultural and Forest Engineering
Tsukuba University
Tsukuba City, Ibaraki 305
Japan
†Department of Physical and Colloid Chemistry
Wageningen Agricultural University
Dreijenplein 6
6703HB, Wageningen
The Netherlands

Received June 20, 1994; accepted November 2, 1994

[1] To whom correspondence should be addressed

Contribution to the International Polymer Colloids Group Newsletter

E.S. Daniels, V.L. Dimonie, M.S. El-Aasser, A. Klein,
O.L. Shaffer, C.A. Silebi, E.D. Sudol, and J.W. Vanderhoff

Emulsion Polymers Institute
Lehigh University, Mountaintop Campus, Iacocca Hall
Bethlehem, Pennsylvania 18015-4732 USA

The titles of our current research projects are given in the **Contents** of our *Graduate Research Progress Reports*, No. 43, January, 1995, which can be found at the end of this report. Summaries of progress in several research areas are presented here.

1. Miniemulsion Copolymerization of Vinyl Acetate and Vinyl 2-Ethylhexanoate Monomers

Ervin L. Kitzmiller

The underlying interest in studying the copolymerization of vinyl acetate (VAc) with vinyl 2-ethyl hexanoate (V2EH) lies with the possible benefits that may be achieved by the successful incorporation of V2EH into the copolymer in comparison to poly(vinyl acetate) alone. Expected improvements include greater film formation and flexibility properties and, in addition, enhanced resistance to alkaline hydrolysis attack.

It has been suggested that incorporation of V2EH into the copolymer chains is affected by the polymerization scheme chosen, i.e., conventional emulsion vs. miniemulsion polymerization. In addition, when using a monomer possessing significantly low water solubility, as is the case for V2EH (<0.01%), the kinetics may be enhanced and the copolymer produced may be more homogeneous using the miniemulsion polymerization approach rather than conventional emulsion polymerization. In parallel with the copolymerizations, homopolymerizations of VAc and V2EH were conducted to better understand their copolymerization.

All of the following homopolymerizations were performed in batch using the Mettler RC1 reaction calorimeter. The polymerization temperature was 60 °C. The reactor was configured with one baffle and agitated at 500 rpm with a pitch 4-blade turbine impeller. A standard recipe was established for studying this system as given in Table 1.

Figures 1 and 2 compare the rate of reaction profiles for the VAc and V2EH systems, respectively, using both conventional and miniemulsion systems. The reactive surfactant TREM LF-40 (HENKEL) was employed in these reactions, which not only can serve as emulsifier, but because of its allylic structure, can also copolymerize with the monomers and/or act as a radical scavenger. The latter attribute of TREM LF-40 is considered to be the cause of the interesting results found when comparing the kinetic results of the miniemulsion polymerizations to the equivalent conventional emulsion polymerizations. As can be seen in both the VAc and V2EH rate profiles, there is an initially faster rate in the miniemulsion polymerizations and for V2EH,

overall faster kinetics are achieved. For the VAc system, these results are thought to be due to chain transfer to the surfactant. For the V2EH system, the slower kinetics in the conventional emulsion polymerizations may result to a small degree from chain transfer to TREM LF-40, but most likely are attributable to the monomer's low water solubility.

Table 1: STANDARD RECIPE USED FOR THE VAc AND V2EH CONVENTIONAL AND MINIEMULSION HOMOPOLYMERIZATIONS

Ingredient	Amount	Mass (g)
Distilled-Deionized Water	80 parts	564.8
V2EH or VAc	20 parts	141.2
TREM LF-40 *or* Hydrogenated TREM	5, 10, 20, 30, 40 mM* 10, 20, 30 mM*	1.2166 - 9.7344 2.4452 - 7.3334
Hexadecane	0 or 80 mM*	0 or 10.23
Sodium Persulfate (NaPS)	4 mM*	0.5376
Sodium Bicarbonate ($NaHCO_3$)	4 mM*	0.1897

* Based upon water

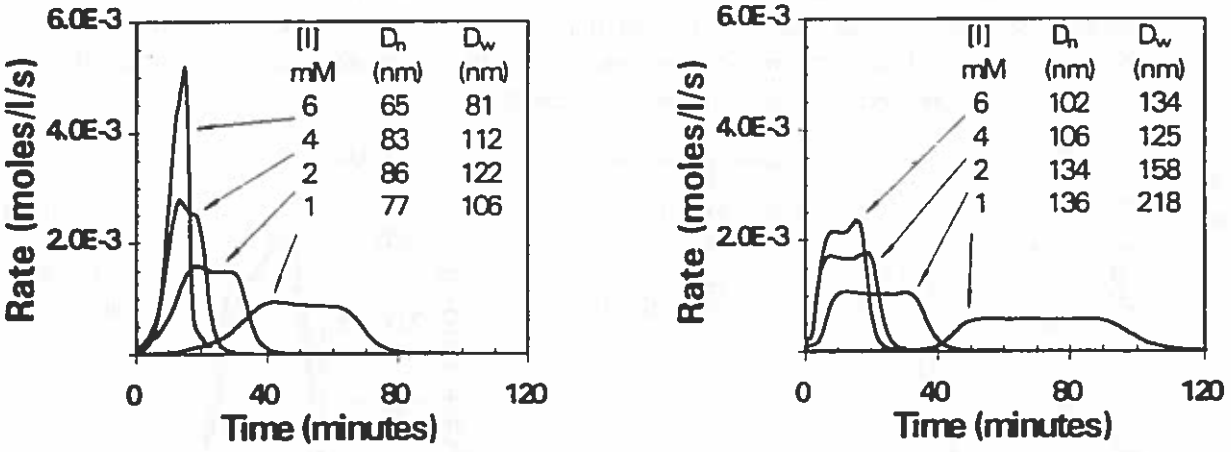

Figure 1: *Effect of initiator concentration on the rate of polymerization and particle size in conventional (left) and miniemulsion (right) polymerizations of VAc using the reactive surfactant TREM LF-40; T_r = 60°C.*

Also reported in Figures 1 and 2 are the resulting particle sizes as determined via transmission electron microscopy. In the VAc system, it can be seen that smaller particles are produced via the conventional emulsion polymerizations in comparison to the miniemulsion polymerizations. However, little effect on particle size is seen with increasing initiator concentration in the conventional emulsion polymerizations whereas in the miniemulsion polymerizations, smaller particles were generated. In the V2EH system, the conventional emulsion

polymerizations also produced smaller particles in comparison to the miniemulsion polymerizations, but the increasing initiator concentration in the conventional system produced smaller particles while no trend in the results for the miniemulsion system were observed.

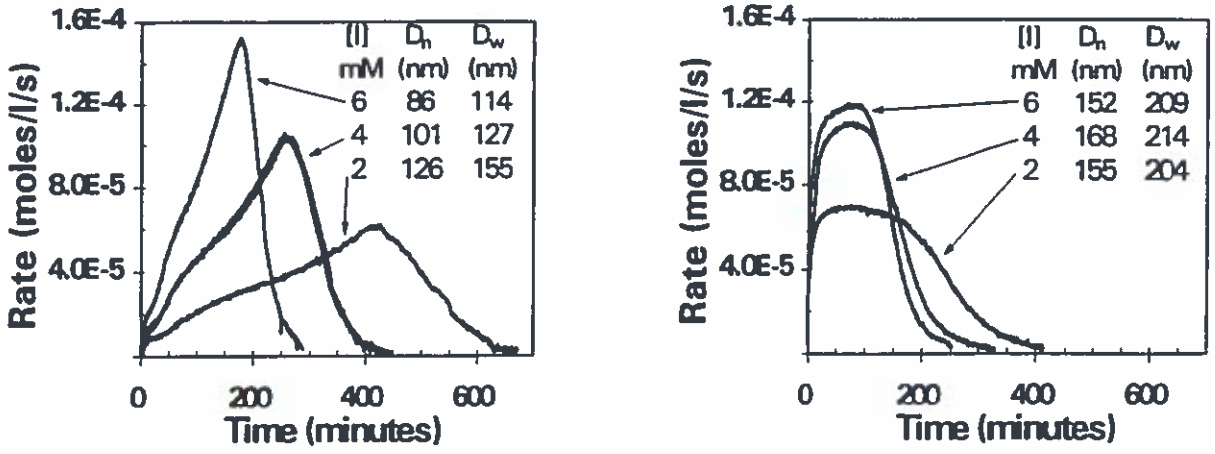

Figure 2: *Effect of initiator concentration on the rate of polymerization and particle size in conventional (left) and miniemulsion (right) polymerizations of V2EH using the reactive surfactant TREM LF-40; T_r = 60°C.*

Figures 3 and 4 show the VAc and V2EH conventional homopolymerization rate profiles, respectively, comparing the use of reactive TREM LF-40 to the nonreactive, hydrogenated TREM. These results clearly show the effect of the chain transfer on the kinetics. For both monomer systems, as the concentration of the TREM LF-40 was increased, the rates decreased; whereas in the polymerizations carried out using the hydrogenated TREM, as the surfactant concentration increased, the rates likewise increased.

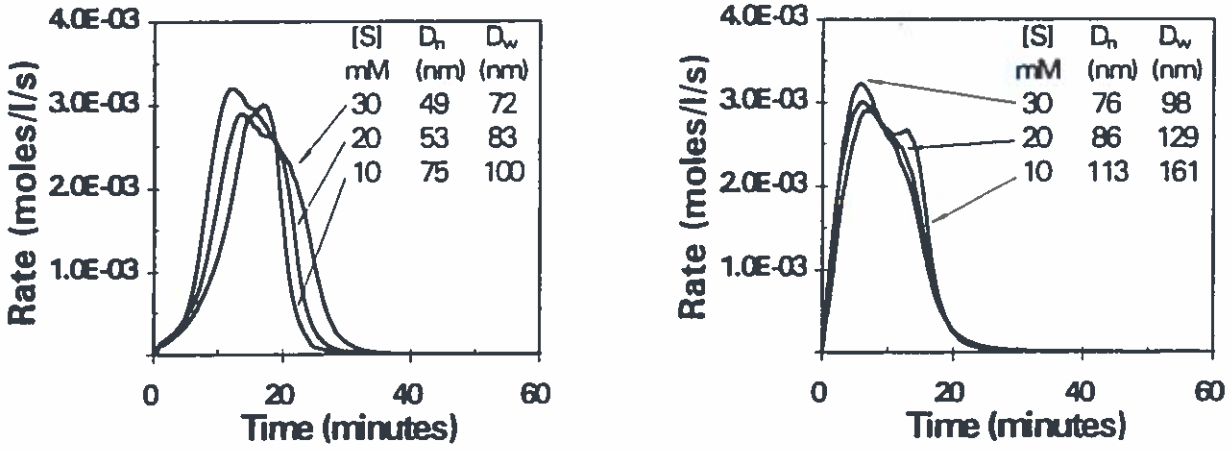

Figure 3: *Effect of surfactant concentration, [S], and type on the rate of polymerization and particle size for the conventional emulsion polymerization of VAc: reactive TREM LF-40 (left); hydrogenated TREM (right); T_r = 60°C.*

Particle size analyses of the latexes showed that, for the VAc system, smaller particles were produced using the reactive TREM LF-40 in comparison to the hydrogenated TREM. In

addition, for both polymerization processes, increasing surfactant concentration resulted in decreasing particle size. In comparison, the V2EH system revealed little difference between the two surfactants. Both produced nearly the same size particles. However, increasing the reactive TREM LF-40 concentration did result in smaller particles, whereas no clear trend was seen for the hydrogenated TREM.

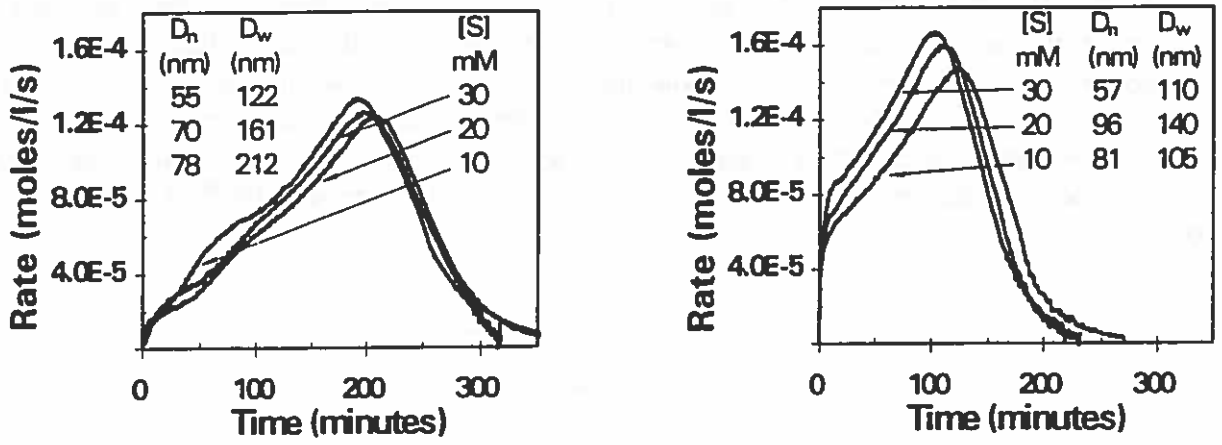

Figure 4: *Effect of surfactant concentration, [S], and type on the rate of polymerization and particle size for the conventional emulsion polymerization of V2EH: reactive TREM LF-40 (left); hydrogenated TREM (right); T_r = 60°C.*

2. Characterization of Poly(Vinyl Alcohol) During the Emulsion Polymerization of Vinyl Acetate Using Poly(Vinyl Alcohol) as Emulsifier

Guadalupe Magallanes

During the emulsion polymerization of vinyl acetate (VAc) using poly(vinyl alcohol) (PVA) as stabilizer and potassium persulfate as initiator, the VAc reacts with the PVA forming PVA - graft - PVAc. When the grafted polymer reaches a critical size it becomes water-insoluble and precipitates from the aqueous phase forming polymer particles. Since particle formation and therefore, the properties of the final latex will depend on the degree of grafting, it is important to quantify and characterize the grafted PVA.

The initial approach used to separate the water-soluble PVA from the grafted water-insoluble PVA was ultracentrifugation (36,000 rpm for 12 hrs at 4°C). By this method, separation of the serum (where the water-soluble PVA remains) from the polymer particles (where the grafted water-insoluble PVA is located) was carried out. However, it was not possible to quantify the amount of linear and grafted PVA because: 1) not all of the water-soluble material could be removed from the polymer particles in a single centrifugation step (more water-soluble material was removed after the precipitate of the first centrifugation was redispersed in water and centrifuged again); 2) good separation could not be achieved at low conversions (~ below 15%); and 3) PVAc water-soluble oligomers were present at all conversions.

To overcome the centrifugation problems, an acetonitrile/water double extraction of the latex (not of the serum film) was carried out to separate the water-soluble PVA from the water-insoluble PVA. In the acetonitrile extraction, the aqueous phase of the latex was replaced with acetonitrile (solvent for PVAc but not for PVA) using a rotary evaporator. The PVAc was dissolved in the solvent while the PVA was suspended in the PVAc/acetonitrile solution. The PVA was separated from the PVAc/acetonitrile solution by centrifugation and then placed in hot water for at least 48 hours in order to separate the mostly linear water-soluble PVA from the grafted water-insoluble PVA. GPC chromatograms of the serum after the first centrifugation and the water-soluble PVA obtained after acetonitrile/water extraction of the latex and the serum are shown in Figure 5, where only a single peak is present, demonstrating that the other peaks, which were present in the serum prior to acetonitrile extraction, were due to PVAc water-soluble oligomers.

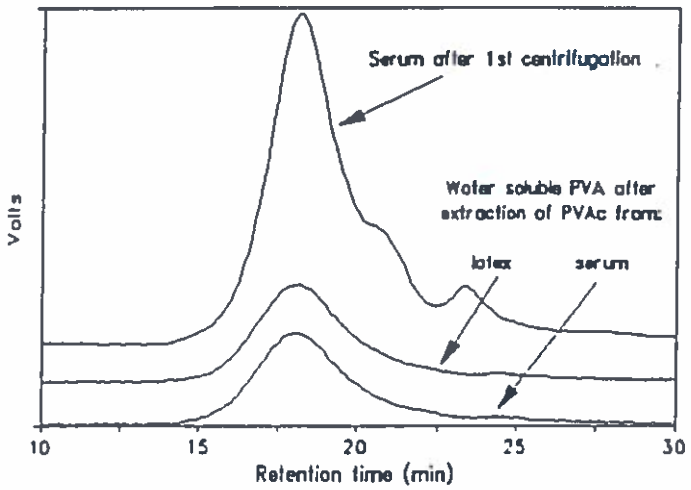

Figure 5: *GPC chromatograms of the water-soluble PVA obtained after acetonitrile/water extraction of the latex and the serum at 11.9% conversion*

Fourier Transform Infrared (FTIR) and ^{1}H and ^{13}C Nuclear Magnetic Resonance (NMR) analyses of each fraction proved that indeed PVAc homopolymer, linear PVA, and grafted PVA had been isolated from the latex. After the acetonitrile/water double extraction of the latex samples, a mass balance was carried out in order to calculate the amounts of PVAc and PVA that were grafted (equations 1 and 2). The calculated amounts for two experiments carried out at different initiator concentrations showed that the amount of PVAc grafted is independent of the initiator concentration, while the amount of PVA grafted is higher at the higher initiator concentration, as shown in Figure 6.

$$PVA_{grafted} = PVA_{recipe} - PVA_{water\text{-}soluble} \quad (1)$$

$$PVAC_{grafted} = VAc_{reacted} - PVAc_{homopolymer} \quad (2)$$

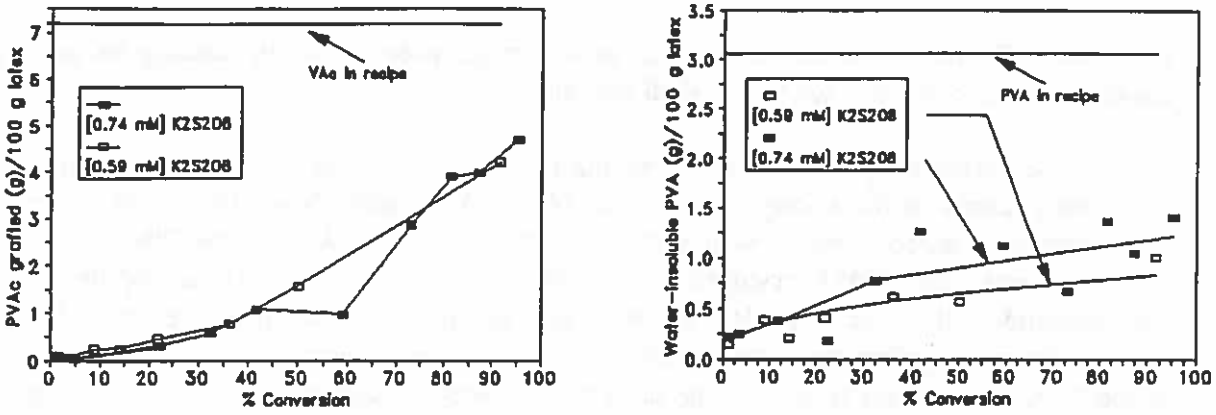

Figure 6: *PVAc grafted (left) and PVA grafted (right) as a function of conversion in the emulsion polymerization of VAc using partially hydrolyzed PVA as emulsifier.* $[K_2S_2O_8]$ *= 0.59 and 0.74 mM;* T_r *= 60 °C.*

3. Copolymerization of Macromonomers as Compatibilizing Agents in Composite Latex Particles

Prapasri Rajatapiti

Composite latex polymers possess properties that cannot be achieved either by physical blending of the constituent polymers or by copolymerization of the corresponding monomers in the same proportion. These polymers are typically prepared by seeded emulsion polymerization, from which a variety of morphological features can be obtained. Design and control of latex particle morphology are often crucial in order to fulfill end-use requirements for these materials. The interfacial tension between the two polymer phases and the interfacial tension between each phase and the aqueous medium are the key factors governing the type of composite particle morphology. In this research project, we are trying to control the degree of phase separation for the poly(n-butyl acrylate)/poly(methyl methacrylate) (PBA/PMMA) polymer pair and increase the coverage of the seed polymer in composite latex particles using a compatibilizing agent as a modifier of the polymer/polymer interfacial tension. The compatibilizing agent is generated by the reaction between a macromonomer and a comonomer. In principle, the formation of graft copolymer by the macromonomer technique is advantageous because it offers control over the graft length, since the molecular weight of the starting macromonomer can be preselected. In addition, the number of grafts per polymer chain can be controlled by adjusting the macromonomer to comonomer molar ratio.

The compatibilizing agents are prepared *in situ* by emulsion copolymerization of n-butyl acrylate (n-BA) in the presence of PMMA macromonomer. Composite latexes of PBA/PMMA are prepared by seeded emulsion polymerization using the PBA seed particles in which the PMMA macromonomers are incorporated. Based on the hydrophilicity of the monomers, it is anticipated that the graft copolymers will be preferentially partitioned at the polymer/water interface of the seed PBA particles because of their relatively more hydrophilic PMMA branches. These copolymers on the surface of the seed particles will decrease the interfacial tension between

the PBA and PMMA phases during the second-stage polymerization, leading to an improved coverage of the core particles by the shell polymer.

The partitioning of the compatibilizing agents was studied by the soap titration method. From the decrease in the average particle size [*IPCG Newsletter*, Nov., 1993] and the increase in the effective cross-sectional area per molecule of surfactant (A_s) on the PBA latex particles copolymerized with PMMA macromonomer compared to that of the PBA homopolymer latex, it was concluded that the particle's surface was modified by the presence of n-BA/PMMA macromonomer copolymers at the interface. To explain the reduction in the average particle size of the PBA seed latexes formed in the presence of PMMA macromonomer, an estimation of the increase in the particle surface hydrophilicity was obtained via interfacial tension measurements between the monomer and water phases. The decrease in the interfacial tension suggested the partitioning of MMA units from the PMMA macromonomer at the oil/water interface. The effect of the compatibilizing agents on the morphology of the resulting composite particles was studied via transmission electron microscopy (TEM). PBA homopolymer seed particles resulted in hemispherical composite particles while the PBA seed prepared in the presence of PMMA macromonomer resulted a majority of core/shell particles plus some smaller hemispherical particles. It is speculated that the core/shell particles were derived from the seed particles in which macromonomer chains had been incorporated, whereas the hemispherical particles resulted from the PBA seed particles in which no macromonomers were present. These PBA homopolymer particles were most likely formed by homogeneous nucleation of n-BA in the aqueous phase. Future work is required to fully understand this phenomenon.

4. On-line Monitoring, Modeling, and Model Validation of Semi-batch Emulsion Polymerization

Vincenzo Liotta and Christos Georgakis

Conducting emulsion polymerizations in a semi-batch mode provides a degree of process flexibility that can be useful in meeting the demand to produce polymer latexes with particular characteristics. The semi-batch process is investigated in this work with the development and validation of a dynamic growth model using data from a newly built emulsion polymerization reactor control facility.

The model, which describes the growth of a monodisperse polystyrene seed as neat monomer is fed to the reactor, incorporates recent findings in radical diffusion and kinetics. While developing the model, particular attention was given to an accurate description of the gel effect as well as the choice of kinetic parameters from the literature. Simulation results include weight fraction polymer inside the particles, conversion, and particle size.

Data to be used for model validation was obtained from a custom-built automated reactor facility. The major components of this facility include a three liter reactor and accessories, a temperature control system, an inlet flow system, an on-line characterization system, and a data acquisition and control framework that ties all the components together. The characterization system, the most sophisticated part of the facility, is comprised of an on-line density meter and an

on-line particle size sensor. Density measurements provide near continuous conversion data while the particle size sensor, an on-line adaptation of capillary hydrodynamic fractionation (CHDF), measures particle size every ten minutes.

Good agreement exists between simulation results and on-line experimental data with the aid of only one adjustable parameter, the mass transfer coefficient for radical entry, k_{mp}. Figure 7 shows a comparison of the evolution of the experimental weight fraction inside the particles and the best model fits for three different monomer feed rates. The model predicts the experimentally observed pseudo-steady state behavior under Smith-Ewart case 2 kinetics (F_m=1.28 mL/min) as well as the autoacceleration phenomenon typical of case 3 kinetics (F_m=0.44 mL/min, F_m=0.86 mL/min). A sensitivity analysis of the model to the adjustable parameter, using the program ODESSA, was also performed and shown to be an important tool in the validation procedure.

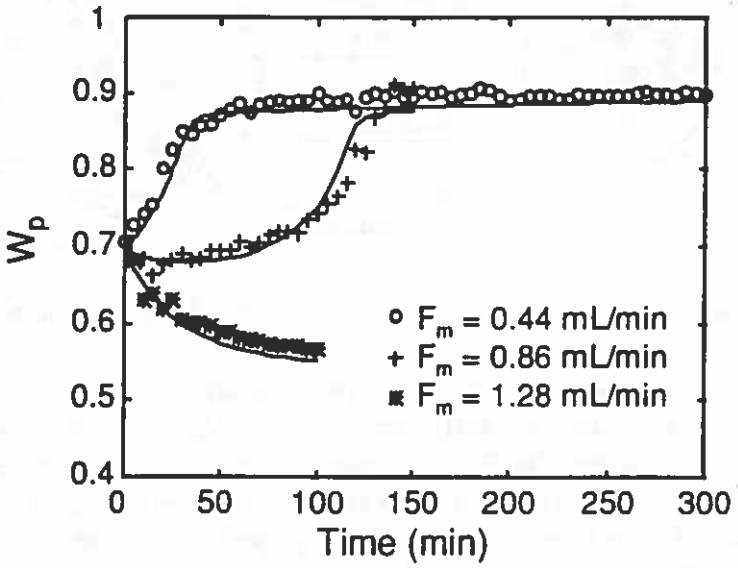

Figure 7: *Weight fraction polymer in the particles as a function of time calculated from densitometer data (points) and best fit model (lines); T_r = 50°C.*

5. Structured Latex Particles for Modification of Polycarbonate

Rong Hu

This project deals with the design of a new kind of impact and damping modifier for thermoplastics to be used in the study of toughening mechanisms of modified thermoplastics. The modifier is a core/shell structured latex particle with an interpenetrating polymer network (IPN) core and a glassy shell. The IPN technology developed in this study will provide a means for studying the cavitation phenomena in the rubber particles that can provide maximum impact resistance for a polycarbonate (PC) matrix.

The IPN core consists of both relatively low and high glass transition temperature materials, polymer A and polymer B, respectively, as depicted schematically in Figure 8. Polymer A has a T_g of 60°C below ambient temperature (i.e., T_g < -40°C) to act as a good toughening agent, while polymer B has a T_g between -30°C and 10°C to provide effective damping by absorbing energy through the onset of coordinated molecular motions, which is similar to the action of sound and vibration damping materials. Polymer B also offers a greater resistance to cavitation. The shell material, polymer C, should provide a good interfacial bonding between the core and the matrix, polymer D. Because poly(styrene-*stat*-acrylonitrile) (SAN) is compatible with PC at certain AN concentrations, SAN was selected to be polymer C.

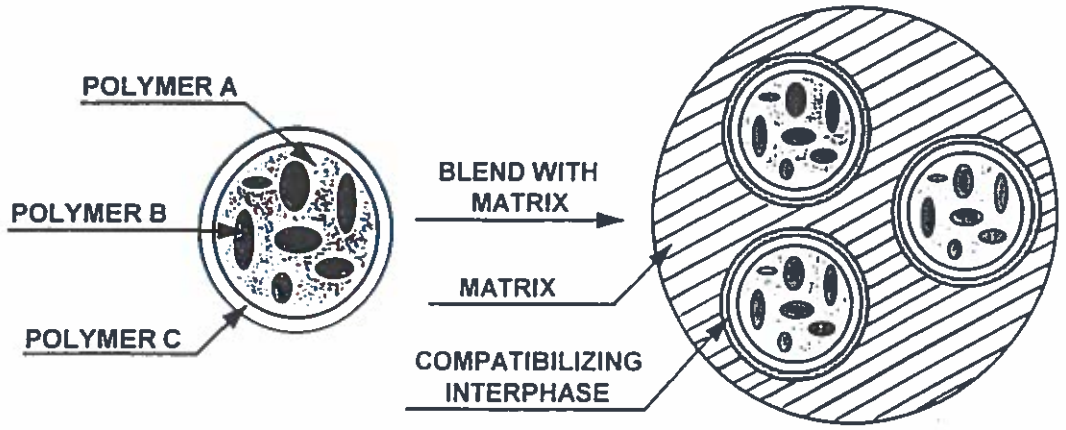

Figure 8: *Possible morphology of the IPN latex rubber particle and toughened thermoplastic.*

The IPN particles were prepared by the sequential technique. Polymer A is poly(butadiene-*stat*-styrene) (P(Bd/S)) (90/10 weight ratio). Since the crosslinking density of the first polymer (polymer A) controls the IPN morphology, two kinds of polymer A with different gel fractions were synthesized by conventional emulsion polymerization. Lithium soap recipes were used as the emulsifiers to prepare monodisperse P(Bd/S) latex particles with two different gel-fractions, 95% and 40%, respectively. Different compositions of polymer B were selected to obtain different IPN morphologies and consequently, different mechanical properties of the core/shell latex particles. The glass transition temperature of polymer B was designed to be around 10°C (as predicted by the Fox equation) in order to have good damping properties at room temperature. Tetra-ethylene glycol dimethylacrylate (T-EGDMA) was used as the crosslinking agent. The P(Bd/S) particles were swollen with the monomer mixture for 24 hours at room temperature and then polymerized by a batch process. It was found that when using P(Bd/S) particles with 95% gel fraction, phase separation occurred with polymer B surrounding the P(Bd/S) particles as a shell or as a half moon morphology when the ratio of polymer A to polymer B was 1/1 or lower. A quite different morphology was observed when the P(Bd/S) core particles had a 40% gel fraction. No core/shell formation was observed with different polymer A to polymer B ratios. When the A/B ratios were 1/1 and lower, the polymer B domains were more obvious, forming a cellular-type morphology. The high crosslink density of the P(Bd/S) core restricted the swelling of the core particles by the second-stage monomers, resulting in the exclusion of polymer B to the exterior of the composite particles, while the P(Bd/S) cores with 40% gel fraction could accept more of the second stage monomers and polymers, resulting in a

uniform distribution of polymer B in polymer A. It was also found that the gel fraction of the IPN particles was increased to approximately 100% after the second stage polymerization, indicating a rise in the gel fraction of polymer A, i.e., P(Bd/S). This was likely to occur during the second stage polymerization since a crosslinking agent (T-EGDMA) was used in the formation of polymer B and the residual double bonds in the P(Bd/S) latex could react with the crosslinking agent and second stage monomers in the presence of free radicals, thus increasing the gel fraction.

IPN core/SAN shell morphology was obtained by employing the semi-continuous addition mode of the shell monomer during the third stage polymerization. Four types of IPN/SAN structured latex particles were synthesized from the different IPN cores with cellular-type morphologies. A 72/28 (weight ratio) S/AN monomer mixture was chosen for the shell composition in order to obtain the maximum adhesion between the PC and the latex particles. Figure 9 shows the tan-delta peaks of these structured latex particles measured by dynamic mechanical spectroscopy (DMS). When using poly(butyl acrylate-*stat*-methyl methacrylate) (P(BA/MMA)) or poly(butyl acrylate-*stat*-styrene) (P(BA/S)) as polymer B, a broad peak starting around -55°C was observed, followed by a SAN shell peak at 111°C. A miscible IPN morphology was obtained with a broad peak between -70 and 10°C and a shell peak at 116°C when using P(Bd/S) (50/50 wt ratio) as polymer B. However, besides two peaks at -64 and 116°C, a third peak around 6°C was also seen in the tan-delta curve when using poly(ethylhexyl methacrylate-

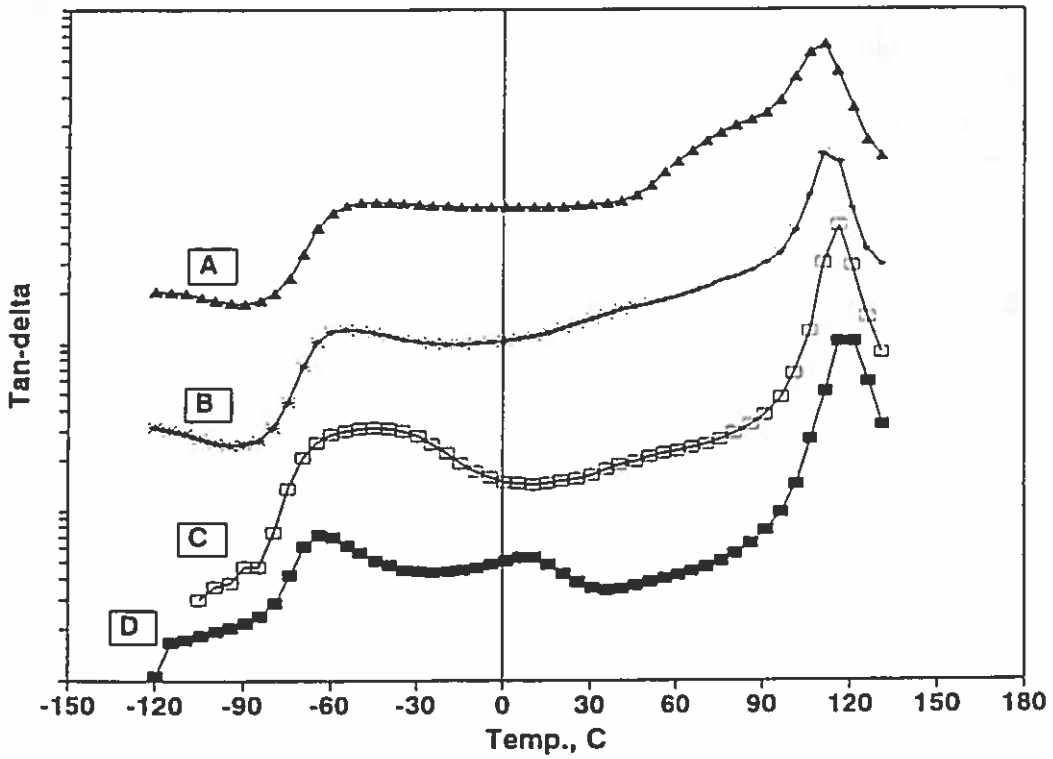

Figure 9: *DMS results of structured latex particles: (A) 1/1/1 P(Bd/S)/P(BA/MMA)/SAN; (B) 1/1/1 (Bd/S)/P(BA/S)/SAN; (C) 1/1/1 P(Bd/S)/P(Bd/S)/SAN; (D) 1/1/1 P(Bd/S)/P(EHMA/S)/SAN.*

stat-styrene) (P(EHMA/S) (85/15 weight ratio)) as polymer B. It can be concluded that the miscibility between polymer B with P(Bd/S) and SAN controls the IPN/SAN morphology. P(BA/MMA) and P(BA/S) are more hydrophilic than P(Bd/S) and P(EHMA/S) and are more miscible with SAN, so the peak around 10°C was not seen in the tan-delta curve, indicating that not enough pure polymer B domains existed in the particles. P(EHMA/S) is less compatible with polymer A than P(Bd/S) (50/50), as a result, a separate peak for polymer B was observed. Since it is unknown what kind of IPN morphology would have an optimum toughening property in PC, all of these structured latex particles will be blended with PC to study their toughening performance.

Recent Ph.D. Dissertations

The Development of Core-Shell Latex Particles as Toughening Agents for Epoxies
Julie Yu Qian

Analytical Separation of Colloidal Particles Using Capillary Electrophoresis
Armistice B. Hlatshwayo

Particle Formation and Growth During Styrene Oil-in-Water Miniemulsion Polymerization
Christopher M. Miller

Interaction of Proteins with Monodisperse Polymer Latexes
Jan-Ming Hou

EMULSION POLYMERS INSTITUTE
Lehigh University

Graduate Research Progress Reports
No. 43 January 1995

Emulsion Polymerization of Styrene in an Automated Reaction Calorimeter (L. Varela de la Rosa)

Emulsion Copolymerization of Styrene and n-Butyl Acrylate in an Automated Reaction Calorimeter (E. Ozdeğer)

Towards an Understanding of the Role of Water-Soluble Oligomers in the Emulsion Polymerization of the Styrene/Butadiene/Acrylic Acid Termonomer System (X. Yuan)

Particle Formation and Growth During Styrene Oil-in-Water Miniemulsion Polymerization (Ph.D. Abstract) (C.M. Miller)

Particle Formation and Growth During Styrene Oil-in-Water Miniemulsion Polymerization (P.J. Blythe and C.M. Miller)

Miniemulsion Copolymerization of Vinyl Acetate and Vinyl 2-Ethylhexanoate Monomers (E.L. Kitzmiller)

Copolymerization of Styrene and Butadiene Monomers via Miniemulsion (D. Li)

The Role of the Polymerizable Surfactant Sodium Dodecyl Allyl Sulfosuccinate in the Emulsion Polymerization of Styrene (J. Chu)

Grafting Reactions in the Emulsion Polymerization of Vinyl Acetate Using Poly(Vinyl Alcohol) as Emulsifier (G. Magallanes)

Evaluation of Dimethyl Meta-Isopropenyl Benzyl Isocyanate (TMI®) in Emulsion Polymerization (S. Mohammed)

Anionic Dispersion Polymerization of Styrene (M.A. Awan)

The Role of Compatibilizing Agents in the Development of Composite Latex Particle Morphology (P. Rajatapiti)

Suprastructured Latex Thermoplastics — A ^{13}C NMR Characterization Study (V. Nelliappan)

The Development of Core/Shell Poly(Butadiene-co-Styrene) / Poly(Methyl Methacrylate) Latex Particles as Toughening Agents for Epoxies (J.Y. Qian)

Elastomeric Films from Structured Latexes (Y. He)

Structured Latex Particles for Modification of Polycarbonate (R. Hu)

Preparation of Micron-Size Poly(n-Butyl Acrylate) / Polystyrene Structured Latex Particles by Dispersion Polymerization (D. Wang)

Electrokinetic Effects Associated with the Motion of Latex Particles in Capillary Hydrodynamic Fractionation (CHDF) (A.D. Hollingsworth)

Analytical Separation of Colloidal Particles Using Capillary Electrophoresis (A.B. Hlatshwayo)

Rheology of Associative Thickener Solutions (L. Zhuo)

Telechelic Polybutadiene: Synthesis, Characterization, and Crosslinking in Latex Films (J. Xu)

Colloidal Stability of Poly(tetrafluoroethylene) (PTFE) Dispersions (C. Wang)

Interaction of Proteins with Monodisperse Polymer Latexes (J.M. Hou)

Interactions at Short Times between Polydisperse Charged Spheres

J.K. Phalakornkul, A.P. Gast, R. Pecora°, G. Nägele†, A. Ferrante†, R. Klein†

Chemical Engineering Department, Stanford University, Stanford, CA 94305

°Chemistry Department, Stanford University, Stanford, CA 94305

†Fakultät für Physik, Universität Konstanz, Postfach 5560, D-7750 Konstanz, Germany

---

Abstract

We investigate the interactions in concentrated polydisperse charged silica spheres suspended in a nearly optically matched solvent by photon-correlation techniques. We study the equilibrium structure and dynamics of the spheres as well as the effects of the intrinsic size polydispersity from the acquired structure factors, diffusion coefficients and hydrodynamic functions. Polydispersity in size suppresses the peak in the structure factor as well as enhancing its value at long length scales. Even at a volume fraction of 0.033 of moderately charged macroions, the diffusion processes are still governed by both the direct interparticle potential and the indirect hydrodynamic interactions. Unlike suspensions of hard spheres, the hydrodynamic interactions hinder the diffusion only at the low and high q limits, but increase the diffusion rate at the intermediate q corresponding to the range of highly correlated macroions. This hydrodynamic enhancement complies with the theoretical prediction of Nägele et al., and diminishes with increasing degree of size polydispersity. Polydispersity of scattering power caused by the optically inhomogenous and polydisperse spheres has a strong effect on the experimentally accessible quantities. Finally, the influences of surface charge density on the interactions are considered, as well.

Self Consistent Field Calculations of Interactions Between Chains Tethered to Spherical Interfaces

Eric K. Lin and Alice P. Gast*

Department of Chemical Engineering
Stanford University
Stanford, CA 94305.

Abstract

Self consistent mean field (SCF) theory is used to investigate the structure of and interactions between layers of polymer chains tethered to a spherical interface. Traditional methods have combined flat geometry results with the Derjaguin approximation to calculate the interaction potentials between curved surfaces, leading to a great overestimation of both the range and steepness of the pair interaction potential. We have improved upon this approach by utilizing the chain configurational statistics from the curved geometry with a modified Derjaguin approximation to calculate pair interaction potentials. By varying the core radius, the degree of polymerization, and the tethering density in an athermal solvent, the tethered layer assumes structures ranging from those in star polymer systems to planar polymer brushes. The interaction potentials are found to be strictly repulsive with varying degrees of range and steepness. These changes in the interaction potential are related to changes in the tethered layer structure. The results are also compared with those from scaling theories. The range of the interaction potential generally correlates with the layer thickness predicted from scaling theory. The functional form of the interaction potentials does not follow previously proposed forms of the interaction potentials.

Long Range Order in Polymeric Micelles Under Steady Shear

[†]Glen A. McConnell, [‡]Min Y. Lin, and [†]Alice P. Gast

[†]Department of Chemical Engineering, Stanford University, Stanford CA 94305-5025

[‡]Exxon Research and Engineering Corporation, Annandale, NJ 08801

May 19, 1995

Abstract

Small angle neutron scattering (SANS) experiments were performed to examine the long range order in polymeric, micellar crystals subjected to linear steady shear. Polystyrene/ polyisoprene (PS/PI) diblocks with varying degree of polymerization and block asymmetry are used to generate both body-centered (BCC) and face-centered (FCC) cubic micellar crystals when suspended in decane. The FCC crystals show a transition from polycrystallinity to $< 1,1,1 >$ sliding layers. This transition is marked by a significant hysterisis in the steady shear stress versus shear rate data. For higher shear rates, we observe $< 1,1,1 >$ layers normal to the shear gradient slipping past each other. As the shear rate increases, the layers do not hop perfectly from one registry site to the next. The BCC crystals subjected to linear shear demonstrate a more continuous deformation of the local crystalline lattice that eventually develops into a BCC twin structure with the $< 1,1,0 >$ layers normal to the shear gradient. The BCC twins advance in portions along the twinning planes, allowing the crystal to flow at moderate shear rates. At higher shear rates we observe a loss of long range order associated with shear melting. These results show an encouraging similarity to other cubic crystals observed in both colloids and diblock melts.

Contribution to the IPCG Newsletter from
the Sydney University Polymer Centre
Reporter: Bob Gilbert
Chemistry School, Sydney University, NSW 2006, Australia.

The following abstracts from various members of the SUPC summarize current research directions.

Pulsed-laser polymerization measurements of the propagation rate coefficient for butyl acrylate. R.A. Lyons, J. Hutovic, M.C. Piton, D.I. Christie, P.A. Clay, B.G. Manders, S.H. Kable, R.G Gilbert and D.A. Shipp. Macromolecules, submitted.

The results are reported for a series of measurements of the propagation rate coefficient (k_p) of butyl acrylate obtained from pulsed-laser polymerization. Previous attempts reported in the literature to use this technique for this monomer have failed because the data did not satisfy the internal consistency tests afforded by PLP. The problem was obviated by carrying out measurements at very low temperatures and with very short times between laser pulses (including through use of two synchronized lasers). Data for k_p were obtained over the range –65 to –7°C which satisfy PLP consistency tests (invariance of the apparent k_p value to laser pulse frequency, etc.). The results fit k_p (dm^3 mol^{-1} s^{-1}) = $10^{6.54}$ exp(–15.5 kJ mol^{-1}/RT); a confidence ellipse for these parameters is provided. These data extrapolate to a value of $k_p = 1.1\times10^4$ dm^3 mol^{-1} s^{-1} at 50°C.

A priori prediction of propagation rate coefficients in free radical polymerizations: propagation of ethylene. J.P.A. Heuts, R.G. Gilbert and L. Radom. Macromolecules, submitted.

A method is derived for calculating Arrhenius parameters for propagation reactions in free-radical polymerization from first principles. Ab initio molecular orbital calculations are carried out initially to determine the geometries, vibrational frequencies and energies of the reactants and transition state. Transition state theory then yields the Arrhenius parameters. The lowest frequencies are replaced by appropriate (hindered or unhindered) internal rotors, to better model these modes in the calculation of frequency factors. It is found that a high level of molecular orbital theory (e.g., QCISD(T)/6-311G**) is required to produce reasonable activation energies, whereas satisfactory frequency factors can be obtained at a relatively simple level of theory (e.g., HF/3-21G), because the frequency factor is largely determined by molecular geometries which can be reliably predicted at such a level. Obtaining reliable frequency factors for quite large systems is thus possible. The overall procedure is illustrated by calculations on the propagation of ethylene and the results are in accord with literature experimental data. Means are also derived for extending the results to propagation of polymeric radicals, without additional computational requirements. The method is expected to be generally applicable to those propagation reactions that are not significantly influenced by the presence of solvent (i.e., relatively non-polar monomers in non-polar solvents). The calculations show that the magnitude of the frequency factor is largely governed by the degree to which the internal rotations of the transition state are hindered. They also suggest that here can be a significant penultimate unit effect in free radical copolymerization. Furthermore, the calculations explain the rate-enhancing effect found upon deuteration of the monomers and explain why the rate coefficients for the first propagation step is larger than that for the long-chain propagation step.

Molecular weight distributions: their cause and cure. R.G. Gilbert, Trends in Polymer Sci., in press.

The average molecular weight ,and the molecular weight distribution, are some of the most important determinants of the properties of a polymer product, strongly

influencing properties such as mechanical strength, minimum film-forming temperature of a latex, and so on. Advances in theory have led to a novel but simple experimental means to obtain information about the events controlling these properties, by straightforward manipulation of the data obtained from conventional GPC. This has the potential to lead to new means of improving polymer products.

Critically evaluated rate coefficients for free-radical polymerization, 1. Propagation rate coefficients for styrene. M. Buback, R.G. Gilbert, R. A. Hutchinson, B. Klumperman, F.-D. Kuchta, B.G. Manders, K.F. O'Driscoll, G.T. Russell and J. Schweer. Macromol. Chem. Phys., in press.

Pulsed-laser polymerization (PLP) in conjunction with molecular weight distribution (MWD) measurement has emerged as the method of choice for determining the propagation rate coefficient k_p in free-radical polymerizations. Detailed guidelines for using this technique (including essential internal consistency checks) and reporting the results therefrom are given by the authors, members of the IUPAC Working Party on *Modeling of kinetics and processes of polymerization*. The results for PLP-MWD k_p measurements from many laboratories for bulk free-radical polymerization of styrene at low conversions and ambient pressure are collated, and are in excellent agreement. They are therefore recommended as constituting a benchmark data set, one that is best fitted by

$$k_p = 10^{7.630}\ \mathrm{L{\cdot}mol^{-1}{\cdot}s^{-1}} \exp\left(\frac{-32.51\ \mathrm{kJ{\cdot}mol^{-1}}}{R{\cdot}T}\right)$$

(the confidence ellipsoid for the Arrhenius parameters is also given). These benchmark data are also used to evaluate the merits of several other methods for determining k_p; it is found that appropriately calibrated EPR appears to yield reliable values of k_p for styrene.

Transfer constants from complete molecular weight distributions. D.I. Christie, R.G. Gilbert, Macromol. Chem. Phys., in press.

Transfer constants to chain-transfer agent (CTA) and to monomer can be obtained by consideration of the complete molecular weight distribution, using the slope of a plot of ln(number molecular weight distribution) against molecular weight, in the limit of high molecular weight and low radical flux [P.A. Clay, R.G. Gilbert, *Macromolecules*, **28**, 552 (1995)]. A variant of this technique is developed here, employing initiation by pulsed-laser polymerisation (PLP). An advantage of using a laser pulse to initiate polymerisation is that the propagation rate coefficient may be measured using the same method of initiation. The method is shown to be suited to measure transfer constants to CTA (although not to monomer), and is applied to the polymerisations of methyl methacrylate (MMA) with added triethylamine (TEA) and with added tert-dodecylmercaptan (TDM). The transfer rate coefficients are found to be 74 (± 20) $dm^3\ mol^{-1}\ s^{-1}$ at 60 °C for the TEA system, and 52 (± 7) $dm^3\ mol^{-1}\ s^{-1}$ at 25 °C for the TDM system.

In addition, the following book has been published:

Emulsion Polymerization: a Mechanistic Approach. R.G. Gilbert. Academic Press, London, 1995; 362 pps. ISBN 0-12-283060-1

* The following publication has appeared since the previous Newsletter:

Chain-length-dependent termination rate processes in free-radical polymerizations. 3. Styrene polymerizations with and without added inert diluent as an experimental test of model. P.A.G.M. Scheren, G. T. Russell, D. F. Sangster, R.G. Gilbert and A.L. German. Macromolecules, 28, 3637-49 (1995).

Contribution to the International Polymer Colloid Group Newsletter
May 1995

from

Finn Knut Hansen

University of Oslo, Dept. of Chemistry
P.O.Box 1033 Blindern, 0315 OSLO, Norway

Presently we are working on the "Associating Polymers" meeting in Loen, Norway, which will take place 25-30 June. We are quite exited, as the meeting is an effort on order to bring together people both with theoretical and more application background on "thickeners" and "gels". We also feel that it will bring together the "polymer colloid" people (as in the IPCG) and the more "gel-oriented" people. This is also a relatively new field where insight into systems and mechanisms are steadily increasing. The program for the meeting may be included in this newsletter.

The activity here in Oslo has been increasing, and 3 of our master students are now finished. We have presently 2 Ph.D. students, one is working on hydrophobically modified polyacrylamide (with F.Candau) and one on monomolecular films of block-copolymers. Below is given some information on the work of one of the master students.

Solubilization of acrylates in micellar systems investigated by means of Pulsed Gradient Spin-Echo Fourier Transform NMR.

Finn K. Hansen, Grete Irene Modahl and Harald Walderhaug

Introduction

To be able to model emulsion polymerization and related processes such as production of hydrophobically modified water soluble polymers, an important parameter is the distribution of monomers between micelles and the aqueous phase. One method that may be used to measure the solubilisation equilibrium is to measure the change in diffusion coefficient(s) of the monomer(s) caused by micellar solubilisation. Because the micelles diffuse as a single unit, the diffusion coefficient is lowered relative to the free monomer. Diffusion coefficients may be measured conveniently by means of Pulsed Gradient Spin-Echo Fourier Transform NMR (PGSE-FT NMR). Advantages with this method are that the system is undisturbed and that several monomers may be measured simultaneously (for co- and ter-polymerisations).

Principle

If the micelles and the bulk solution are regarded as two separate phases, the distribution of an organic substance (solubilisate), A, between these two phases may be considered as an equilibrium process,

$$A_{aq} \leftrightarrow A_{mic} \quad \text{with} \quad [A]_{mic}/[A]_{aq} = K_C \tag{1}$$

where K_C is the equilibrium distribution constant. A characteristic physical property, such as the diffusion coefficient for the solubilisate, will have a contribution both from the free aqueous phase monomer and the solubilised monomer. This may be expressed by,

$$\langle D \rangle = p\, D_{mic} + (1-p)\, D_{aq} \tag{2}$$

where $\langle D \rangle$ is the measured mean diffusion coefficient and p is the fractional partition of monomer in micelles. This may be determined from the (measured) mean diffusion coefficient when the separate diffusion coefficients are known. D_{mic} may be measured by solubilisation of practically insoluble substances (p=1). Tetramethyl silane (TMS) is often used. For the determination for D_{aq} the obstruction effect of the micelles must be taken into consideration. The parameter p will be directly connected to the probability for micellar particle nucleation and will increase with increasing surfactant concentration. We have measured p as a function of surfactant concentration for several acrylates and surfactants.

In process simulation, p may be calculated by means of the equilibrium equation

$$K_C = \frac{[A]_{mic}}{[A]_{aq}} = \frac{p/V_{mic}}{(1-p)/V_{aq}} = \frac{p}{1-p}\cdot\frac{V_{aq}}{V_{mic}} = \frac{p}{1-p}\frac{1}{X_{mic}} \tag{3}$$

where $X_{mic} = V_{mic}/V_{aq}$ and V_{aq} and V_{mic} are the volumes of the aqueous and (swollen) micellar phases, respectively. X_{mic} may be calculated from

$$X_{mic} = (C_s - CMC)v_s\rho \tag{4}$$

where C_s is the surfactant concentration, CMC the critical micelle concentration, v_s the partial molar volume of the surfactant in micelles and ρ is the solvent density (water). It is here assumed that the solubilisate does not perturb the micelles, which is often a questionable assumption. For a solution saturated with solubilisate, v_s will be independent of p, but higher than for the pure surfactant, while for unsaturated solutions, v_s will decrease with decreasing amount of solubilisate per micelle. Also v_s may vary because of the change in aggregation number caused by the solubilisation and may also be dependent on the type of solubilisate. It may therefore be difficult to calculate p from Equ. (3) using K_C and v_s as constants. For a saturated solution, K_C may rather be expressed by

$$K_C = \frac{p}{1-p}\left[\left(\frac{p}{1-p}\right)a + X_{mic}\right]^{-1} \tag{5}$$

where a is a constant proportional to the solubility of the solubilisate in the continuous phase. Here X_{mic} is expressed by Equ. (4) with v_s as the molar volume for the pure surfactant. We may therefore write

$$\frac{p}{1-p}\frac{1}{X_{mic}} = \frac{K_C}{1-K_C a} = K_C' \qquad (6)$$

K_C' will be a constant as long as a is constant.

Experimental

Solubilisation was determined in heavy water (D_2O) of the acrylates ethyl-, buthyl-, penthyl, hexyl-, and ethylhexyl-acrylate and the methacrylates methyl-, ethyl-, buthyl-, isobuthyl, hexyl- and cyclohexyl-methacrylate. The surfactants were sodium dodecylsulfate (SDS) and nonyl-phenyl ethoxylates with 10, 20 and 40 EO-units ($NP\text{-}EO_{10}$, $NP\text{-}EO_{20}$ and $NP\text{-}EO_{40}$). The diffusion measurements were performed on a Bruker CXP 200 with a proton field-gradient probe. Measurements were performed both at room temperature and at elevated temperatures up to 40°C.

Results

In Fig. 1 (below) the partition coefficient, p , is given for the acrylates MMA, EMA and BA in sodium dodecyl sulfate (SDS). The dotted lines are calculated by means of Eq. (3) or (6). The variable X is the degree of saturation of monomer in the aqueous phase. We see that the results

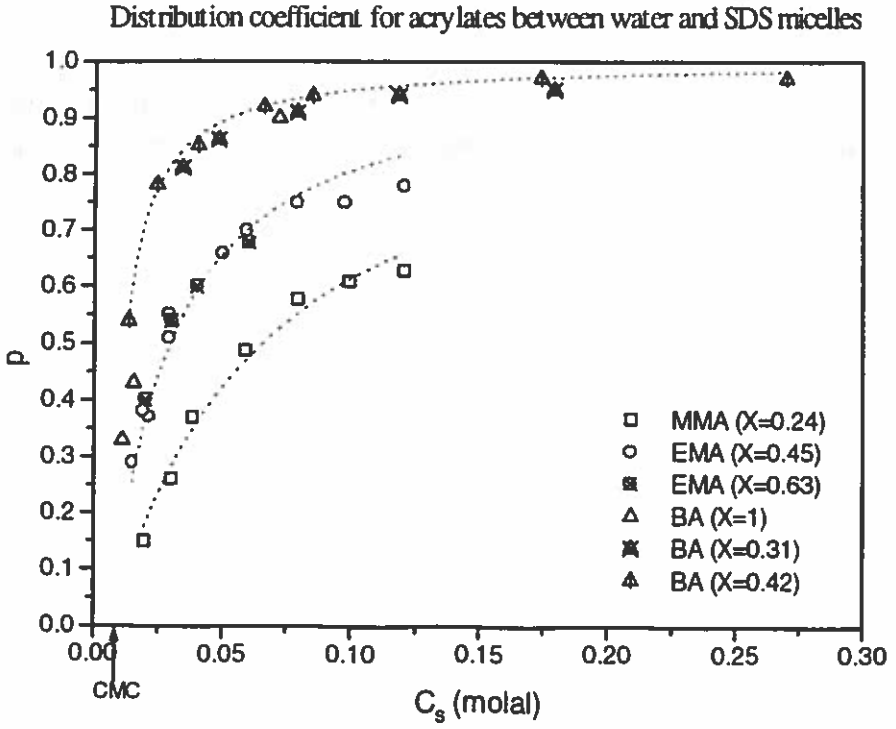

are relatively well described by this equation and there is little variation with the degree of saturation (which should be the case if K_C is a true equilibrium constant). Values for K_C' for

the monomers are calculated to 61 (MMA), 133 (EMA) and 461 (BA). If measurement errors are small, only a single (or a few) measurement(s) would be required to calculate K_C'. Some results for the nonionic surfactants are shown in Table 1. The error in the K_C' values calculated in this way is ca 20%.

Monomer	Surfactant	C_S (mmolal)	v_s (L/mol)	p	K_C'
EA	SDS	15	0.250	0.11	56
	NP-EO_{10}	9	0.608	0.11	20
	NP-EO_{20}	9	0.969	0.15	18
	NP-EO_{40}	9	1.70	0.14	9
BA	SDS	15	0.250	0.43	343
	NP-EO_{10}	9	0.608	0.54	193
	NP-EO_{20}	9	0.969	0.45	85
	NP-EO_{40}	9	1.70	0.16	11

Table 1

We se from this table that the nonionic surfactants solubilise more than SDS on a molar basis, but much less on a weight basis, because the nonionics have a higher molecular weight. Also K_C' decreases as the number of EO-groups increases, but this is less evident in p, indicating that the monomer is mainly solubilised in the hydrophobic core.

The present technique is very promising for the evaluation of solubilisation of monomer mixtures because the PGSE-FT NMR technique can measure several diffusion coefficients simultaneously. The technique is not ideal for very insoluble monomers, as p becomes too close to 1.

Because of NMR instrument breakdown, we have not had the opportunity to widen the experimental results yet, but a new instrument is installed in these days, and we hope for more interested students. Postdocs are also welcome.

M9506

INTERNATIONAL POLYMER COLLOIDS GROUP NEWSLETTER

Contribution from T. Konishi and Norio Ise, Central Laboratory, Rengo Co., Ltd., 186 - 4 - 1 Ohhiraki, Fukushima, Osaka 553, Japan, and K. Ito, T. Muramoto, and H. Kitano, Department of Chemical and Biochemical Engineering, Toyama University, Toyama 930, Japan.

Reporter: Norio Ise

I. Ultra-small-angle X-ray Scattering Study of Colloidal Silica Crystals

(a) Six-fold Symmetry

A detailed study was carried out on a colloidal silica dispersion by using an ultra-small-angle X-ray scattering (USAXS) apparatus (T. Konishi, N. Ise et al. Phys. Rev. B. 51, 3914 (1995)). The z-average radius of the particles and its standard deviation were 560 A and 8 %, respectively, which were obtained by fitting observed USAXS profiles under high salt conditions to the form factors for isolated spheres. The net charge density of the particles were 0.06 $\mu C/cm^2$ by conductometric measurements, with the analytical charge density being 0.24 $\mu C/cm^2$. After extensive purification, the silica concentration was 3.76 vol.% by dry weight using 2.2 g/cm^3 for its specific gravity. The dispersion was introduced into a glass capillary (length: 70 mm) of an inner diameter of 2 mm together with ion-exchange resin particles [AG501-X8(D), Bio-Rad Lab., Richmond, CA]. The upper part of the capillary (separated by a nylon mesh) and the lower part were filled with the resin particles. The middle part, where the X-ray beam (width: about 1 mm, height: about 15 mm) hits, was free from the resin particles. The dispersion inside the capillary was iridescent.

Figure 1 shows the scattering profiles observed for the dispersion kept vertically for 84 days after the dispersion was introduced into the capillary. Sharp peaks (curve (a)) were observed at diffraction angles of (150 x n)", with n being an integer. Since strong and sharp peaks with n up to five could be observed, it was concluded that a very large "single" crystal had grown in the dispersion. The same profile as curve (a) was observed at each multiple angle of 60 $\pm$ 1°, in other words, at rotation angle of capillary ω of (60 x m) $\pm$ 1° with m being an integer, when the capillary was rotated around its vertical axis.

Furthermore the dispersion displayed similarly sharp peaks at diffraction angles of (85 x n)" when the capillary was rotated by (30 + 60 x m) $\pm$ 1° (curve (b)).

All the information could be explained only when a bcc lattice was assumed with [111] direction of the single crystal being vertically upward and parallel to the capillary axis. It was concluded that the curve (a) corresponds to the diffraction from the (110) planes. By using the Bragg equation, the distance (d_{110}) between the (110) planes was determined to be

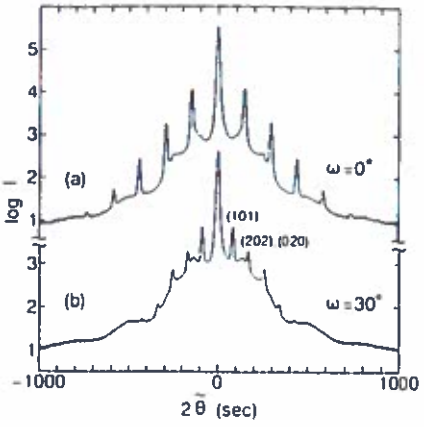

Figure 1. The logarithm to base 10 of the USAXS intensity $I(2\tilde{\theta})$ in counts per second versus the rotation angle $2\tilde{\theta}$ of the second crystal in the Bonse-Hart camera system. Sample: 3.76 vol. % water dispersion of colloidal silica particles (radius: 560 A, standard deviation: 8 %). Curve (a) for the rotation angle (ω) of the capillary = 0^{o}, curve (b) ω = 30^{o}. Temp.: 25^{o}C.

2100 A.

The situation is represented in Figure 2 for the case of $\omega = 0^{o}$. The first and second order peaks of the curve (b) are the (101) reflections, while the second one may be simultaneously the first order of the (020) reflection. The third-order peak is probably due to the (121) reflection. From d_{110} the diffraction angles 2θ from the (101) and (020) planes were calculated to be (150 x n)" and (210 x n)", respectively. As demonstrated in Figure 3, the true diffraction angle 2θ (the angle made by the incident X-ray in the horizontal plane with the scattered x-ray) is equal to $2\tilde{\theta}/\cos\phi$, where $2\tilde{\theta}$ is the angle between a vertical plane including the path of the incident X-ray and that containing the path of the scattered X-ray. For the (110), (101) and (020) planes, ϕ values are 0^{o}, 54.7^{o} and 35.3^{o}, respectively. Thus, the first order of the (020) reflection is at $2\tilde{\theta}$ = 170", while that of the (101) reflection is at 85". These values are in good agreement with the observed ones, as clear from Figure 1.

The lattice constant a obtained by using $d_{hkl} = a / (h^2 + k^2 + l^2)^{1/2}$ for cubic lattices with the value d_{110} was 3000 A.

It should be pointed out that Sogami and Yoshiyama recently found by the Kossel line analysis for the present dispersion that the lattice structure is bcc and its lattice constant is 3140 A, in agreement with the present results (I. S. Sogami and T. Yoshiyama, to be published).

Figure 2. A top view of the bcc lattice maintained in the capillary for the rotation angle of the capillary = 0^{o}, with the [111] direction of the lattice being vertically upward and parallel to the capillary axis.

(b) Four-fold Symmetry

Recently, the same dispersion as discussed above was found to display a new symmetry, four-fold symmetry, in a different capillary (T. Konishi and N. Ise, publication in preparation). Figure 4 shows the scattering profiles for the four-fold symmetry. As before, sharp peaks were observed but at different diffraction angles of (149 x n)". The curve (a) was also observed

at (90 x m) $\pm$ 1^{o}. Figure 5 shows the top view of the bcc lattice providing the four-fold symmetry for ω = (90 x m)^{o}.

Furthermore, similarly sharp peaks were observed at diffraction angles of (109 x n)" when the capillary was rotated by (45 + 90 x m) $\pm$ 1^{o} as shown by curve (b). No clear peaks could be observed at $\omega \neq$ (45 x m)^{o}. The profiles in Figure 4 can be explained by assuming a bcc structure with the [001] direction of the single crystal being vertically upward and parallel to the capillary axis (Figure 5) and with a lattice constant a of 3000 A. It is possible to conclude that the profiles at ω = (90 x m)^{o} correspond to diffraction from the (110) planes with ϕ = 0, while those at ω = 45^{o} are from the (011) and (01$\bar{1}$) reflections with ϕ = 45^{o}. The $2\bar{\theta}$ values calculated were (150 x n)" [observed: (149 x n)"], (212 x n)" [observed:(218 x n)"], and (106 x n)" [observed: (109 x n)"] for the (110) (0$\bar{1}$1) and (01$\bar{1}$) reflections, respectively. Thus all the observed values of 2θ could be consistently explained by the bcc lattice with a single value for a (3000 A).

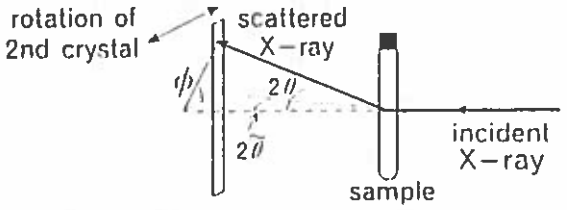

Figure 3. Diffraction from a crystal in the capillary out of the horizontal plane. Definitions of $2\bar{\theta}$ and 2θ

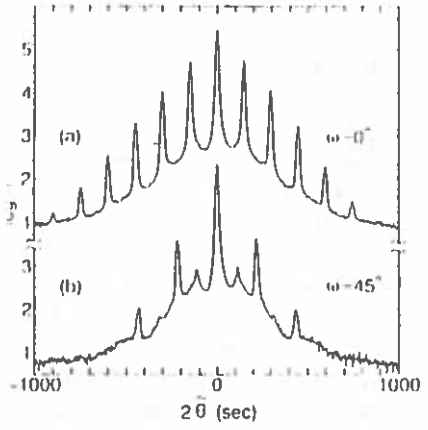

Figure 4. The scattering profiles of a four-fold symmetry of a colloidal silica water dispersion. Conc.:3.76 vol.% The measurements were done four days after the dispersion was introduced into capillary. Curve (a):rotation angle of the capillary ω = 0^{o}, curve (b): ω = 45^{o}.
Temp.: 25^{o}C .

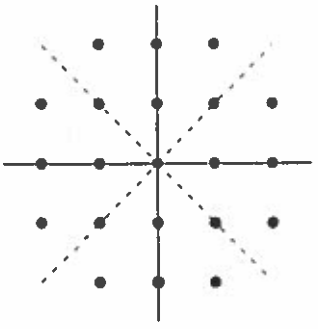

Figure 5. A top view of the bcc lattice with the [001] direction being vertically upward and parallel to the capillary axis for the rotation angle of the capillary = (90 x m)^{o}.

(c)Size of the Single Crystal

The Hosemann plot and the application of the Scherrer equation to determine the size of the crystals were unsuccessful: the crystal was too large under the present conditions. Visual observation of iridescence indicated that the crystals had sizes comparable to the scattering volume (about 1 x 2 x 15 mm).

(d)Why the Six-fold or Four-fold Symmetry?: The Ostwald Ripening and Crystallization at the Interface

For both the six-fold and four-fold symmetries, two or three of the {110} planes of the bcc structures are required to be parallel to the vertical (not horizontal) surface of the capillary. This result is consistent with previous observations of colloidal crystals obtained by microscopy (K. Ito, H. Nakamura, and N. Ise, J. Chem. Phys. **85**, 6143 (1986)) and by Kossel line analysis (I. S. Sogami and T. Yoshiyama, Phase Transitions **21**, 171 (1990)). The fact that the most densely packed plane of bcc structures, namely {110}, are parallel to the surface suggests the presence of an attractive interaction between the surface and particles. As will be mentioned below, Thomas et al. reported positive adsorption of positively charged surfactant micelles near a positively charged surfactant monolayer by a neutron reflection study (R. K. Thomas et al. J. Phys. Chem. **97**, 13907 (1993)). Ito et al. found by a confocal laser scanning microscope that the concentration of negatively charged polymer latex particles at a separation of 5 μm from negatively charged glass surface was twice as high as the bulk concentration and decreases (not increases) with increasing separation (K. Ito, T. Muramoto and H. Kitano, J. Am. Chem. Soc. **117**, 5005 (1995)). It would be easily understood that the increased concentration favors the {110} planes being parallel to the surface and facilitates crystallization near the surface.

In the early stage of crystal growth, there must be a large number of rather small, nascent crystals with [111] or [001] direction parallel to the capillary axis near the capillary-dispersion interface. (Simultaneously, there would be a large number of small, nascent crystals in the interior of the dispersion. However these crystals appear not to play the most important role in the process of the orientation determination, since they show rotational diffusion so that a specific orientation cannot preferred to.) The observed fact indicates that these crystals near the interface simultaneously cannot grow to the single crystal with one definite orientation. Selection processes must exist. Here the Ostwald ripening mechanism steps in. In other words, a large crystal grows to the single crystal at the expense of smaller ones, whichever of the two orientations it may have.

It is also noteworthy that we have never observed any other orientations for large crystals of the colloidal silica particles under investigation.

(d)Non-Space-Filling Crystal and the Long-range Attractive Interaction

On the basis of various experimental observations, we have been claiming the presence of a long-range attractive interparticle interaction in addition to a widely accepted repulsive interaction. The present USAXS study also provides convincing evidence for the attractive interaction. Unlike in

our previous scattering study, the USAXS work on the silica dispersion gave five order of diffraction, which indicates conclusively the existence of a three-dimensional lattice structure in the dispersion. The scattering peaks could be characterized by the lattice constant (3000 A). For bcc symmetry, the closest interparticle spacing ($2D_{exp}$) is given by $(3^{1/2}/2)x$ a to be 2600 A. At the given concentration, the average interparticle spacing ($2D_0$) is 2900 A [$(3^{1/2}/2)x\ (8\pi/3c)^{1/3}$ x R, where c and R are the particle concentration and particle radius.] Obviously $2D_{exp} < 2D_0$. This implies that particles, which are to be separated from each other by 2900 A in the absence of interaction, are brought together to 2600 A in the process of crystallization. Such a contraction has been reported not only by us but also by Kamenetzky et al. (Science, **263**, 207 (1994)). One of the simplest interpretation of this contraction is to accept an attraction between particles.

By simple arithmetic the single crystal occupies 0.72 [= $(2600/2900)^3$] of the total dispersion volume and the rest (0.28) must contain voids and/or free particles for the present case. Unfortunately, it is not possible to uniquely determine the size of the voids by a scattering method.

Needless to say, if the widely accepted repulsion-only assumption (the DLVO concept) is correct, we should observe $2D_{exp} = 2D_0$. This was not experimentally the case, however.

In our previous studies, it was concluded on the basis of single, broad X-ray diffraction peak for ionic polymer solutions or microscopic observation for latex dispersions that non-space-filling ordered structures coexist with disordered macroions (the two-state structure). This conclusion has often been questioned on the ground that the single broad peak is not necessarily reminiscent of ordered arrangements. The basis of this questioning can now be positively denied, since the conclusion is substantiated also by the several order of diffraction obtained by the USAXS measurements. In other words, the single, broad peak reflects ordered structures, though probably fairly highly distorted.

II. Positive Adsorption of Charged Latex Particles near a Like-Charged Glass Plate

It has been often noticed by a confocal laser scanning microscope that negatively charged latex particles were accumulated near a glass surface, which was believed to be negatively charged (See for example, see Figure 14 of a review article by Dosho et al. Langmuir **9**, 394 (1993)). Ito et al.(K. Ito, T. Muramoto, and H. Kitano, loc. cit.) reinvestigated the problem in a systematic manner.

The latex particle was styrene-styrenesulfonate copolymer latex (MSS-17, diameter 0.56 μm, charge density -5.5 $\mu C/cm^2$). The observation cell was made of a Pyrex glass tube with a cover glass glued to the bottom. Before being glued, the cover glass was dipped in concentrated sulfuric acid to clean the surface and was rinsed repeatedly with deionized water. The ζ-potential of the glass surface thus treated was conveniently determined from the electrophoretic velocity profile of charged latex particles dispersed in a rectangular cell made of the same materials as the cover glass. It was found out to be - 70 to -90 mV depending on

the added NaCl concentration in the range of 10^{-4} - 10^{-6}M. The velocity profiles were measured using a Laser Zee Meter Model 501. A reversed-type confocal laser scanning microscope LSM410 (Carl Zeiss) was used to count the number of particles as a function of the distance (z) from the cover glass.

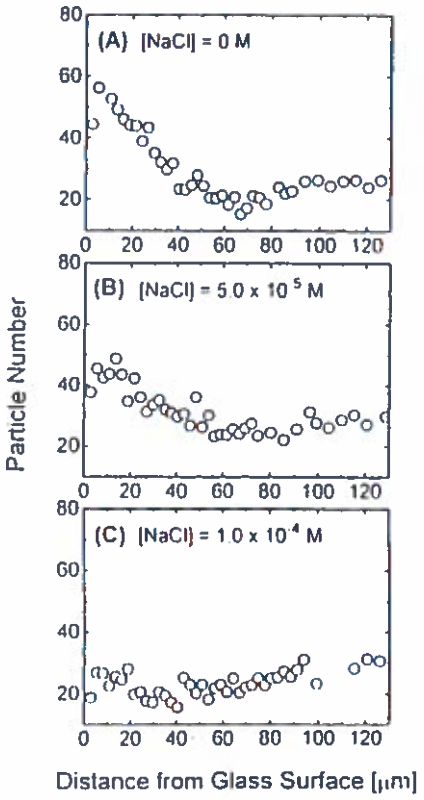

Figure 6. The number of particles as a function of distance from the cover glass: (A)deionized dispersion; (B)[NaCl] = 5.0 x 10^{-5} M; (C)[NaCl] = 1.0 x 10^{-4}M. [Latex]:0.065 vol %. Attempts were made to attain better particle images by adjusting the contrast so that the effective depth of focus was not fixed but in the range 2 - 3 μm. By using this value and the area covered, the average particle number was estimated to be 20 - 30.

The number of particles (N) in the observation area (37 x 31 μm^2) near the cover glass is shown as a function of z in Figure 6. In the deionized dispersion, the particle number in the vicinity of the interface (z: 5 - 10 μm) was larger than that in the interior by a factor of about 2 and decreased with z. Obviously positive adsorption took place. However, addition of salt decreased the adsorption and the particle distribution at [NaCl] = 10^{-4}M became homogeneous. The salt concentration dependence indicates that the adsorption is caused by electrostatic interaction between the particles and the plate. Similar measurements were carried out in a density-matched condition using heavy water, confirming that the observed effect was not due to gravitational sedimentation. It is highly plausible that the charged plate attracted the particle through the intermediary of counterions in between, which in turn attracted distant particles through the same mechanism.

Because both the particles and the plate were in focus at closer than about 2 μm, the particle distribution could not be determined in this range.

Though so far overlooked, such an electrostatic positive adsorption

is in complete contradiction with the standard double layer interaction theory, at least as far as the z range covered (5 - 100 μm) is concerned. As was mentioned above, a similar kind of positive adsorption was observed by Thomas et al. for a cationic micelle solution by using the neutron reflection study.

Publications from October, 1994 to April, 1995

(1) N. Ise and H. Matsuoka, "Repulsion-only Assumption or the Long-Range Attraction-Repulsion Assumption", Macromolecules, 27, 5218 (1994)

(2) N. Ise and M. V. Smalley, "Thermal compression of colloidal crystals: Paradox of the repulsion-only assumption", Phys. Rev. B. 50, 16722 (1994)

(3) T. Konishi, N. Ise, H. Matsuoka, H. Yamaoka, I. S. Sogami, and T. Yoshiyama, "Structural study of silica particle dispersions by ultra-small-angle x-ray scattering", Phys. Rev. B. 51, 3914 (1995)

(4) J. Yamanaka, N. Ise, H. Miyoshi, and T. Yamaguchi, "Experimental examination of the Booth theory on the first-order electroviscous effect in ionic colloidal dispersions", Phys. Rev. E. 51, 1276 (1995)

(5) K. Ito, T. Muramoto, and H. Kitano, "Positive adsorption of charged particles near a like charged glass plate", J. Am. Chem. Soc. 117, 5005 (1995)

(6) T. Konishi and N. Ise, "Ultra-small-angle x-ray Scattering Profile of colloidal silica crystal of four-fold symmetry", submitted.

Ostwald ripening of concentrated alkane emulsions.

Leon Bremer [1,2], Bruno De Nijs [1], Luc Deriemaeker [1], Robert Finsy [1]

Erik Geladé [2], Jacques Joosten [2]

Abstract.

Fiber optic dynamic light scattering (FODLS) is used to study the kinetics of ageing processes in emulsions of n-alkanes stabilised by a surfactant. The method is particularly useful for this aim because it enables measurements in concentrated emulsions. Complications that may occur in traditional DLS due to the extreme dilution, like solubilisation of the particles in the medium can be easily avoided in this way.

Experimental results show that the main ageing process is Ostwald ripening. The results are in agreement with theoretical predictions based on the Lifshitz-Slyozov-Wagner (LSW) theory as far as it concerns the relation between the molecular solubility of the n-alkanes (in the aqueous phase) and the Ostwald ripening rate. This illustrates that the main rate determining factor is the molecular diffusion of the alkane molecules through the continuous (aqueous) phase. The Ostwald ripening rate is affected by the concentration of surfactant but is in all situations higher than expected from LSW.

1 Dr. Ir. Leon Bremer , Ir. Bruno De Nijs , Ing. Luc Deriemaeker,
Prof. Robert Finsy
Theoretical Physical Chemistry, Vrije Universiteit Brussel
Pleinlaan 2 - B - 1050 Brussel, Belgium.

2 Dr. Ir. Leon Bremer, Dr. Erik Geladé, Dr. Jacques Joosten
Department of Physical Analytical and Computational Chemistry, DSM-Research,
P.O. Box 18, 6160 MD Geleen, The Netherlands

Contribution to the International Polymer Colloids Group Newsletter

by

Haruma Kawaguchi

Department of Applied Chemistry, Keio University
3-14-1 Hiysohi, Yokohama 223 Japan
TEL: +81-45-563-1141 ext.3456 FAX: +81-45-562-7625
e-mail: polymer1@applc.keio.ac.jp

Precipitation Polymerization to Prepare Monodisperse Hydrogel Microspheres

Precipitation polymerization generally results in the formation of coagulum but, in rare cases, gives stable monodisperse microspheres. Polymerization of N-isopropyl-acrylamide and crosslinker in hot water, developed by Pelton, et al. (Colloids Surfaces (1986) 20, 247), is such a rare case to form monodisperse, submicron microspheres. No additional stabilizer was necessary to prepare them.

Polymerization of acrylamide (AAm) and methylenebisacrylamide (MBAAm) in ethanol formed coagulum, but addition of methacrylic acid (MAc) to the polymerization recipe changed the situation drastically and resulted in the formation of monodisperse microspheres. In this precipitation polymerization system, MAc sequences seem to serve as a stabilizer formed *in-situ* (H.Kawaguchi, et al., Polym. International, (1993) 30, 225). Because of the difference in polymerizability among three monomers, the composition of growing microspheres changed every moment in the course of polymerization. Owing to this, the swellability of growing microspheres decreased in the initial stage of polymerization, took the minimum around 40% conversion and then increased in the later stage of polymerization as shown in Fig. 1.

The inner structure of the microspheres was uneven and included heterogenuity in terms of crosslink density. The details of microstructure is now being studied by SAXS in cooperation with Professor K.Kajiwara's group, Kyoto Institute of Technology (Fig. 2). The heterogenuity became less distinct with increasing MBAAm fraction in monomer. The degree of equilibrium swelling of these hydrogel microspheres changed discontinuously around the MBAAm fraction of 0.08 - 0.10.

When p-nitrophenylacrylate was copolymerized with MAc, (AAm) and MBAAm in ethanol or isopropanol, we could obtain monodisperse, reactive hydrogel microspheres. The microspheres were converted to amphoteric hydrogel microspheres by reacting their active ester groups with diamine or polyamines and exhibited an interesting response to pH (M.Kashiwabara, et al., Colloid Polym. Sci., in press). Further works are now in progress.

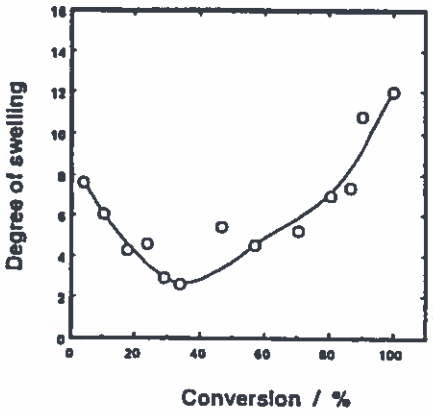

Fig. 1 Dependence of degree of swelling on conversion.

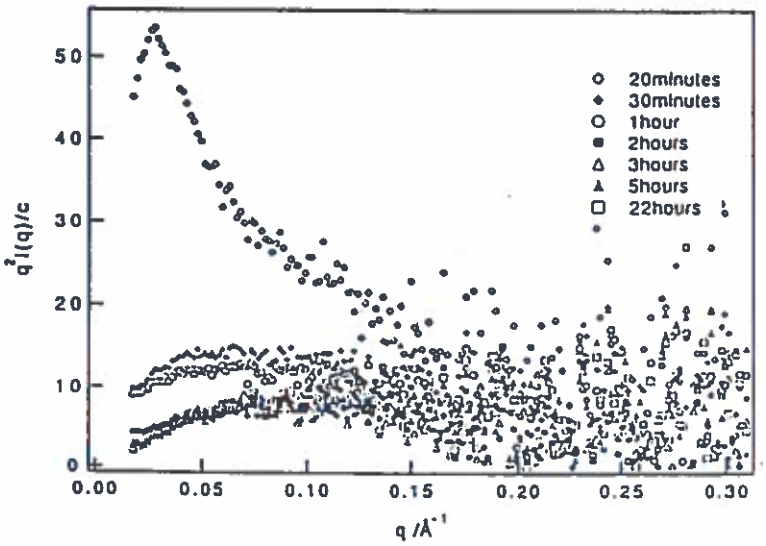

Fig. Kratky plots of hydrogel microspheres in water at various conversions.

Ph.D. Theses from H.K. group (March, 1995)

Yukio INOMATA

"BIOSEPARATION USING AFFINITY LATICES"

Abstract

First, latex particles suitable for a bioseparator were designed and prepared. They should be little susceptable to nonspecific adsorption of proteins and have reactive sites to bind biospecific compounds. Polystyrene-core / poly(glycidyl methacrylate)-shell particles satisfied these conditions. Then, sequence-specific DNAs, fragment of a transcription factor, RGDS, and a kind of hormone were immobilized onto the particles to collect and purify the respective complementary components. In DNA immobilization, double-stranded (ds) DNAs having single-stranded (ss) chain ends of suitable length could be effectively bound to the particles via coupling between amine groups on ss-part of DNA and epoxy groups on the particle surface.

Bioseparation was carried out by a batch-wise operation. Namely affinity latex particles collected target compounds specifically through bioaffinity and were separated from supernatants. The specifically collected compounds were then released from the particles to a fresh medium by adding salts or others, warming, etc. The bioseparation uisng affinity latices was found to be superior to column chromatography in terms of purification efficiency and processability, especially in ultra-minute scale of purifications.

References

1 Y.Inomata, H.Kawaguchi, M.Hiramoto, T.Wada, and H.Handa,
Direct purification of multiple ATF/E4TF3 polypeptides from HeLa cell crude nuclear extracts using DNA affinity latex particles.
Anal. Biochem., 206, 109-114 (1992)

2 Y.Inomata, T.Wada, H.Handa, K.Fujimoto, H.Kawaguchi,
Preparation of DNA-carrying affinity latex and purification of transcription factors with the latex.
J. Biomater. Sci., Polym. Ed., 5, 293-302 (1994)

3 Y.Inomata, Y.Kasuya, K.Fujimoto, H.Kawaguchi,
Purification of membrane receptors with peptide-carrying affinity latex particles.
Colloids Surfaces B. Biointerfaces, in press.

4 Y.Inomata, H.Kawaguchi, T.Wada, H.Handa,
Improvements in DNA-carrying affinity latex for the purification of transcription factors.
Kobunshi Ronbunshu, 48, 335-340 (1991) (in Japanese)

Toshifumi SHIROYA

"APPLICATION OF POLYMER-PROTEIN HYBRIDS"

Abstract

This article is concerned with the preparation of polymer-protein hybrids and their application to biotechnology. The polymers included water-soluble, thermosensitive polymers, thermosensitive polymeric microspheres and rigid polymeric microspheres. The proteins used in this study were enzymes, trypsin and peroxidase, and a transcription factor. In the study on trypsin-immobilized poly(N-isopropylacrylamide) particles, the dependence of enzymatic activity on temperature was focused on. Relative activity droped down above the lower critical solution temperature of PNIPAM. This temperature-dependence was suppressed when the enzyme was immobilized on the particles via hydrophilic spacers. Protein-carrying affinity latex particles are one of the hybrids. A kind of transcription factors was immobilized onto microspheres composed of terpolymer of styrene, glycidyl methacrylate and methylenebisacrylamide, through a hydrophilic spacer, to separate and purify transcription factor Ⅱ A. The spacer was necessary for effective separation.

References

1 D.Ma, H.Watanabe, F.Mermelstein, A.Admon, K.Oguri, X.Sun, T.Wada, T.Imai, T.Shiroya, D.Reinberg, H.Handa,
Isolation of a cDNA encoding the largest subunit of TF Ⅱ A reveals functions important for activated transcription.
Genes & Dev., 7, 2246-2257 (1993)

2 T.Shiroya, M.Hatakeyama, K.Fujimoto, H.Watanabe, T.Wada, T.Imai, H.Handa and H.Kawaguchi,
J. Chromat., Submitted.
3 T.Shiroya, M.Yasui, K.Fujimoto, H.Kawaguchi,
Control of enzymatic activity using thermosensitive polymers,
Colloids Surfaces B. Biointerface (in press)
4 T.Shiroya, N.Tamura, M.Yasui, K.Fujimoto, H.kawaguchi,
Enzyme immobilization on thermosensitive hydrogel microspheres.
Colloids Surfaces B. Biointerfaces (in press)

Other recent papers by H.K. Group

* T.Kato, K.Fujimoto and H.Kawaguchi,
Permeation control by thermosensitive shell layer of submicron microspheres
Polymer Gels Networks, 4, 307-313 (1994)
* K.Makino, S.Yamamoto, K.Fujimoto, H.Kawaguchi and H.Ohshima,
Surface structure of latex perticles covered with temperature-sensitive hydrogel layers.
J. Colloid Interface Sci., 166, 251-258 (1994)
* Y.Urakami, Y.Kasuya, M.Miyamoto, K.Fujimoto and H.Kawaguchi
Phagocytosis of microspheres with modified surfaces.
Colloids Surfaces B: Biointerfaces, 3, 183-190 (1994)
* R.Yoda, S.Komatsuzaki, E.Nakanishi, H.Kawaguchi and T.Hayashi,
Preparation and properties of A-B-A type block copolymer membranes consisting of poly(N-hydroxypropyl-L-glutamine) as the A component and polyisoprene as the B component.
Biomaterials, 15, 944-949 (1994)

INTERNATIONAL POLYMER COLLOIDS GROUP NEWSLETTER

Contribution from the Department of Chemical Engineering,
Yonsei University, 134, Shinchon-dong, Sudeamoon-ku, Seoul, Korea.

Reported by Jung-Hyun(Jay) Kim

Current researches accomplished in our lab. include: (1) The Controlled Agglomeration Mechanism of S/B Latex by Carboxylated Model Colloid (2) The Morphology of PB/PMMA Structured Latex by Direct Emulsification Method (3) Simulation of Monomer Addition Rate for Prevention of Composition Drift in Emulsion Copolymerization. Some of the results were summarized in the following contributions.

The Controlled Agglomeration Mechanism of S/B Latex by Carboxylated Model Colloid

W. C. Shin, J. H. Kim

The agglomeration mechanism of S/B latex by carboxylated model colloids has been investigated. It was found that the agglomeration capability of the agglomerating agent was proportional to its hydrophilicity, that is, the stronger is the hydrophilicity of the agglomerating agent, the larger is the size of the agglomerated S/B latex particle. The origin of the hydrophilicity lies in the dissociation of the polymer chain of the acrylic acid polymerized onto the surface of the agglomerating agent. The hydrophilicity of the agglomerating agent was adjusted by the amount of acrylic acid copolymerized onto its surface and the pH of the medium. The driving force behind agglomeration phenomena is the compressive osmotic pressure between the hydrophilic agglomerating agent and the S/B particle.

Table. Agglomeration results

	Zeta Potential(mV) of Agglomerating Agent		Agglomerated S/B Particle Size, D_n(nm)	
	AGG1 (pH 2.1, 189 μC/cm^2)	AGG2 (pH 2.2, 110 μC/cm^2)	AGGD1	AGGD2
pH 9	-65	-55	507	347
pH 10	-60	-54	470	321
pH 11	-56	-43	415	317
pH 12.2	-53	-40	399	284

※ S/B particle size : 103nm
AGGD1 : S/B latex agglomerated by AGG1(85nm, 189 μC/cm^2)
AGGD2 : S/B latex agglomerated by AGG2(74nm, 110 μC/cm^2)

Reference :

1. Igaraci utaka, Japan, Pat., No., 61-260791, (1986)
2. Robert J. Hunter, "Foundations of Colloid Science", 2nd Ed., p. 483-484, Oxford Univ. Press, New York, (1989)
3. Francosie Candau, Ronald H. Ottewill, "An Introduction to Polymer Colloids", p. 153, Kluwer Academic Publishers, (1990)
4. S. Asakura, F. Oosawa, J. Polym. Sci., Vol. 33, 183, (1958)
5. A. Elaissari, E. Pefferkorn, J. Colloid Interface Sci., Vol. 141, 522, (1991)
6. E. Pefferkorn, A. Elaissari, J. Colloid Interface Sci., Vol. 138, 187, (1990)

The Morphology of PB/PMMA Structured Latex by Direct Emulsification Method

Y. J. Suh, J. H. Kim

One of the disadvantages of thermoplastic material is the low impact strenght. Many kinds of elastomer were used as impact modifier to improve this defect. But their impact strenght was declined rapidly when used outdoors. For the solving of this problem, it was suggested that elastomer was exchanged by the core/shell structured polymer. In this research, the direct emulsification method was used to control the particle sizes of the cores, and the amounts of the emulsifier at the direct emulsification were changed to control the PB/water interfacial tension. And the final structured latex was prepared by the seed polymerization. The morphology of the latex was predicted by modeling. The variables were particle size and PB/water interfacial tension. According to the TEM of the final latex, the seeds which had smaller than 100nm became structured particles whereas the seed larger than 100nm were almost seperated. This result almost agreed with the model.

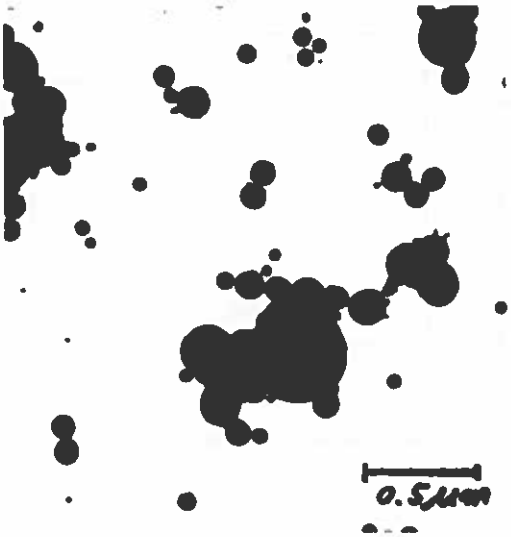

Fig. TEM of the PB seed

Fig. TEM of the PB/PMMA structured latex.

Reference :

1. Vanderhoff et al., U.S. Patent 4,177,177 1979
2. Y. G. J. Durant & J. Guillot, Coll. & Polym. Sci. , 271, 6, 1993
3. Y. C. Chen, Ph. D. Dissertation, Lehigh University, 1991
4. J. L. Lando and H. T. Oakley, J. Coll. Interf. Sci., 25, 526 (1967)

Simulation of Monomer Addition Rate for Prevention of Composition Drift in Emulsion Copolymerization

I. W. Cheong, J. H. Kim

In conventional emulsion copolymerization, particles with homogeneous composition cannot be produced because of different solubility and reactivity of monomers. During the process, composition between centre and surface of particle varies largely. To prevent composition drift, the feed rate of monomer which has good reactivity must be controlled. In this studies, the monomer feed rate using semi-starved condition was simulated to obtain a homogeneous composition particle and the main parameters effect on the feed rate control was investigated. The main parameters are reactivity ratio, average number of radical per particle and the number of reaction loci. The monomer partitioning is determined by a thermodynamic balance between the gain of interfacial free energy upon swelling and the loss of free energy due to polymer-monomer mixing. The consumption rate of monomer is determined by the emulsion kinetics.

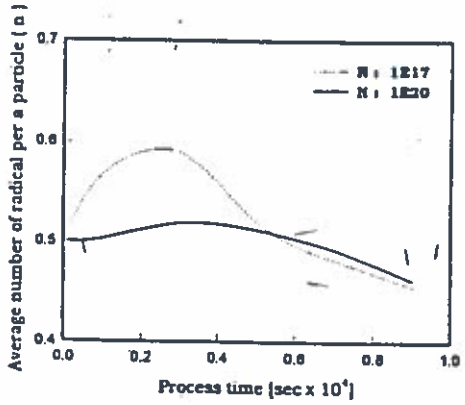

Fig. Average number of radical vs. process time

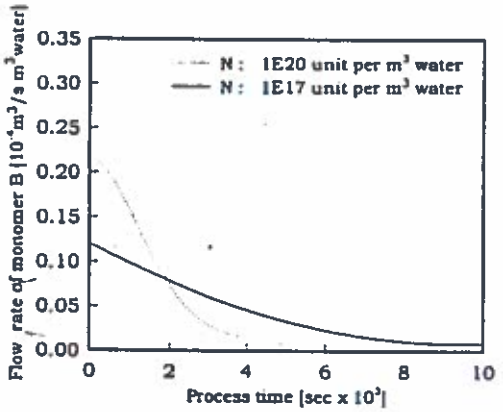

Fig. Flow rate vs. process time (A : B = 50 :50)

References :

1. G. Arzamendi & J.M.Asua, J. Applied Polymer Science, Vol.38, 2037 (1989)
2. G. H. J. Van Doremaele, H. A. S. Schoonbrood, J. Juria, and German, J. Applied Polymer Science, Vol.45, 957-966 (1992)
3. Shinzo Omi, Koji Kushibiki and Mamoru Iso, Polymer Eng. & Sci, March, 1987, Vol.27 No.6
4. Harold. A. S., etc., J. Applied Polymer Science, Vol.49, 2029-2040 (1993)

Contribution to IPCG Newsletter

by

Dr. Peter A. Lovell

Polymer Science & Technology Group, Manchester Materials Science Centre
University of Manchester & UMIST, Grosvenor Street
Manchester, M1 7HS, United Kingdom

For this issue I have decided to give brief outlines of current projects.

Toughening Unsaturated Polyester Resins using Multi-Phase Particles

Research Student: Mr. O.M. Munyati
Collaborator: Dr. R.J. Day
Sponsor: The Beit Trust

Following on from my work on the use of multi-phase particles for toughening of PMMA and epoxy resins, this project is concerned with similar studies into toughening of polyester resins. The resins are extensively used in composite materials but suffer from poor toughness. Although the ability to toughen these systems is greatly restricted by the high crosslink density of the cured resins, small increments in toughness, if carried through to the composites, are considered to be valuable by the industry. The principal objective of this project has been to prepare and evaluate three-layer toughening particles in a commercial unsaturated polyester resin. Differences in particle size, morphology and chemistry are being probed and the effects of the particles upon the micromechanics of deformation investigated.

Preparation of Particles for Toughening Styrene-Acrylonitrile Copolymer (SAN)

Research Workers: Dr. Y. Yang and Mr. S. Steenbrink
Collaborator: Dr. R.J. Gaymans (Twente University, The Netherlands)

The aim of this collaborative project is to investigate the effect of rubber particle diameter upon the toughness of rubber-toughened SAN. The project has involved the preparation of two-layer toughening particles comprising crosslinked poly(n-butyl acrylate) rubber cores and poly(methyl methacrylate) shells. Four types of particle have been prepared with rubbery core diameters in the range 0.15 - 0.45 μm. The particles are being blended with SAN and the effect of rubbery core diameter on toughness and deformation mechanisms studied at Twente University, where there is considerable experience in the mechanical characterisation of SAN.

High-Performance and Environmentally-Friendly Adhesives

Research Assistant: Mr. J. Garrett
Sponsor: EC Brite Euram Project joint with Jowat, Lobers & Frank Gmbh (Germany), Evode Ltd. (UK) and the University of Bielefeld (Germany)

This collaborative research project began about 18 months ago and is concerned with research into high-performance adhesives, environmentally-friendly adhesives as replacements for existing solvent-based systems and alternative crosslinking mechanisms and manufacturing technologies. Our part of the programme is focused on research into reactive acrylic latexes as environmentally-friendly replacements for solvent-based contact adhesives.

A Study on Microgel Dispersions

W.Mächtle, G.Ley, J.Streib
BASF AG, 67056 Ludwigshafen, Germany

Fourteen PnBMA-latices have been made by emulsion polymerization with particles increasingly crosslinked by copolymerizing up to 10% by weight of methallylmethacrylate (MAMA).

First, all aqueous dispersions were well characterized using the different techniques of static (SLS) and dynamic light scattering (DLS) and of analytical ultracentrifugation (AUC) determining particle size and size distributions, particle density and density distributions, sedimentation and diffusion coefficients. From these measurements it was shown that each sample contains nearly monodisperse particles of about 60 nm diameter and uniform particle density which increases with increasing MAMA concentration.

Then we transfered these particles into tetrahydrofuran (THF), which is a good solvent for PnBMA by stirring a small amount of the original latex into a large excess of THF. We characterized the suspensions in THF using the same techniques of LS and AUC respectively. In the solvent particles without or with a low MAMA content dissolved completely into single solvated coiled polymer chains with a mean molecular mass Mw of about 7*10**5. Particles with high MAMA content are only swollen by THF. Its molecular mass is about 7*10**7 and within the limits of error equal to that of the particles in water. This indicates that all polymer chains in each latex particle are bond to the network of the microgel particle. At intermediate MAMA concentrations both swollen microgel particles and molecularly dissolved polymer chains are observed. This is possible because the appearence of both species in the Schlieren-optics of the AUC is very different: turbidity bands for microgels and Schlieren-peaks for dissolved macromolecules. The swelling ratio q of the microgels (which is defined as its volume in THF devided by that in water) decreases strongly with increasing MAMA-content characterizing a continuous transition from only weakly to very densily crosslinked microgels. The values of q determined independently from the AUC and DLS measurements are in good agreement. The microgel formation can be described satisfactorily by FLORYs theory of network formation from preformed linear polymer chains.

Also the hydrodynamic behaviour of the microgels as characterized by the quotient of the radius of gyration Rg (SLS) and the hydrodynamic radius Rh (DLS) clearly shows the transition from coils of linear chains (about 1.6) over "hairy balls" (intermediate) to "hard spheres" (0.78). For quantification of this transition the strong decrease in the concentration dependence of the sedimentation coefficient seems to be useful.

Modelling of Single Polymer Aggregates in Solution.

O.A. Evers, G. Ley, E. Hädicke
BASF AG, 67056 Ludwigshafen, Germany

At the Gordon Conference on Polymer Colloids in 1993 we presented a Poster on the modelling of single polymer dispersion particles. In the SCHEUTJENS-FLEER-model applied all possible conformations of the polymer chains on a spherical lattice are evaluated using a self-consistent mean field method. The energetic interactions are accounted for by a FLORY-HUGGINS type approach. Our model allows for the self-consistent computation of the equilibrium segment densities and the equilibrium segment potentials in space through a set of non-linear equations in both variables taking into account the constraints arrising from the segment connectivities in the polymer chains. Only nearest neighbor interactions are taken into account using the FLORY-HUGGINS-Parameter Chi(xy) defined as the energy change in units of kT associated with the transfer of a segment of type x from a surrounding of pure x into a surrounding of pure y. The spherical lattice consists of concentric layers of lattice sites which are occupied by either a polymer segment or a solvent molecule. Within each layer we assume a homogeneous distribution of the various segments and solvent molecules: a mean field approximation. Therefore, inhomogeneities are taken into account in one dimension only, i.e. the radial direction of the particle.

In the meantime details of the model have been published elsewhere [1]. The model gives detailed information on the inner structure of dispersed particles e.g. enrichment of chain ends, shorter polymer chains and (solvated) end groups in the interfacial layers. It showed further that in monomer-polymer-particles there is no extended concentration gradient but a distinct enrichment of monomer in the thin outer "hairy surface layer" of the particle (a few nanometers only). The monomer seems to function as an envelope for the chain ends shielding them from the energetically unfavorable contacts with the dispersion medium [2].

For composite particles made of two chemically different polymers the model predicts a distinct internal structuring of the particle even for mixtures of fully compatible polymers if there is any difference in their interaction with the solvent. In this case the inner structure of the polymer strongly depends on particle size. If the surface of the particle is saturated with the "shell-forming" polymer, the thickness of the "shell" seems to be determined mainly by the radius of gyration of the "core-forming" polymer. If the difference in the interaction of the polymer segments with the solvent increases, gross demixing of the compatible polymers is found like in the case of incompatible polymers. This is mostly due to the increasing solvent concentration in the "shell-forming" polymer.

If the polymers are incompatible particles with a distinct "core-shell-structure" are formed due to gross demixing. Again the "shell" is formed by the polymer with the lower repulsive interaction with the solvent. Its thickness is determined mainly by the fraction of the "shell-forming" polymer. The thickness and the structure of the

interpenetration region between "core" and "shell" is determined by the interaction of the polymer segments, the chain length of the polymers and its polydispersity, the difference in the interaction energy with the solvent and, consequently, by the degree of swelling of the "shell" by the solvent.

But remember: In our simulations the formation of a "core-shell-structure" of the particle is enforced by the superimposed symmetry of the spherical lattice used and the mean field assumption for its layers! Therefore, despite we think that its predictions on the segment size level (e.g. of the degree of demixing, the concentration profiles and the fine structure at the interfaces) already are close to reality, our model cannot predict the gross geometrical arrangement of the different polymer "phases" gouverned by macrophysics (e.g. interfacial tensions, Youngs-equation) which - together with a vast number of non-equilibrium structures - may give rise to the "particle zoo" found in numerous different polymer dispersion systems. In order to improve the fit of the concentration gradients to reality we are currently developing a "lattice-free" model using density funtionals.

[1] O.A.Evers, G. Ley, E.Hädicke, Macromolecules 26 (1993) 2885

[2] O.A.Evers, E.Hädicke, G.Ley, Colloids and Surfaces A 90 (1994) 135

Contribution to the International Polymer Colloid Group Newsletter May 1995

Voltammetric metal titration of particle dispersions.

Jeannette H.A.M. Wonders*, Herman P. van Leeuwen and Johannes Lyklema.
Dept. of Colloid and Physical Chemistry, Dreijenplein 6, 6703 HB, Wageningen, The Netherlands
E-mail: Wonders@fenk.wau.nl Fax: +31.8370.83777 Tel: +31.8370.84100

Keywords: LATEX, HEAVY METAL

Introduction.

Characterization of surface groups by voltammetric titration is more complex than often assumed [1]. There are a number of complications which affect the relationship between the measured voltammetric current and the metal speciation in solution. A primary complicating factor is the difference between the diffusion coefficients of the free metal and the complex species. The work by de Jong *et al.* [2, 3, 4] has dealt with this problem, especially for the case of a large excess of ligand over metal. For practice the problem is that during a titration, the metal-to-ligand ratio changes and this means that the electrochemical lability changes as well. Hence, homogeneous kinetics may be important in one part of the curve, but not applicable in another. Likewise, a mean diffusion coefficient $\overline{D}$ may be operational for only a part of a titration curve. These features lead us to consider the changes of kinetics and the validity of$\overline{D}$ in the course of a titration.

The metal complexing ligands to be titrated are core-shell latices (coded as AOY types) and a polystyrene latex without such a shell (coded as AKB 20). For details about these latices we refer to a forthcoming thesis and papers based on it [12]. The results in terms of metal-binding affinities and capacities will be compared to those obtained from the potentiometry and conductometry.

Theory.

We shall mainly base our considerations on the case where metal-binding sites S are titrated with the electroactive metal ion M, forming the electroinactive complex MS (charge signs are omitted for clarity):

$$M + S \underset{k_d}{\overset{k_a}{\rightleftharpoons}} MS \qquad (1)$$

The rate constants k_a (surface complex formation) and k_d (surface complex dissociation) are related to the stability constant K, via $k_a/k_d = K$. Although our treatment is valid for any combination of values for the diffusion coefficients D_M and D_{MS}, the typical situation for M/particle systems is that $D_{MS}(\approx D_S) << D_M$.

Region A, large excess of sites to metal ions

General

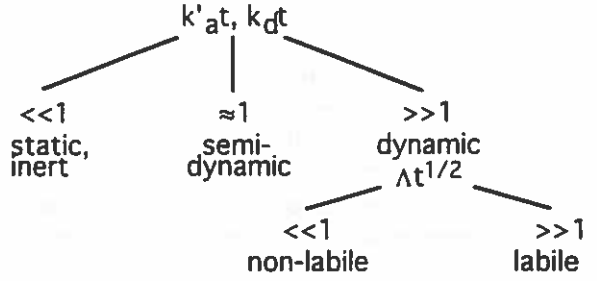

Figure 1. A schematic representation of the characteristic regimes of metal complex systems. Further explanation in text.

In the region of low metal-to-site ratios, the site concentration is approximately constant. The complexation reaction can then be considered as quasi-monomolecular:

$$Kc_S = K' = k'_a/k_d = c_{MS}/c_M \qquad (2)$$

where $k'_a = k_a c_s$. The chemical kinetic constants k'_a and k_d are key parameters since the voltammetric experiment is of a dynamic nature. For a metal complex system, containing different metal species with unequal diffusion coefficients, the ensuing criterion for voltammetric lability has been formulated on the basis of a rigorous theory [3, 4]. For a dynamic system, i.e. with $k'_a t$, $k_d t >> 1$, it says:

$$\Lambda t^{1/2} >> 1 \qquad (3a)$$

where $$\Lambda t^{1/2} = \frac{J_{diff}}{J_{kin}} = \frac{k_d^{1/2}\varepsilon^{-1/2}(\varepsilon^{-1} + K')}{K'(1+K')^{1/2}} t^{1/2} \qquad \text{and } \varepsilon = D_{MS}/D_M \qquad (3b,c)$$

The system is labile, when the lability criterion (equation 3a) is obeyed. A labile system is featured by: $\phi(t)$=constant and $\Delta E(t)$=constant. For a non-labile system, the lability criterion $\Lambda t^{1/2} << 1$ (Fig 1) and both $\phi(t)$ and $\Delta E(t)$ are proportional to $t^{1/2}$. ϕ is the normalized current and ΔE the shift of the peak potential (with respect to the blank). The derivation of Equation 3 is based on comparing the flux due to production of free metal from dissociation of the complex (J_{kin}) with the flux for semi-infinite linear diffusional transport to the electrode surface (J_{diff}). Equation (3) shows that metal complexes are only labile for certain ranges of values of (a) the rate constants for association/dissociation of the complex, (b) the diffusion coefficients of the metal complex and the free metal, and (c) the time scale of the dynamic experiment.

Inert or static complexes

In contrast to the dynamic case, the inert or static complex is determined by very low kinetic rates: $k'_a t$, $k_d t << 1$. The current density directly reflects the concentration of free metal in solution, irrespective of whether the complexation reaction is at equilibrium or not:

$$\phi(t) = c^*_M / c^*_T = (1+K')^{-1} \qquad (4)$$

with $c^*_T = c^*_M + c^*_{MS}$, all in the dimensions of volume concentrations. Since the complex does not contribute to the current, there is no potential shift.

Labile complexes

Electrochemically labile complexes are very common in environmental systems such as heavy metals in humic acids [5, 6]. Voltammetric speciation on the basis of analysis of currents is only possible by the grace of the difference between the diffusion coefficients of the labile complex and the free metal. The simultaneous diffusion of MS and M towards the electrode surface gives rise to a diffusion layer with a thickness that is intermediate between those for pure MS and pure M. It has been explained that a mean diffusion coefficient $\overline{D}$ is operative [7, 8, 9]:

$$\overline{D} = \frac{c^*_M}{c^*_T} D_M + \frac{c^*_{MS}}{c^*_T} D_{MS} \qquad (5)$$

For the case of semi-infinite linear diffusion, the response of a labile system obeys the general proportionality:

$$I \propto c^*_T \sqrt{\overline{D}} \qquad (6)$$

where I is the current. The situation described by equation (5) is only achieved if the number of conversions of M into MS and vice versa is much higher than unity, *i.e.* if the equilibrium is sufficiently dynamic. There is a shift in potential which is independent of the time. Note that in the case of a labile system, a practically immobile particle, forming labile complexes, can contribute greatly to the current, thereby drastically modifying the measured signal. Physically, this is explained by the fact that inside the diffusion layer the complex produces free metal ions as a result of the adjustment of its concentration to the local free metal concentration.

Other types of complexes
As can be seen in the schematized representation, the labile and the inert complexes are not the only types, which occur in nature. The analysis of a titration curve for such systems is complicated. More information can be found in a forthcoming paper and thesis [12].

It is repeated to note that in the course of a titration the lability of a given complex is not fixed. The site concentration, while still being in excess over the total metal concentration, decreases upon addition of metal. This means that k'_a and K' decrease as well and, according to criterion (3), the lability increases. Thus, on going from region A to region B in a titration curve, the slope may increase for purely kinetic reasons. For practice the lability change in the initial region A has no consequences, since the extent of change is small there.

Regions B and C, around and beyond the equivalence point

Our findings concerning the determination of the equivalence point for a voltammetric titration curve are summarized in Table 1. The two extreme cases are clear and simple: with an inert complex one has to extrapolate to the c_T^*-axis, whereas with a strong, labile complex one has to take the intersection point found by double extrapolation. For the different cases in between these two, the procedure becomes more complicated, if not hopeless.

Table 1.
Evaluation of the equivalence point in a voltammetric metal complex titration

Nature of the complex	Procedure
Inert	Extrapolation to c_T^*-axis (b in Figure 1)
Quasi-labile	None (existing extrapolation procedures all yield erroneous results)
Labile: strong ($Kc_S^* >> D_M/D_{MS}$)	Intersection of double extrapolation (a in Figure 1)
Labile: intermediate and weak	Interpretation only possible if D_{MS} is known (extrapolation procedures fail)

Results and Discussion.

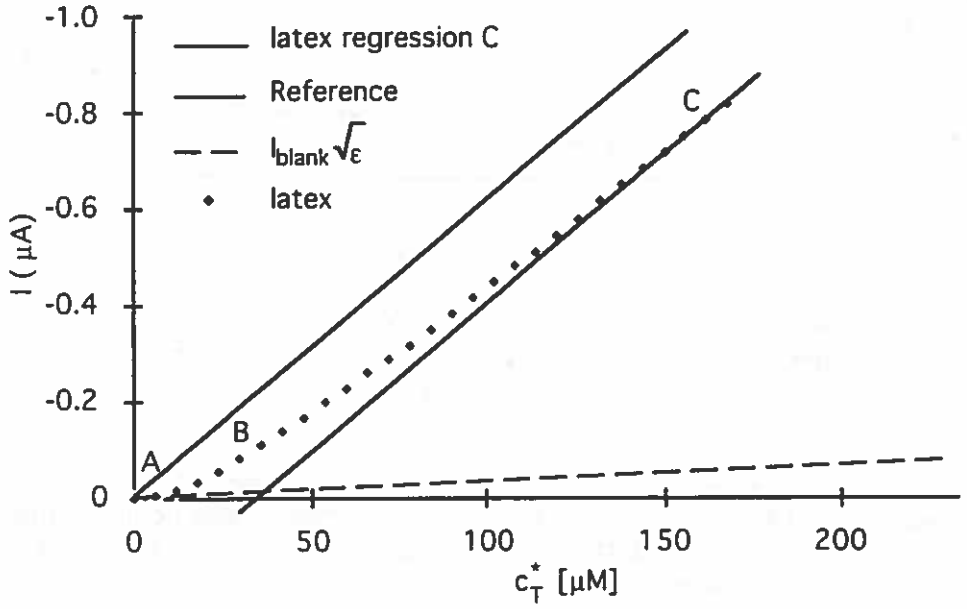

Figure 2. Titration of latex AOY 5 dispersion in 25 ml 0.01 M KNO_3 with cadmium(II). The pH was 7.67 and the degree of dissociation 0.95.

We observe that the titration curves reach the slope of the blank, albeit for quite an excess of cadmium. To find the cadmium bound in a labile complex, we should extrapolate from region A and extrapolate from region C. As shown by Figure 2, extrapolation using region A is not possible. We studied region A in more detail. In region C the peak potential gradually returns to the blank value. The behaviour of the peak potential is also regular. As expected, DPP peaks in region A and B shifted towards negative potentials compared to the blank.

Region A
We examined region A more closely by performing separate experiments in which more latex and a lower concentration of metal is used. In this way it is possible to see whether the complexes are labile, by checking that $\phi > \sqrt{\varepsilon}$ and that there is a shift in the peak potential towards negative direction (ΔE). The quantities ϕ and ΔE should be independent of the pulse time. This has been confirmed for all latices using different voltammetric techniques. All latices form labile complexes, except AKB 20 at high pH. Further, consistency of the stability constants from the shift of potential with the ones from the normalized current was verified.

In contrast to the results for the core-shell latices, the current measured for latex AKB 20-complexes at pH 6.5 is lower than the minimum value for labile complexes (Figure 4). Only for a pH lower than 6.1, the current exceeds the minimum. This complex certainly does not appear to be labile in region A, in correspondence with earlier findings [10, 11]. DPP peaks for AKB 20 complexes gave a potential shift compared to the blank. These complexes indeed are neither labile nor inert.

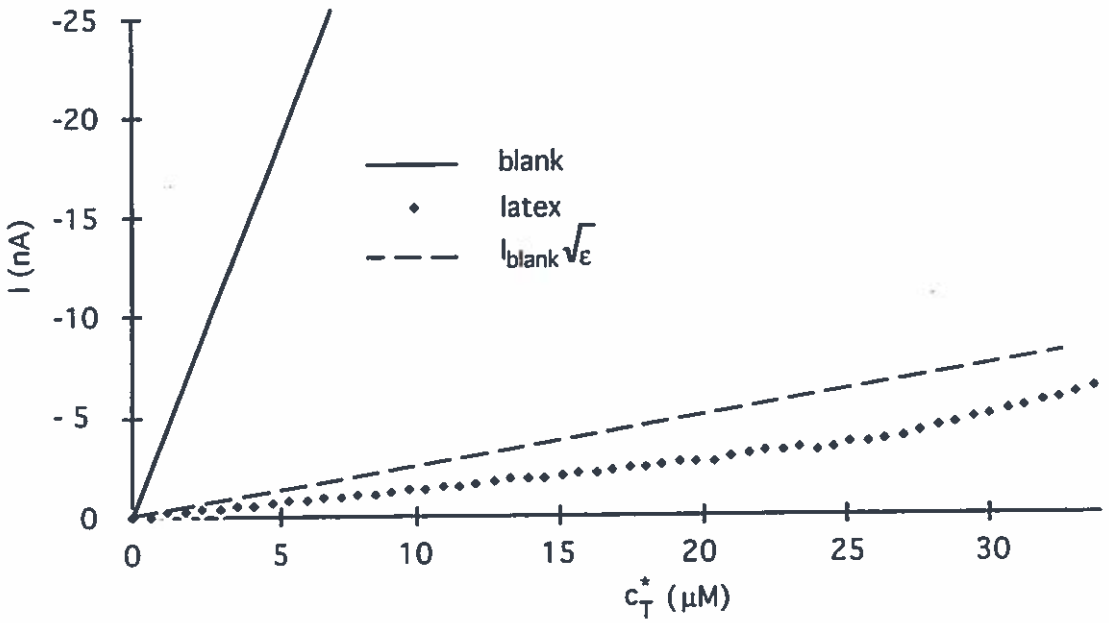

Figure 4. Voltammetric titration of latex AKB 20, dispersed in 0.01 M KNO_3 with cadmium(II) under excess of sites. The pH of the dispersion was 6.5±0.05 and the degree of dissociation 0.10. c_T^* is the concentration of total cadmium(II) in dispersion. .

Complete titration curves
Titration measurements were performed at a pH of 8-8.5, which is the limit for determining cadmium(II) with DPP. For all latices, the peak shifts towards a less negative potential as more metal ions are added. This is due to an increasing ratio of free over bound metal ions. No flocculation of latices was observed.

For systems proven to be labile, we treated the results as described in the theoretical section. These amounts are given for each latex in Table 2. Furthermore, Table 2 reflects the amount of deprotonated surface groups, determined using the amount of hydroxide added and the pH.

The slope of the curve in region A of the metal titration of latex AKB20 appears almost equal to zero. This system is not labile, but quasi-labile or perhaps semi-dynamic. It may be labile in region C. Anyway, we took the intercept of the regression line drawn in Region C with the x-axis as an estimate of the minimum amount of metal bound (Table 2). To find the amount of cadmium complexed for a similar, but labile system, the amount of cadmium complexed given in Table 2 would have to be multiplied by $(1-\varepsilon^{1/2})^{-1}$, a factor which for this system is equal to 1.069. We are not stating that the "real" amount is necessarily somewhere between these two values, but it can be seen that ε is an impression of the error's magnitude caused by incorrect treatment of the voltammetric titration results. For the present system, ε is not too big, hence the error cannot be huge.

For all latices, the amounts of surface groups which bind cadmium(II) are lower than the total amounts of groups which bind protons as determined by conductometry. Even if we use a binding ratio of 1:2 for cadmium, the amounts are lower. When we compute the ratio (ν) of cadmium(II) bound by (charged) carboxylic groups for the core-shell latices using the data of latex ARC 24, we find that these ratios are equal to the results for latex AKB 20. Hence, we can conclude that the binding capacities for cadmium of carboxylic groups and sulphonic groups are roughly 80% and 30%, using a binding ratio of 1:2. This ratio may not be a strict limitation. It is very likely that cadmium(II) partially binds to surface groups of latex according to the one to one ratio and partially according to the one to two ratio. The binding is discussed in more detail in the forthcoming thesis [12].

Table 2. Amounts of bound cadmium(II) determined by voltammetric titration of various latices together with some of their data obtained from potentiometry and conductometry.

latex	ARC 24	AOY8	AOY 5	AKB 20
$\sqrt{\varepsilon}$ (using D_M Cd: 7.2 10^{-10} m^2/s)	3.80 10^{-2}	5.67 10^{-2}	5.64 10^{-2}	6.47 10^{-2}
surface group density (moles/m^2)	4.9 10^{-7}	5.7 10^{-7}	9.0 10^{-7}	1.0 10^{-5}
fraction of sulphonic surface groups	1.00	0.35	0.29	0.00
pH	7.7	7.1	7.7	6.3
degree of deprotonation (α_d)	1.00	0.96	0.95	0.83
total charged surface group density (moles/m^2)	4.9 10^{-7}	5.5 10^{-7}	8.6 10^{-7}	8.6 10^{-6}
cadmium(II) adsorbed (moles/m^2)	7.4 10^{-8}	1.7 10^{-7}	2.9 10^{-7}	3.3 10^{-6}
ν (bound cadmium(II)/charged groups)	0.15	0.31	0.33	0.41
ν (Cd/COO^-) for ν (Cd/OSO_3^-)=0.15	- -	0.40	0.42	0.41

References

1. H.P. van Leeuwen, *Sci. Total Environ.* **60** (1987) 45.
2. H.G. De Jong, H.P. Van Leeuwen, *J. Electroanal. Chem* **235** (1987) 1.
3. H.G. De Jong, H.P. Van Leeuwen, *J. Electroanal. Chem.* **234** (1987) 17.
4. H.G. De Jong, H.P. van Leeuwen, K. Holub, *J. Electroanal. Chem.* **234** (1987) 1.
5. J. Buffle, *J. Electroanal. Chem.* **125** (1981) 273.
6. C.J.M. Kramer, J.C. Duinker, *Complexation of Trace Metals in Natural Waters.* Nijhoff/Junk Publ., The Hague, 1984.
7. R.F.M.J. Cleven, H.G. de Jong, H.P. van Leeuwen, *J. Electroanal. Chem.* **202** (1986) 57.
8. D.R. Crow, *Polarography of Metal Complexes.* Academic Press, London, 1969.
9. J. Koutecky', *Collect. Czech. Chem. Commun.* **19** (1954) 857.
10. J.M. Díaz-Cruz, J.H.A.M. Wonders, H.P. van Leeuwen, *Electroanalysis* (to be published).
11. J.M. Díaz-Cruz, J.H.A.M. Wonders, H.G. de Jong, H.P. van Leeuwen, *J. Electroanal. Chem.* **375** (1994) 127.
12. J.H.A.M. Wonders, *PhD. Thesis*, Agricultural University Wageningen, 1995.

Reprinted from Macromolecules, 1995, 28.

Characterization of Pauci-Chain Polystyrene Microlatex Particles Prepared by Chemical Initiator

Chi Wu,*,† Kam Kwong Chan,† Ka Fai Woo,† Renyuan Qian,‡ Xinhui Li,‡ Liusheng Chen,‡ Donald H. Napper,§ Guilan Tan,§ and Anita J. Hill∥

Department of Chemistry, The Chinese University of Hong Kong, Shatin, N. T., Hong Kong, Institute of Chemistry, Academia Sinica, Beijing 100080, China, School of Chemistry, The University of Sydney, Sydney, NSW 2006, Australia, and Faculty of Engineering, Monash University, Clayton, Melbourne, Victoria 3168, Australia

Received May 10, 1994; Revised Manuscript Received December 2, 1994[⊗]

ABSTRACT: Pauci-chain polystyrene (PCPS) particles, each containing a few polystyrene chains, were prepared by microemulsion polymerization using a chemical initiator. Laser light scattering (LLS), including the angular dependence of the absolute integrated scattered intensity (static LLS) and of the line-width distribution (dynamic LLS), together with fluorescence, positron annihilation lifetime spectroscopy (PALS), and porosimetry, was used to characterize PCPS both in dispersion and as PCPS glasses. The fluorescence spectra showed that ~1% of monomer styrene exists in the PCPS. The LLS results suggest that, on average, one PCPS particle prepared using chemical initiator was composed of only ~6 PS chains confined to the very small volume of the particle (~1000 nm³). PALS studies showed that the average radius of the free volume cavities inside PCPS is larger than that found in conventional PS latex or bulk PS. The density of PCPS (0.95 g/cm³) obtained from porosimetry is 9.5% lower than both that of conventional PS latex and bulk PS (1.05 g/cm³). The density and PALS free volume results suggest that the average intermolecular distance between the segments of the many different interpenetrating polymer chains in bulk or conventional latex PS is smaller than that in PCPS, even though the PS chains in PCPS were confined to a very small volume. This implies that the intersegmental approach inside PCPS was more difficult than that inside a conventional PS latex or bulk PS.

Reversible Swelling of Poly(vinyl acetate) Latex Particles in Sodium Dodecyl Sulfate Solution

Peter Hidi, Donald H. Napper, and David F. Sangster*

Division of Physical and Theoretical Chemistry, University of Sydney, Sydney, NSW, Australia 2006

Received October 17, 1994; Revised Manuscript Received May 31, 1995[⊗]

ABSTRACT: Dynamic light scattering and ultracentrifugation studies have shown that, in aqueous solutions of some anionic surfactants such as sodium dodecyl sulfate (SDS), poly(vinyl acetate) (PVAc) latex particles swell up to 60 times their original volume. The process is reversible on dilution. This unexpectedly large swelling always commences at a surfactant concentration below the critical micelle concentration, *e.g.*, at 4.5 mM for SDS. The swelling rate is best expressed by a Kohlrausch–Williams–Watts dispersive kinetics expression—initially very fast and then becoming progressively and continuously slower. Swelling is inferred to be due to the formation throughout the particle of polymer–micelle complexes, the structure of which is similar to those reported in systems containing certain water-soluble synthetic polymers and surfactants. The swelling is reversible and on dilution the particles contract rapidly to slightly less than their original size. The difference is due to the escape of some lower molecular weight material from the particles. The reversibility shows that a degree of morphological integrity of the particle is preserved on swelling. This is attributed to the existence of microdomains of intrinsic entanglements probably formed during the original emulsion polymerization process.

ELSEVIER

Colloids and Surfaces
A: Physicochemical and Engineering Aspects 98 (1995) 93–106

COLLOIDS AND SURFACES A

The effects of different electrolytes on the fractal aggregation of polystyrene latexes coated by polymers

Peng Wei Zhu, Donald H. Napper *

School of Chemistry, The University of Sydney, Sydney, N.S.W. 2006, Australia

Received 3 November 1994, accepted 18 January 1995

Abstract

The effects of different electrolytes on the aggregation kinetics and fractal dimensions of aggregates of polystyrene latex particles coated by poly(*N*-isopropylacrylamide) (PNIPAM) and poly(ethylene oxide) (PEO) have been studied using dynamic light scattering. Whilst PNIPAM is soluble in water at low temperatures, on increasing the temperature and/or adding electrolyte it adopts a globular conformation and becomes hydrophobic, in comparison to the more hydrophilic PEO. For the PNIPAM-coated latexes, the aggregation induced by various sodium salts was found to decrease in the following order: $NaCl > NaBr > NaNO_3 > NaI > NaSCN$. This sequence is similar to that found previously for latexes coated by PEO. The concentrations of electrolyte required to reach the same fractal dimension at longer times corresponded to the reverse order. The longer time fractal dimensions were found to increase with increasing electrolyte concentration so that the aggregate structures tended to become more densely packed. All the results can be correlated with the sequential order of the viscosity coefficients B_η of the electrolytes studied. For the PEO-coated latex, the fractal dimension was found to be insensitive to electrolyte concentration. With respect to temperature, the fractal dimension changed only slightly between 40 and 47.5 °C, but dropped dramatically up to 50 °C. The observations have been interpreted in terms of the nature of the interparticle interactions.

EUROPHYSICS LETTERS

10 December 1994

Europhys. Lett., 28 (8), pp. 603-608 (1994)

Collapse of Tethered Chains Due to *N*-Clusters, When Binary Interactions are Weakly Repulsive, but Ternary Interactions are Weakly Attractive.

W. L. MATTICE(*), S. MISRA(*) and D. H. NAPPER(**)

(*) *Institute of Polymer Science, The University of Akron*
Akron, OH 44325-3909, USA
(**) *Department of Physical and Theoretical Chemistry, University of Sydney*
New South Wales, 2006 Australia

(received 14 June 1994; accepted in final form 25 October 1994)

PACS. 68.25 - Mechanical and acoustical properties of solid surfaces and interfaces.
PACS. 82.70D - Colloids.

Abstract. - The collapse of tethered chains of 100 and 400 bonds has been simulated on a tetrahedral lattice. The density of the unperturbed tethered chains ranges from extremely dilute to weak overlap. When the binary interactions are weakly repulsive, attractive ternary interactions can produce a sharp collapse of the chains. The collapse is initiated from the «inside» (≡ near the grafting/tethering surface). It takes place over a narrow range of the ternary interaction if the chains are monodisperse. Since the value of the ternary interaction required for collapse depends on the number of bonds, the transition may not appear sharp if it is measured with polydisperse chains.

Contribution to the IPCG Newsletter April, 1995

Tsuneo Okubo
Department of Polymer Chemistry, Kyoto University, Kyoto 606-01, Japan
Phone 81-75-753-5611, Fax 81-75-753-5609,
e-mail A51325@JPNKUDPC.BITNET

Main activity of our group is on (1)colloidal crystals(morphology, crystal growth, etc.), and (2)deionized polyelectrolyte solution. Following papers are presented at the 44th annual meeting of the Society of Polymer Science, Japan held in Yokohama, end of May, 1995.

(1)**Dynamic Light Scattering of Colloidal Crystals of Polystyrene Spheres,** by T.Okubo, K.Kiriyama, H.Yamaoka and N.Nemoto.

(2)**Light Scattering Studies on the Formation Mechanism and Crystal Structure of Giant Single Crystals of Silica Spheres in Diluted Suspension,** by N.Nemoto, H. Hashimoto, M. Koike and T.Okubo.

(3)**Dynamic Light Scattering of Colloidal Liquids,** by T.Okubo and N.Nemoto.

(4)**Kinetic Analysis of Crystal Growth of Colloidal Crystals. I,** by T.Okubo, S. Okada and H. Yamaoka.

(5)**Direct Observation of Growing Processes of Colloidal Single Crystals under an Alternating-Current Electric Field,** by T.Okubo and N. Nemoto.

(6)**Crystal Growth of Colloidal Single Crystals in a Color Display Cell,** by T.Okubo, S. Kobata and H. Yamaoka.

(7)**Electro-optic Effects in Colloidal Crystals of Silica Spheres,** by M. Stoimenova and T.Okubo

Publications(1994-)

(1)"**Another Look at the Melting Temperature of Colloidal Crystals in the Completely Deionized Suspension**", T.Okubo, *Colloid Polymer Sci.*,**271**, 440-446(1994)

Melting temperature(T_m) of colloidal crystals of monodispersed polystyrene and silica spheres has been measured for the completely deionized suspensions as a function of sphere concentration. More than 3 weeks are needed before achievement of the completelydeionized state. T_m increases substantially are the deionization process of the suspension proceeds. The most reliable values of T_m observed for the completely deionized suspension are successfully analyzed again with the theory of Williams et al. The new T_m values are compared also with the theory of Robbins et al., which treats the repulsive Yukawa potential between colloidal spheres.

(2)"**Phase Diagram of Ionic Colloidal Crystals**", T.Okubo, ACS Symposium Ser.548, "Macro-ion Characterization. From Dilute Solutions to Complex Fluids"K.S.Schmitz(ed), 364-380,ACS, Washington,DC(1994).

Very large single crystals(3 to 8 mm) are observed with the naked eye in the highly deionized colloidal suspensions of monodisperse polystyrene

and silica spheres. Deionization is carefully made with the mixed beds of ion-exchange resins more than three weeks. Two kinds of single crystals,i.e., block-like crystals from homogeneous nucleation in the bulk phase far from the cell wall and the pillar like ones from the heterogeneous nucleation along the cell wall are observed. Size of the single crystals increases sharply as the concentration of spheres decreases, and is largest at the concentration slightly higher than the critical concentration of melting(ϕ_c). ϕ_c and the melting temperature(T_m) have been measured again for the completely deionized suspensions. New fc values are very small compared with the previous data, whereas T_m values are high. Important role of the long Debye-screening length around spheres and the intersphere repulsion is strongly supported.

(3)"**Sedimentation Velocity of Colloidal Spheres in Deionized Suspension**", T.Okubo, *J.Phys.Chem.*,**98**,1472-1474(1994).

Sedimentation velocities(S) of silica spheres(diameter 311 and 507 nm) and heavy polystyrene spheres(diameter 937 nm) are measured in the completely deionized suspensions and in the presence of sodium chloride. S decreases slightly and then starts to increase as the ionic concentration of the suspension decreases. The first decrease is explained with the retarded Brownian movement of colloidal spheres coated with the electrical double layers. Increase of S in the completely deionized suspension is much more significant for the small spheres. One of the most plausible reasons for the increase is the strengthened gravitational forces on the colloidal particles coated with the expanded double layers. The other factor will be the reduced surface charges on the colloidal spheres in the deionized suspension. The experimental results show clearly that the expanded electrical double layers play an important role on the translational self-diffusion of colloidal spheres especially in the exhaustively deionized suspension.

(4)"**Giant Colloidal Single Crystals of Polystyrene and Silica Spheres in Deionized Suspension**", T.Okubo, *Langmuir*, **10**, 1695-1702(1994).

Shape and size of colloidal single crystals of polystyrene and silica spheres ranging 81 and 212 nm in diameter(d) are studied mainly with the close-up color photographs in the diluted and exhaustively deionized suspensions with ion-exchange resins. Two kinds of single crystals, (1)block-like crystals grown up from the homogeneous nucleation mechanism in the bulk phase far from the cell wall and (2)pillar-like ones from the heterogeneous nucleation along the cell wall are observed clearly. Size of the colloidal single crystals is very large(3 to 8 mm) at the sphere concentration slightly higher than the critical concentration of melting(ϕ_c). ϕ_c-values are around 0.0002 in volume fraction irrespective of sphere diameter ranging 90 and 210 nm, and much high for the spheres smaller than 90 nm,e.g., 0.0036 and 0.0014 for colloidal silica(CS-61, d=81 nm) and polystyrene spheres(D1C25, 85 nm), respectively. Crystal size decreases very sharply as sphere concentration increases, since number of nuclei increases substantially with sphere concentration.

(5)"**Colloidal Single Crystals of Silica Spheres in Alcoholic Organic Solvents and Their Aqueous Mixtures**", T.Okubo, *Langmuir*, **10**, 3529-3535(1994).

Single crystals of colloidal silica spheres, 110 nm±4 .5 nm in diameter, are visually observed in suspensions of purely alcoholic organic solvents,i.e., methyl alcohol, ethyl alcohol, and ethylene glycol and in their aqueous mixtures in the exhaustively deionized conditions. Single crystals appear also for aqueous mixtures of propyl alcohol and n-butyl alcohol. Close-up color photographs of the single crystals are taken. Two kinds of colloidal single crystals,i.e., block-like crystals grow up from the homogeneous nucleation mechanism in the bulk phase far from the cell wall and the pillar-like ones from the heterogeneous nucleation mechanism along the cell wall, are observable in these solvent systems clearly. The size of the single crystals increases significantly as the sphere concentration decreases, and the largest crystals appear at sphere concentrations slightly higher than the critical concentration of melting(ϕ_c, in volume fraction). ϕ_c values are around 0.0002 in pure water and increase sharply as the fraction of organic solvent increases. The ϕ_c values in 100% of methyl alcohol, ethyl alcohol and ethylene glycol range from 0.01 to 0.02, which are substantially low compared with the reference values reported hitherto. The change in ϕ_c is explained well with the change in the dielectric constants of the solvent mixtures. The important role of the expanded Debye-screening length around spheres and the intersphere repulsion is supported strongly.

(6)"**Surface Tension of Structured Colloidal Suspensions of Polystyrene and Silica Spheres at the Air-Water Interface**", T.Okubo, *J. Colloid Interface Sci.*, in press.

Surface tensions, γ, of nineteen kinds of colloidal spheres of monodispersed polystyrene and silica(6 - 460 nm in diameter) in crystal-like, liquid-like and gas-like suspensions are studied systematically at the air-water interface by the Wilhelmy method. γ-values of the aqueous suspensions of colloidal silica spheres are close to that of pure water, though very weak surface activity[maximum in $\Delta\gamma$(surface tension of suspension minus that of water) is ca. -2 mN/m only] is detected for silica spheres of diameters ranging from 100 to 200 nm. Surface activity of polystyrene spheres, on the other hand, is high especially for spheres of diameters between 100 and 200 nm. The maximum in $-\Delta\gamma$ is ca. 20 mN/m. The large difference in the surface activity between the two kinds of spheres is due to the difference in surface characters,i.e., highly polar and strongly hydrophobic for silica and polystyrene spheres, respectively. Furthermore, surface tension lowering of the crystal-like suspensions is substantial when compared with that of the liquid-like or gas-like suspensions. It is highly plausible that the intersphere distance in the two-dimensional colloidal crystals at the interface is shorter compared with that in the bulk phase by the shortened electrical double layers at the interface.

(7)"**Rigidity of Colloidal Crystals as Studied by the Diffusion Equilibrium Method**", T.Okubo, *J. Chem. Phys.*, in press.

Rigidity of the colloidal crystals of monodispersed silica and polystyrene spheres has been measured by the diffusion equilibrium method, in which the stock suspension of the crystal state(ca. 0.1 in volume fraction of spheres) is introduced carefully in the bottom of the observation cell. The interface between upper water and lower crystals keeps clear whole the period of the measurements, one to two months for silica spheres. The initial ascending velocity of the interface increases significantly as the ionic concentration of suspension decreases. The translational mutual-diffusion coefficients, D_{tr} of the colloidal spheres are evaluated from the ascending velocities. The D_{tr} values of the deionized suspensions are surprisingly large, ca. 700-fold compared with that calculated using the Stokes-Einstein equation, and decrease sharply as ionic concentration of suspension increases. The lattice spacings at various heights in the crystal phase are determined in a diffusion equilibrium from the reflection spectroscopy. The rigidity and the fluctuation parameter, g-factor, of the colloidal crystals are evaluated and compared with the previous data from the sedimentation equilibrium method, for example.

(8)"**Dynamic Properties of Giant Colloidal Single Crystals. Dynamic Light Scattering of Monodispersed Polystyrene Spheres(192 nm in diameter) in Deionized Suspension**", T.Okubo, *Colloids Surfaces*, in press.

Diffusive processes of colloidal *gases*, *liquids* and *crystals* of monodispersed polystyrene spheres in the exhaustively deionized suspension are investigated with a dynamic light scattering(DLS) technique. A single diffusive mode and then a single value of diffusion coefficient, D (or the effective diameter, d_{eff} derived from the coefficient) is evaluated for the *gas-like* suspensions from the cumulant and histogram analyses. D increases as ionic concentration of the suspension increases, which is due to a decrease in the width of the electrical double layers surrounding the spheres with increasing ionic strength. The intensity autocorrelation function for the *liquid-like* and *crystal-like* suspensions deviates greatly from the single exponential type of decay function. Generally, two or occasionally three dynamical processes are observed for the colloidal liquids and crystals from the histogram analyses. The fast and slow modes in the liquids are assigned to the quasi-synchronous fluctuation of spheres, and to the restricted translational Brownian movement of spheres coated with the electrical double layers in the liquid cage. The fast mode of the colloidal crystals may be assigned to the fast Brownian movement of spheres in a strongly interacting crystal lattice. The medium mode of fluctuation is assigned to the synchronous fluctuation of spheres and the surrounding electrical double layers in the crystal lattice, which is the main component among the two or three modes. The slow process is ascribed to the wavy propagation of the strains in the crystal lattice. D and d_{eff} are rather independent of the scattering vector except *crystal-like* structures at high sphere concentrations.

(9)"**Electro-optic Effects in Colloidal Crystals of Silica Spheres** ", M. Stoimenova and T.Okubo, J. Colloid Interface Sci., in press.

The electro-optic behavior of isotropic colloidal crystals of silica spheres is investigated by the electric light scattering method. The electro-optic responses observed at low frequencies(Hertz range) are consistent with sphere concentration fluctuations induced by charge transport and convection. A oscillational resonance frequency due to the shear wave of the crystals is detected, at which the decay of the electro-optic response is visco-elastic. The increase of field intensity introduces electrohydrodynamic effects similar to those observed in the nematic liquid crystals.

AN ALTERNATIVE PROCESS FOR PREPARING COMPOSITE PARTICLES

A B Schofield, R H Ottewill, J A Waters,

School of Chemistry, University of Bristol.

Abstract

A process for preparing composite particles and for generating colloidal encapsulation is described. It is based on the mixing of a dispersion of polymer with another dispersion of preformed particles. The mixing is performed under conditions where heterocontact is generated between the dissimilar particles. It is believed that with correctly selected or modified surfaces for the particles, the process is thermodynamically driven by a reduction in interfacial energy which arises with composite particle formation. On contact, at temperatures exceeding the glass transition, the polymer particles appear to spread over the surface, or engulf, the particles of the other type.

Introduction

Many variations in the structure of composite latex particles have been observed and described. Internal rearrangement of the particle morphology, presumably toward a more thermodynamically favoured structure, has been reported (ref 1). In extreme cases, such morphological rearrangement can lead to gross changes in the dispersion characteristics (ref 2). A number of conditions have been identified which appear to hinder the rearrangement. These include having the 'matrix' polymer in the glassy state (below the effective glass-transition-temperature) or including a crosslinked phase within the particles. A number of papers have attempted to predict the structure of particles at equilibrium (refs 3-5). In some of these studies, a relationship between the favoured arrangement and the volume ratios of the components was established (ref 6).

These observations and predictions prompted development of a process for preparing composite particles such as composite latex particles. The process involves generating a heterocontact between two preformed, dissimilar polymer particle types under controlled conditions such that one particle type spreads around the surface of, or engulfs, the other (ref-6). Colloid stability is maintained throughout. It is believed that the process is thermodynamically driven by a reduction of the total interfacial energy of the system. The engulfing particle comprises polymer and the process is conducted at a temperature above it's effective Tg. The other particle may comprise a second polymer, some other organic material such as a bio-active compound or it may be inorganic such as a pigment or a filler.

The Thermodynamic Condition for Engulfment

It has been found (refs 6,7) that if two dissimilar particles of radius (R) are considered, the interfacial energy for a core-shell arrangement is less than that where the two particles remain separated if

$$(\gamma_{CW} - \gamma_{CS}) / \gamma_{SW} > (1-\nu_S^{2/3}) / \nu_C^{2/3}$$

where γ denotes the interfacial energy for the respective interfaces and ν is the relative fractional volume such that

$$\nu_C + \nu_S = 1 \quad \text{and} \quad \nu_C = R_C^3 / (R_C^3 + R_S^3)$$

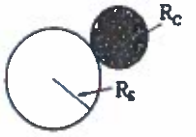

SEPARATED
(NO ENGULFMENT)

CORE-SHELL
(FULLY ENGULFED)

Further, by computing the total interfacial energy from 'separated' through progressive engulfment to 'core shell' it has been suggested (refs 5,7) that the fully engulfed structure is favoured over all other structures, including intermediate structures (partially engulfed), if the interfacial energy expression

$$(\gamma_{CW} - \gamma_{CS}) / \gamma_{SW} > 1 \qquad \text{(I)}$$

This is consistent with the Young-Dupre equation where

$$(\gamma_{CW} - \gamma_{CS}) / \gamma_{SW} = \cos\theta$$

for a droplet of S spreading over a surface of C under an environment of W. For complete spreading, $\theta = 0$ and $\cos\theta = 1$.

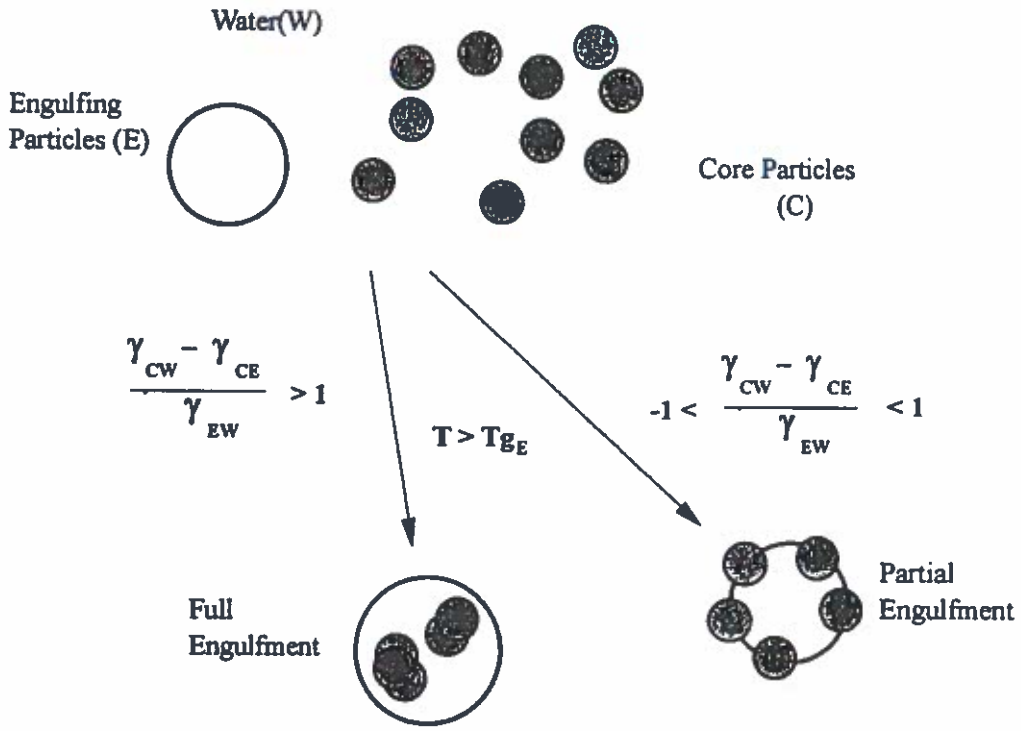

The thermodynamic driving force to the fully engulfed structure appears to increase with increasing value for the interfacial energy expression (refs 5,7). Therefore the engulfment process will benefit by running with a value for the expression which is considerably in excess of 1. The value may be increased by

(a) Increasing the value of γ_{CW}, that is in aqueous systems, by making the core particle more hydrophobic or

(b) Decreasing the value of γ_{CS}, by making the surface of the core particle similar to the interior of the shell particle or

(c) Decreasing the value of γ_{SW}, by ensuring that in aqueous systems the surface of the shell particles is very hydrophilic, for example by attaching water-soluble oligomer or polymer chains (which will also provide steric stabilisation for the shell particles and the final composite particles).

A combination of these factors may be used.

Preparing Composite Particles by an Engulfment Process

The process involves the mixing of dispersions of the two dissimilar, preformed particles under controlled conditions. The required surface characteristics for the particles are either 'built-in' before the process or they are achieved by 'in-situ' modification during the process. For example, in an easily controlled operation, the core particles (to be engulfed) are anionically stabilised and during the process the core particles and a cationic surfactant are added slowly and separately; the latter adsorbs on the core particle surfaces and serves to both destabilise the particles and to increase their hydrophobic character. By selecting engulfing particles which are sterically stabilised, it is possible to maintain colloidal stability throughout the process; also such particles have surfaces with enhanced hydrophilic character as described above.

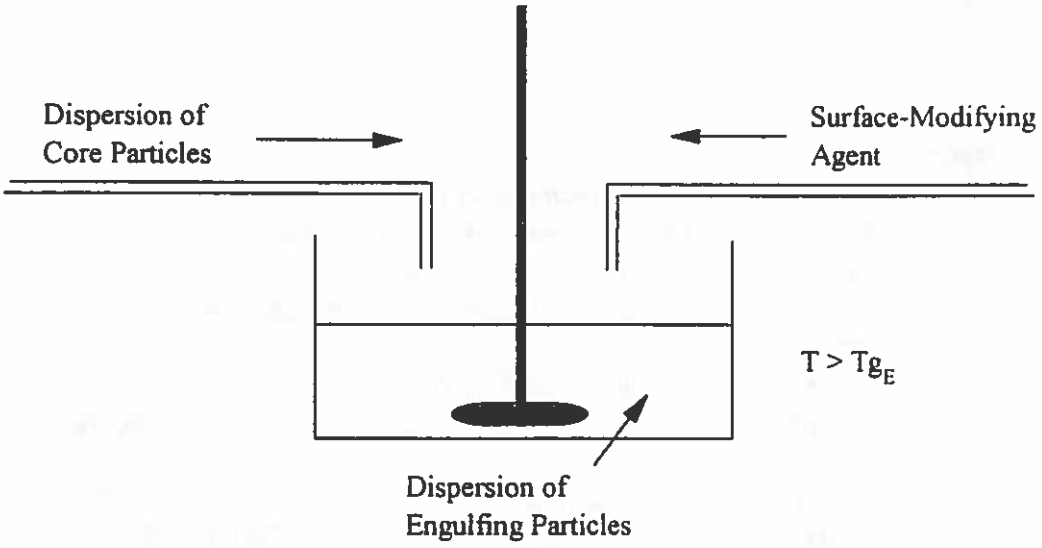

Many different types of composite particles have been prepared by an engulfment process (ref 6). In some recent studies, to be described, poly(butyl methacrylate) constituted the engulfing particles and polystyrene the core particles (ref 8).

Composite Particle Characterisation

Electron Microscopy

Where the engulfing and core particles had significantly different mean sizes, it was possible to use electron microscopy to confirm the virtual disappearance of one particle type; to show that with full engulfment the final particles were spherical and that the size of the particles had increased. Also by embedding composite particles in resin, taking ultrathin sections and staining, it has been possible to see engulfed polystyrene particles within individual acrylic particles (ref 8).

Disc Centrifuge Photosediometry

A Brookhaven Disc Centrifuge was used to characterise the starting and the final particles. It was possible to confirm the 'disappearance' of the core particles and to compare the size of the derived composite particles with theoretical expectations.

Tests for Steric Stabilisation

Simple but effective tests were used to show that the final composite particles were sterically stabilised, as were the engulfing particles. Under the same tests, the ionically-stabilised core particles, examined separately before engulfment, showed gross flocculation.

References

1. J Ugelstadt, *Science & Technology of Polymer Colloids*, Ed. G W Poehlein, R H Ottewill & J W Goodwin, *NATO ASI Series E, Applied Sciences* no. 68, 1983.
2. J S Keith and J A Waters, to be submitted.
3. J Berg, D Sundberg and B Kronberg, *Polymer Materials Science & Engineering, ACS Symp.* Ser. 54, 1986.
4. Y C Chen, V Dimonie and M S El-Aasser, *J Appl. Polym. Sci.* 45, 487, 1992.
5. J A Waters, *Colloids & Surfaces A:Physicochemical and Engineering Aspects*, 83, 167, 1994.
6. Imperial Chemical Industries, *European Patent* 327,199 (1989). Imperial Chemical Industries, *U S Patent* 4,997,864 (1989).
7. J A Waters, *Colloidal Polymer Particles*, Ed. J W Goodwin & R Buscall, 1995.
8. A B Schofield, R H Ottewill and J A Waters, to be submitted.

The association of aqueous phenolic resin with polyethylene oxide and poly(acrylamide-co-ethylene glycol).

Huining Xiao, Robert Pelton*, and Archie Hamielec

McMaster Centre for Pulp and Paper Research
Department of Chemical Engineering
McMaster University
Hamilton, Ontario, Canada L8S 4L7

ABSTRACT

Comb copolymers formed from acrylamide and poly(ethylene-glycol) methacrylate macromonomer, (PAM-co-PEG), were compared to poly(ethylene oxide), (PEO), with respect to hydrogen bond complex formation with water-borne phenolic resins. The behaviors of the two types of high molecular weight polyethers were similar. Complex formation gave a transient increase in viscosity followed by precipitation. Copolymers with pendant PEG chain lengths ≥ 9 formed complexes with phenolic resin whereas PEG homopolymer with a molecular weight of 2000 did not form a complex.

For both copolymer and high molecular weight PEO, the tendency of the complex to precipitate increased when the pH was decreased from 7 to 4. Acridine orange, a cationic dye, bound to the phenolic resin and, after the addition of PEO, yielded visible complex gels with diameters about 20 μm.

Evidence for two forms of SDS binding to poly(N-isopropylacrylamide).

Yulin Deng and Robert Pelton*

McMaster Centre for Pulp and Paper Research, Department of Chemical Engineering, McMaster University, Hamilton, Canada L8S 4L7

Abstract:

The interactions of sodium dodecyl sulfate, SDS, with aqueous poly(N-isopropylacrylamide), polyNIPAM, microgel latex were probed by conductivity and evidence is presented to support the hypothesis that the surfactant binds with the polymer in two ways. At low total SDS concentration, monomeric surfactant molecules bind to the gel particles whereas at high total surfactant concentrations where the monomer concentration equals the CMC, micelles bind with the gel.

Flocculation of Polystyrene Latex by Polyacrylamide-co-poly(ethylene glycol)

Huining Xiao, Robert Pelton* and Archie Hamielec

McMaster Centre for Pulp and Paper Research
Department of Chemical Engineering
McMaster University
Hamilton, Ontario, Canada L8S 4L7

Comb copolymers with long polyacrylamide (PAM) backbones and short poly(ethylene glycol) (PEG) pendant chains were used to flocculate aqueous latex in conjunction with a phenol-formaldehyde resin (PFR). Flocculation efficiency was determined as a function of molecular weight (MW), PEG content and PEG pendant chain length. The results indicated that high copolymer MW was crucial. More than 70 % of latex removal was achieved by copolymer with MW higher than 3 million. Moreover, only 0.3 to 0.8 % (mole) of PEG acrylate and methacrylate esters were required to be incorporated in the high MW copolymers. The minimum PEG pendant chain length for successful removal of the latex was as low as 9 ether repeat units. An empirical equation to relate the flocculation efficiency and the copolymer structures has been derived.

The copolymers exhibited similar flocculation performance to poly(ethylene oxide) (PEO) (molecular weight > 4 million). However, the copolymers did not exhibit a loss of flocculation ability with time.

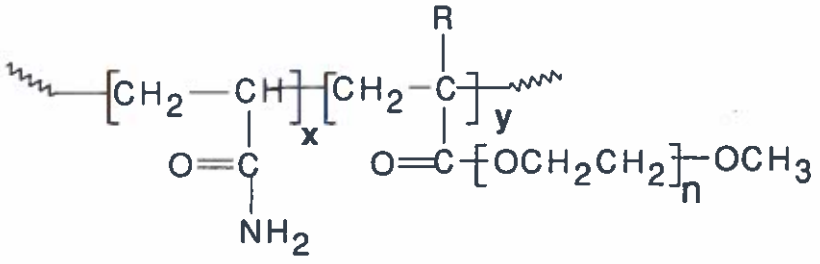

R = H or CH_3

Figure 1. Structure of PAM-co-PEG copolymer

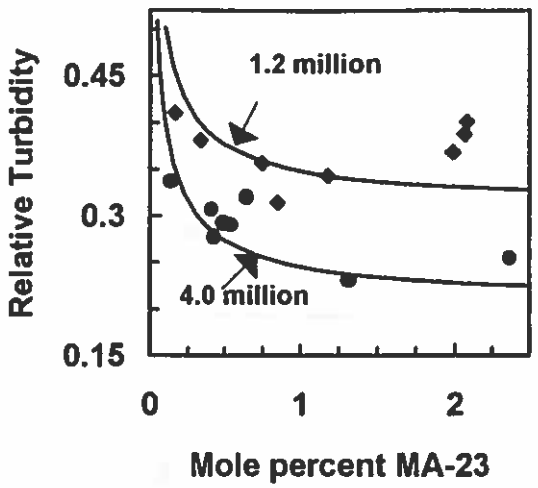

Figure 5. Relative turbidity versus composition of copolymers. Copolymerizations of AM and MA-23 were conducted at 25°C(•) and 40°C(♦). The concentrations of copolymer and phenolic resin were both 2 mg/L. The curves were calculated from the empirical Equation for a pendant chain length of 23 and the molecular weight values shown in the figure.

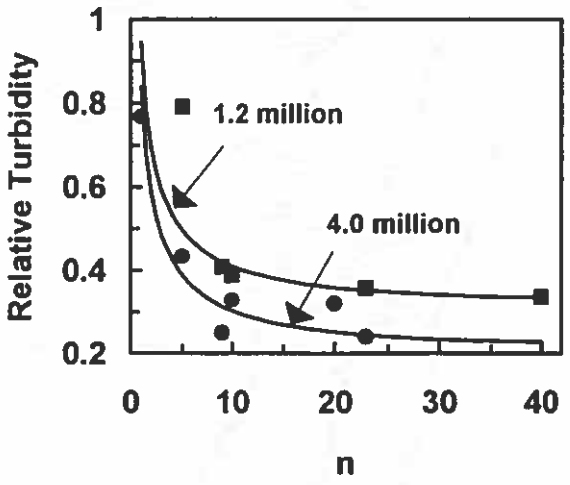

Figure 6. Relative turbidity as a function of PEG pendant length n in copolymers which were polymerized at 25°C(●) and 40°C(■). The concentrations of copolymer and phenolic resin were both 2 mg/L. The curves were calculated from the empirical Equation assuming constant composition of 0.9 % (mole) macromonomer and the molecular weight values shown in the figure.

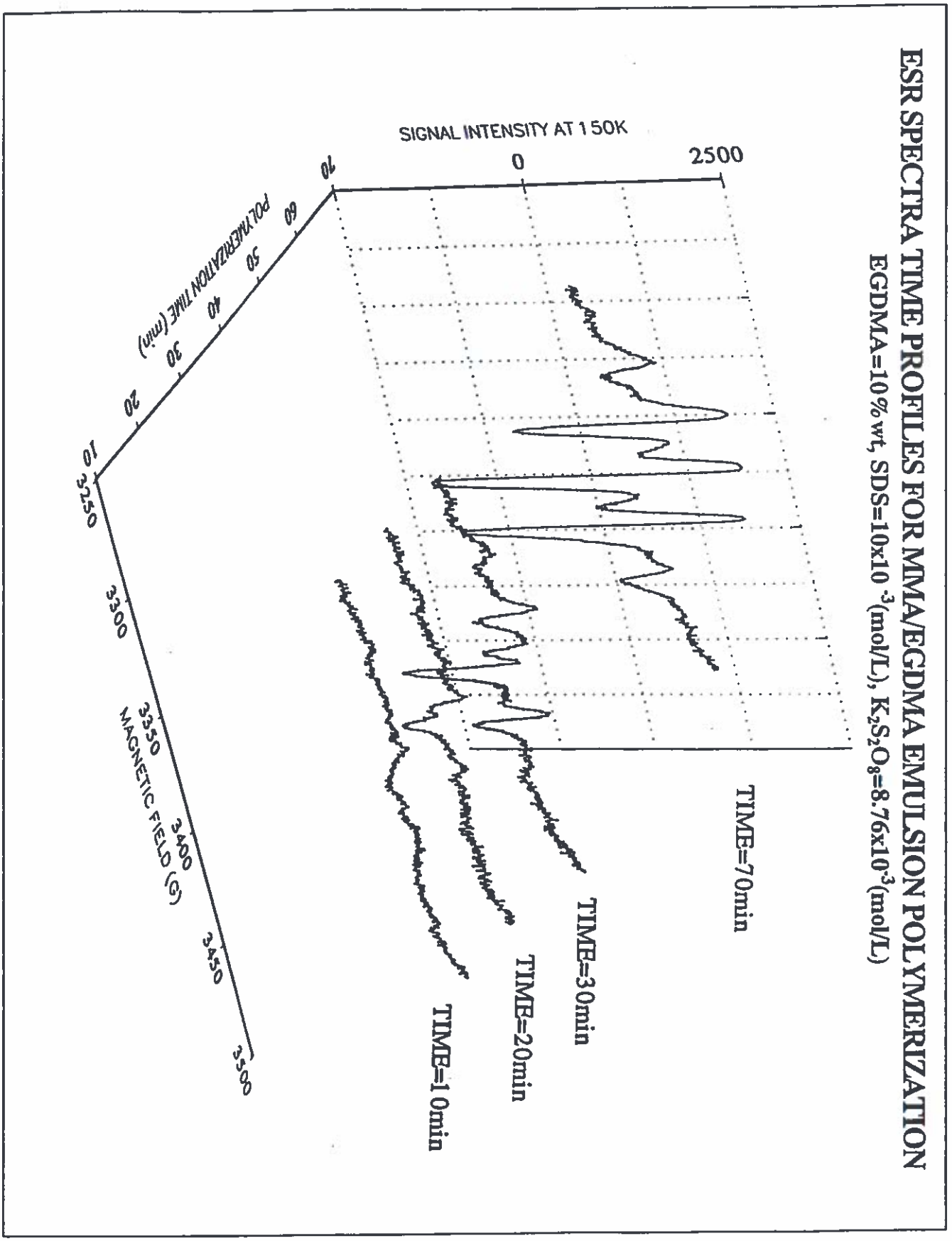

ESR SPECTRA TIME PROFILES FOR MMA/EGDMA EMULSION POLYMERIZATION

EGDMA=10% wt, SDS=10x10 $^{-3}$(mol/L), $K_2S_2O_8$=8.76x10^{-3}(mol/L)

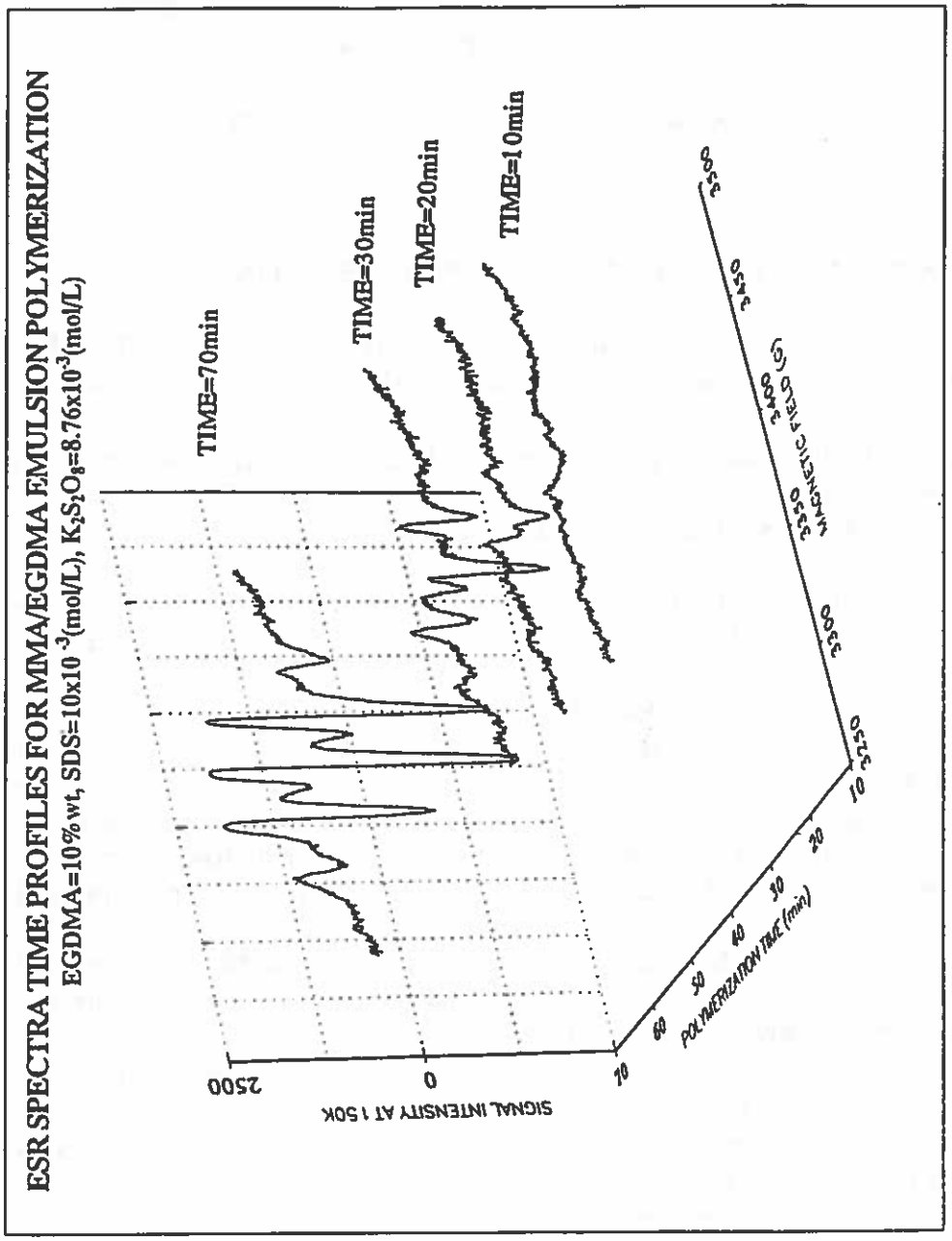
ESR SPECTRA TIME PROFILES FOR MMA/EGDMA EMULSION POLYMERIZATION
EGDMA=10% wt, SDS=10x10 -3(mol/L), K2S2O8=8.76x10-3(mol/L)
TIME=70min
TIME=30min
TIME=20min
TIME=10min
SIGNAL INTENSITY AT 1.50K
2500
0
10
20
30
40
50
60
70
POLYMERIZATION TIME (min)
3210
3300
3330
3360
3450
3500
MAGNETIC FIELD (G)

Contribution to IPCG Newsletter From Laboratoire de Chimie des Procédés de Polymérisation (LCPP-CNRS) and Unité Mixte CNRS-bioMérieux Lyon-France

(submitted by A. Guyot and C. Pichot)

I) RESEARCH ACTIVITIES AT LCPP (CPE-LYON)

A) The thesis of Frédéric Vidal has been defended on March 30, 1995; The following publications are extracted from his work. Abstracts are as follows:

Steric stabilization of polystyrene colloids using thiol-ended polyethylene oxide.
Frederic Vidal, J. Guillot and A. Guyot- CNRS-LCPP BP24 69390 Vernaison France.
Abstract: (in press, Polym. for Adv. Tech.)
Thiol-ended polyethylene oxide (I) are prepared from esterification of thioglycolic acid with monomethylether of polyoxyethylene glycol. Emulsion polymerization of styrene (and, in a few cases, methylmethacrylate as comonomer) is carried out in the presence of I using either water-soluble azo initiator or t-butylhydroperoxide. In the former case, bimodal particles size distribution is obtained while monodisperse latexes can be prepared in the latter case. Then a redox system is formed from I and t-BuOOH so that I is both an initiator and a transfer agent.Good steric stabilization of the latexes are observed. The polyethylene oxide (PEO) sequence of I is partly incorporated at the surface of the latex particles, but the incorporation yield remains limited (in between 7 and 18 %). Most of the residue of I remains in the serum.

Non ionic thiol-ended surfactants-Synthesis and NMR characterization.
F. Vidal, T. Hamaide . C.N.R.S. LCPP BP. 24. 69390 Vernaison. France.
Summary: (in press, Polymer Bulletin)
Non ionic thiol-ended surfactants have been prepared either by esterification of thioglycolic acid with poly(ethylene oxide) methyl ether or by anionic coordinated polymerisation of ethylene oxide in the presence of bromo-11-undecanol as transfer agent followed by reaction with thiourea and subsequent hydrolysis. The surfactants have been characterized by ^1H NMR, as well as the possible by-products. The transfer constants are in the range 16-19 and decrease with the chain length.

Inifer surfactants in emulsion polymerization-A. Guyot and F. Vidal
CNRS - LCPP- BP. 24 - 69390 Vernaison (France)
Abstract: (in press, Polymer Bulletin)
Thiol-ended non-ionic surfactants, used in combination with t-butyl hydroperoxide are components of a redox system able to initiate the emulsion polymerization of styrene, as well as control the molecular weight by transfer. Most of the surfactants remain as side products in the water phase, while multimodal molecular weight distributions of polymer are observed depending on the structure of the surfactant,

the conversion of the monomer and the process used for feeding the reactor. The maximum incorporation yield of these reactive surfactants in the polymer is 40%.

Thiol-ended polyethylene oxide as stabilizer in styrene emulsion polymerisation-F.Vidal and A.Guyot -CNRS-LCPP B.P. 24 - 69390 Vernaison France.

Abstract: (in press, New Journal of Chemistry)

Emulsion polymerization of styrene is carried out in the presence of thiol-ended poly(ethyleneoxide) (PEO) acting both as a reducing agent in the redox initiation system with t-butylhydroperoxide, and as transfer agent in the radical polymerization. In the absence of Sodium Dodecyl Sulfate (SDS) as cosurfactant, the reproducibility of the polymerization kinetics is rather poor, but good results are obtained even if limited amounts of SDS are used. Depending on the process used(batch or semibatch), the yield of incorporation of the PEO sequence at the surface of the latex particles does vary between 18 and 25%. Most of the PEO is found in the serum as dimers containing about 1 styrene unit. The particle size distribution is not monodisperse but reasonably narrow. The latex show good stability versus addition of electrolyte and freeze-thawing, at least if the grafting density of the PEO sequences at their surface is high enough, depending on the lenghts of these sequences. The mechanisms of initiation, nucleation and PEO grafting are discussed.

Surfactants with transfer agent properties (transurfs) in styrene emulsion polymerization-F. Vidal, J. Guillot and A. Guyot

CNRS - LCPP, BP. 24 - 69390 Vernaison France

Abstract: (in press, Colloid and Polymer Science)

Styrene emulsion polymerization have been carried out at 70°C using 2-2' Azobis (2 methyl, N-(2 hydroxyethyl) propionamide as initiator and thiol-ended surfactants (I) HS-C11H22 - (OCH2CH2)nOH with n from 17 to 90 units. The kinetics of monomer conversion, the evolution of particle size, particle size distribution, molecular weight and molecular weight distribution have been studied.After washing the final latex, the incorporation yield of the surfactant moieties in the particles has been measured. Most of the experiments have been carried out in batch; complementary experiments used semi batch or seeded process. In some experiments the two functions of transfer agent and surfactants have been decoupled using either dodecylmercaptan (oil soluble) or thioglycolic acid(water soluble) as transfer agent and the bromine ended precursor of (I) as surfactant. The discussion of the results is chiefly oriented towards both the molecular weight distribution and the incorporation of the surfactant to the latex.

B) The three following papers are related to the encapsulation of silica through emulsion polymerization.

Surface functionalized colloidal silica particles from an inverse microemulsion sol gel process - P. Espiard(*) and A. Guyot CNRS - LCPP BP24- 69390 Vernaison -France
J.E. Mark, Polymer Research Center, University of Cincinnati
Cincinnati-OH 45221-0172 USA
(*)Present Adress: ELF ATOCHEM Cerdato 27470 Serquigny France.

Abstract: (paper to be published in J. of inorganic and organometallic polymers)

Colloidal silica particle are prepared via a sol gel technique carried out in an inverse microemulsion of water in a toluene solution of tetraethoxysilane (TEOS)

stabilized by either an anionic surfactant AOT or isopropanol. Functionalized material was obtained using a functional coupling agent (RO)3Si(CH2)3-.X, X being a functionnal group such as methacryloyl,thiol, vinyl, amino group or a chlorine atom. The functionalization way be carried out either directly in one step of copolycondensation of TEOS and the coupling agent, or in a two step of core-shell polycondensation of the coupling agent onto preformed silica particles. Kinetic study of the copolycondensation are carried out using either ^{29}Si NMR analysis or liquid chromatography. They show that the consumption of TEOS is more rapid than that of the coupling agent. The materials are characterized either chemically (elemental analysis, FTIR,^{13}C and ^{29}Si NMR CPMAS analysis) or by their particle size. The silica functionalized with a polymerizable methacryloyl group are encapsulated by a polymer layer in an inverse emulsion polymerization of acrylic acid, after inversion of the emulsion in water, the resulting material is covered with a layer of hydrophobic polymer through a conventional emulsion polymerization experiment.

Composite Polymer Colloid Nucleated by Functionalized Silica

E. Bourgeat-Lami(l), P. Espiard(1), A. Guyot(l), S. Briat(2), C. Gauthier(2),G. Vigier(2), and J. Perez(2)
(1)LCPP-CNRS, B.P. 24, 69390 Vernaison, France
(2)GEMPPM, Institut National des Sciences Appliquées, URA 421-CNRS Villeurbanne-France

Abstract: (paper in Hybrid organic-inorganic composites-ACS Symp. series 585 (1995)
Emulsion polymerization of ethylacrylate has been carried out in the presence of functionalized and non-functionalized commercial silica. Bothpolymerization kinetics and particle size were studied. Paricular attention was focused on the characterization of grafting onto the silica surface. It is demonstrated that the nature of the interface depends on the type of silica employed. Polyethylacrylate formed is only adsorbed to the surface of non- functionalized silica, while the existence of a chemical bond between polymer molecules and functionalized silica has been demonstrated using different techniques. Because of this bonding to the rigid surface, the molecular mobility of the attached polymer chains is hindered and their molecular conformation is changed. As a consequence, we show that the mechanical strength of the composites is strongly influenced by the nature of the interfacial interaction between the continuous and dispersed phase.

Emulsion polymerization in the presence of colloidal silica particles - Application to the reinforcement of polyethyl acrylate films.

E. Bourgeat-Lami1, P. Espiard1 and A Guyot1
C. Gauthier2, L. David2 and G. Vigier2
(1)CNRS - LCPP- BP 24, 69390 Vernaison, France
(2) INSA - GEMPPM- URA 421 du CNRS, Villeurbanne. France.

Abstract: (paper to be presented in Athens conference (july 1995) and published in "Progress for organic coatings")
Emulsion polymerization of ethyl acrylate was carried out in the presence of different kind of functionalized and non functionalized silica particles. Trimethoxysilylpropylmethacrylate, hydroxyethylmethacrylate and triethoxysilylpropanethiol grafting agents were examined. We demonstrated that

when the first two coupling agents are used, it results a latex able to give films which display remarkable mechanical properties similar to those of vulcanized elastomers reinforced with solid particles. A qualitative model is then set up to give account for these properties. It is proposed that part of the polymer is covalently bound to silica as tight loops giving rise to a set of strong entanglements with the non-grafted polymer during film formation. This model is supported by stress-strain measurements and some validation experiments are described using the third grafting agent of the series.

II) RESEARCH ACTIVITIES AT UNITE MIXTE CNRS-BIOMERIEUX (ENS LYON)

1) Interaction studies between a model nucleic probe and highly functionalized amino latexes.

F. Ganachaud, A. Elaïssari and C. Pichot
CNRS/bioMérieux, ENS Lyon, 46 allée d'Italie 69364 Lyon, France.

Polystyrene-based latex particles bearing amino groups have been prepared by emulsion copolymerization of styrene with a water soluble monomer, vinyl benzyl amine hydrochloride (VBAH). They were used for studying the adsorption behavior of a model nucleic probe, a polythimidylic acid (poly(T)) 35 bases. Measurements were performed in a batch process, *i.e.* by titrating the residual amount in the serum by HPLC. The kinetics of the adsorption was found to be instantaneous, which denotes a strong affinity between the two species. The influence of the pH was important on the maximal amount of adsorbed poly(T), as long as the amino groups on the surface of the latex are ionogenic; then, the adsorption decreases upon decreasing the pH. Similarly, the higher the surface charge density, the larger the adsorbed nucleic probe. The nucleic probe adsorbed amount levels off with the ionic strength at 10^{-3} M, which seems to correspond to the contribution of hydrophobic interactions. Studies are currently investigated concerning the adsorption behavior according to the nature of the nucleic probe, as well as the influence of modifying the latex surface by adsorbing surfactant.

2) Fluorescence energy transfer study of oligonucleotide conformation on the surface of polystyrene latex particles.

Marie-Thérèse Charreyre, Olga Tcherkasskaya[#], Mitchell A. Winnik[#], Thierry Delair, Philippe Cros, Christian Pichot.
[#] University of Toronto, 80 St George Street, Toronto, M5S 1A1, Canada
Unité Mixte CNRS-BioMérieux, ENS Lyon, France

One of the numerous applications of latex particles in the biomedical field is their use as support of biomolecules. For example, oligonucleotides (DNA fragments) can be covalently attached to the surface of latex particles in order to perform the capture of complementary target oligonucleotides present in the medium. For a better efficiency, the bound oligonucleotides must be in an expanded conformation (and not in an adsorbed conformation) on the particle surface. Fluorescence energy transfer method can provide useful information about the conformation of these oligonucleotides. The strategy consists in labeling the oligonucleotide free end with

an energy transfer donor (fluorescein) whereas the acceptor (tetramethylrhodamine) is chemically introduced onto the aminofunctionalized surface of the polystyrene latex particles. Steady-state fluorescence energy transfer experiments are being carried out to study the influence of pH and ionic strength on the conformation of the bound oligonucleotides.

3) Recent papers and thesis:

Synthesis and characterization of cationic amino functionalized polystyrene latexes.
T. Delair, V. Marguet, C. Pichot, B. Mandrand
Colloid Polym. Sci., 272, 962 1994

Recent developments in the design of functionalized polymeric microspheres.
C. Pichot, B. Charleux, M.T. Charreyre, J. Revilla,
Macromolecular Symp., " Frontiers in Polymerization" 88, 71, 1994

Adsorption of rhodamine 6G onto polystyrene latex particles with sulfate groups at the surface.
M.T. Charreyre, P. Zhang, M.A. Winnik, C. Pichot, C. Graillat
J. Interface Colloid Sci.,170, 374, 1995

Heterocoagulation of sensitized latexes in the presence of HCG protein (The pregnancy test).
L. Ouali, E. Pefferkorn, A. Elaïssari, C. Pichot, B. Mandrand
J. Colloid and Interf. Sci.,171,276, 1995

Adsorption and desorption studies of polyadenylic acid onto positively charged latex particles
A. Elaïssari,C. Pichot, T. Delair, P. Cros, R. Kürfurst
Langmuir, 11,1261 (1995)

NMR Techniques in emulsion polymer investigation.
M.R. Llauro, R. Pétiaud, M. Hidalgo, J. Guillot, C. Pichot
Macromolecular Symp. "Radical copolymers in dispersed media" 92, 117, 1995

Thesis: Javier Revilla (December 1994, Univ. Lyon I): "Synthesis and characterization of surface-active monomers with saccharidic moieties-Studies of their radical copolymers in solution and in emulsion with a view to preparing hydrophilic latex particles for biological applications."

I. PIIRMA

Polymerized Microemulsions as Controlled Release Systems.

Edward Davis and H. Michael Cheung, The University of Akron, Akron, Ohio

Controlled release devices are finding wide use in the pharmaceutical and agriculture industries. They are typically used to provide a constant release of a chemical agent over an extended period of time after a single application of the device. In some cases the desired effect is a variable or pulsed release of the agent. The typical controlled release device consists of dispersed agents in a polymer matrix in which the concentration of agent in the polymer network is above the solubilization limit for the agent in the polymer. This results in a constant drug concentration at saturation in the polymer and thus a pseudo zeroth order release from the matrix. This release profile lasts until the agent concentration in the matrix reaches the solubilization limit. The release then proceeds as a first order process. Other devices utilize a porous polymer network surrounding a concentrated pellet of active agent. The concentration of drug at the inner surface of the polymer layer is maintained at saturation and thus also results in a pseudo zeroth order release. Hydrophilic closed cell polymer networks can release agents enclosed within the pores through a cell bursting effect that results from water diffusing through the polymer and swelling the pores by an osmotic mechanism.

It has been demonstrated that microemulsions containing monomer components can be polymerized. Water in oil, bicontinuous, and oil in water microemulsions have been successfully polymerized. The resulting polymer morphology ranges from closed isolated cells through open celled networks, up to and including polymer latex particles. Our lab has polymerized microemulsions containing acrylic acid (AA), methyl methacrylate (MMA) and water as well as similar systems derived by the addition of surfactants. The goal of this work is to determine the usefulness of the closed cell and open cell polymer matrices synthesized from these systems as controlled release devices.

Current efforts are focusing on the case where the active agent is incorporated into the polymer network as a component of the precursor microemulsion. This is done by creating a pseudo component of active agent and water which is then used as the aqueous component of the microemulsion. The left figure demonstrates typical release profiles and was obtained from systems in which the active agent, cetyl pyridium chloride (CPC), concentration in the aqueous phase as well as the overall aqueous to organic ratio was varied. These curves were then fitted to an exponential decay rate model. The effects on the rate constant, k, by the CPC concentration and the aqueous to organic ratio are shown in the right figure. Studies of the effects of the AA to MMA ratio as well as the effects of the release environment such as pH, temperature and salinity are planned.

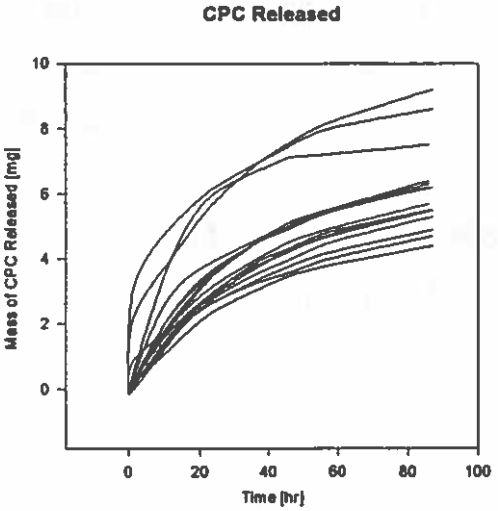

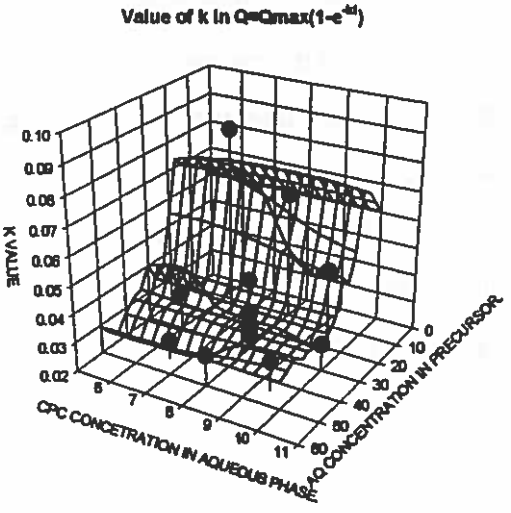

Synthesis and Characterization of Composites Formed from Polymerization of Microemulsions Containing Organic and Inorganic Monomer Species

Student : Ramachandra Mukkamala. ; **Advisor** : Dr. H. Michael Cheung

The Dept. of Chemical Engineering, The University of Akron, Akron, OH-44325-3906.

Microemulsions are thermodynamically stable, microstructured, isotropic systems containing hydrophilic, hydrophobic and amphiphilic components. The polymerization of an organic monomer in microemulsions to yield high surface area polymeric solids is a recent development in the field of microemulsions. These polymeric solids are porous and posses controlled morphology characteristics. It was found that the thermal degradation temperatures of these porous solids is about 270°C and the membranes made from these precursors posses poor tensile properties.

This research attempts to further improve the thermal stability of these precursors, to allow their use in advanced technological and industrial applications. This research is also aimed at improving the tensile properties of the membranes obtained from them. To achieve these goals, a five-component microemulsion system, methyl methacrylate (MMA), acrylic acid (AA), tetraethoxy silane (TEOS), and water stabilized by the surfactant, cetyltrimethylammonium bromide, (CTAB) was formulated. A novel methodology was also developed by coupling the fundamental aspects of microemulsion polymerization to that of ceramics synthesis. Polymerization of microemulsions was carried out using visible light. Using this method, microporous composites with high thermal stability at elevated temperatures were obtained. The composites thus obtained exhibited controlled morphology and uniform pore-size distribution characteristics.

This research also attempts to investigate the possible use of these composite precursors as protective coatings in arresting crack propagation in fiber modules at elevated temperatures.

Characterization and Polymerization of Microemulsion Formulated by Commercial Polymerizable Surfactant

Student : Bhavin R. Patel
Advisor : Dr. H. M. Cheung
Chemical Engineering Department
The University of Akron
Akron, Ohio 44325

Microemulsions are isotropic, clear, or translucent, thermodynamically stable dispersions of two immiscible fluids generally oil and water, containing one or more surface active species. Polymerization of monomer containing microemulsions for obtaining microporous solids is a recent development in the field of microemulsion technology. The objectives of this research is to relate the structure of microemulsion systems to the properties of polymeric material synthesized by polymerizing a hydrophobic monomer (methyl methacrylate) and hydrophilic monomer (acrylic acid) in polymerizable anionic microemulsion media.

The transparent polymeric solids is obtained by photopolymerization of precursor microemulsions containing reactive polymerizable surfactant (TREM LF-40). The polymeric solids thus obtained are microporous and posses controlled morphology characteristics. These polymeric solids also exhibit uniform pore size distribution over single phase microemulsion region. The results indicate that the open cell porous structures of transparent polymers can be obtained from those precursor microemulsions with aqueous content higher than 20% or the closed cell structures from those with less than 20%. The results also indicate the glass transition temperature (Tg) and degradation temperature (Tm) of the polymeric solids is higher than that of homopolymer due to the presence of the crosslinking agent EGDMA and formation of terpolymer.

FORMATION AND CHARACTERIZATION OF POLYMERIZABLE MICROMEULSION PRECURSORS ON BRAIDED FIBERGLASS

Student : Prerak Shah **Advisor** : Dr. Cheung
Department of Chemical Engineering, University of Akron, Akron, OH 44325-3906

Microemulsions are thermodynamically stable, isotropic, microstructured systems composed of hydrophilic and hydrophobic components, stabilized using one or more surface active chemical species.

The presence of microstructure in the microemulsion system and the possibility of synthesizing polymers with unique features makes polymerization of microemulsions a novel process. The unique characteristics such as super absorptivity, high surface area, and morphology control has of late tremendous attention.

The present study is aimed at investigating advanced technological applications of these microemulsion precursors. In this regard, a microemulsion system consisting of methyl methacrylate (MMA), acrylic acid (AA), and water (H_2O) is being studied. Braided fiberglass was dip coated with selected compositions of the precursors and subjected to photo and/or thermal polymerization using 2,2 - dimethoxy, 2-phenyl acetophenone (DMPA) or azobisisobutyronitrile (AIBN) respectively. Ethylene glycol dimethacrylate (EGDMA) was used as cross-linking agent. The coated polymerized fiberglass is being investigated for properties such as absorbing capacity, thermal stability and mechanical strength.

An attempt for investigating the application of these coated fiberglass tubes as modules for separation processes is also being made.

KINETIC MODELLING OF DISPERSION POLYMERIZATION

Gary W. Poehlein and Syed Farid Ahmed, Georgia Institute of Technology

MAY 1995

Introduction

Dispersion polymerization is known to exhibit charecteristics of both solution and heterogenous polymerization[1 - 4]. Radical generation, chain propagation and termination takes place in the continuous phase as well as inside the growing particles. Rate of polymerization in both reaction loci can be significant. Nucleation of particles is thought to be by homogenous nucleation and subsequent homo and heterocoagulation. Nucleation of new particle stops once a sufficient number of stable polymer particles are formed by adsorption of the polymeric stabilizer. Subsequent growth of stabilized particles occur by both polymerization within the particles (disperse phase) and by absorption of polymer chains and unstable primary particles formed in the continuous phase. The process is influenced by miscibility of the growing chains in the continuous phase (medium and monomer) and thermodynamic equilibrium between the phases.

The mechanism by which radicals or polymer chains are transferred to the particles is important in understanding both the nucleation process and subsequent particle growth process. Polymer chains generated in the continuous phase grow to a critical chain length before they precipitate to form a primary particle. Before these chains grow to the critical length, these radicals may also undergo termination or be absorbed by the stable polymer particles already formed. Primary particles absorb monomer and some of the continuous phase and may undergo homocoagulation with other primary particles before their eventual heterocoagulation with stable particles. Growing radicals within the primary particles may undergo chain transfer and subsequent desorption of the monomeric radical. They may also undergo termination either when another radical is absorbed from the continuous phase or when the primary particle undergo homocoagulation with another primary particle containing an active radical.

In order to gain a better understanding of the dispersion

polymerization process, seeded batch polymerization of two distinct particle populations and simulation modelling of monomer conversion as well as the size evolution of the seed polymers have been employed. Competitive growth of bimodal seed dispersions have been used as a tool for understanding emulsion polymerization kinetic mechanisms[5]. Continuous polymerization of a seed dispersion in a CSTR is another method that has been employed for studying particle growth and for estimation of rate constants for various radical transport processes[6 - 8].

Experimental

Seed dispersions with narrow particle size distribution were prepared by dispersion polymerization of styrene in absolute ethanol. Poly-N-Vinyl Pyrrolidone, PVP K-90 (Sigma Chemical) with a nominal molecular weight of 360,000 was used as the polymeric stabilizer. Polymerization was initiated with AIBN.

Competitive growth of two seed dispersions during batch polymerization were carried out at different temperature and initiator levels. Monomer conversion during polymerization was determined by gravimetric analysis. Size characterization of the seed dispersion and final polymer particles from the bimodal polymerization was done by Scanning Electron Microscopy. The particle size distribution was obtained with a Zeiss Endtler optical size distribution analyzer.

Seed dispersions with 10 - 20 % by weight of final solids were prepared using 1.5 - 2.0 % by weight of PVP stabilizer (12.3 - 16.5 gm/dm^3) and an initiator level of 0.5 - 2.0 % by weight of monomer. Weight average diameter of seed particles were between 1.13-3.46 μm with polydispersities of 1.01 - 1.06 and number densities of 10^{13} - 10^{14} per dm^3 (ethanol). Process conditions for competitive growth reactions were adjusted to ensure that the number of seed particles remain constant during the reaction i.e. new particles are not generated and seed particles do not coagulate among themselves. The following table summarizes the process conditions and size evolution of seed particles during competitive growth.

COMPETITIVE GROWTH : PARTICLE SIZE EVOLUTION					
RUN ID	#126	#223	#702	#704	#715
SEED POLYMER					
Seed#1, Dw, micron	1.31	1.13	1.31	1.31	1.20
Seed #2, Dw, micron	2.60	1.79	3.46	3.46	1.68
Volume Ratio	7.80	4.00	18.42	18.42	2.76
FINAL POLYMER					
Particle#1, Dw, m	2.58	2.05	2.40	2.42	2.02
Particle#2, Dw, m	3.59	2.64	4.37	4.49	2.63
Volume Ratio	2.69	2.14	6.04	6.39	2.21
PROCESS CONDITION					
Stabilizer, gm/dm3(e)	7.4	10	6.6	6.4	8.2
Initiator, gm/dm3(e)	0.93	0.39	3.00	2.92	2.19
Temperature, C	70	80	60	80	80
Initiation Rate,x10^7†	2.5	3.8	2.1	28.7	21.6

† mole/dm3(e).sec

Particle Growth and Polymerization Model

The rate of volume growth of seed particles i are expressed as :

$$\frac{d\,v_{P\,i}}{dt} = \left[\frac{M_M}{N_A\ d_P}\right]\left\{\frac{R_{P\,di}}{N_{S\,i}} + \frac{R_{P\,C} + R_{P\,P}}{N_S}\frac{v_i^m}{\langle v^m\rangle}\right\}$$

where $v_{P\,i}$ is the unswollen volume of the seed particle, M_M is molecular weight of monomer, d_P is density of polymer, $N_{S\,i}$ and N_S are molar density of seed particles, $R_{P\,C}$ and $R_{P\,P}$ are rate of polymerization in the continuous phase and in the primary particles and v_i is the swollen volume of seed particles. The exponent m is set equal to 1/3, assuming the rate of polymer absorption is proportional to the radius of the seed particles.

To solve the particle growth equations, we need to know the rate of polymerization in the continuous and disperse phases throughout the course of the polymerization. This requires knowledge of monomer and initiator

concentrations as well as the radical concentrations in each phase, the primary particle concentration and the propagation and termination rate coefficients.

Monomer concentrations in the continuous and disperse phases are obtained by assuming thermodynamic equilibrium and equating the partial molar free energies of monomer and solvent in the disperse phase to their partial molar free energies in the continuous phase[9, 10] . The oil soluble initiator is assumed to be equally soluble in the both phases.

Radical concentration in the continuous phase is obtained from radical balance taking into account initiation, termination, radical absorption by seed and primary particles, radical desorption from primary particles and homogenous nucleation. The primary particle concentration is obtained from primary particle balance taking into account the rate of homogenous nucleation and rates of heterocoagulation with seed particles and homocoagulation between primary particles. Radical balances for the seed population takes into account the rate of initiation as well as rate of absorption from continuous phase and from primary particles. The average number of radicals per primary particle is used as an adjustable parameter.

The total rate of polymerization at any time is the sum of the contributions from polymerization in the continuous and particle phases and in the primary particles. The propagation and termination rate constants are obtained from literature[11, 12]. The effect of polymer chains on the bimolecular termination rate (gel effect) and on the rate of propagation(glass effect) are incorporated into the model based on the free volume available in the seed particles[13]. The rate coefficients for the radical transport processes are modelled based on generally accepted mechanisms and parameter values with appropriate adjustments.

Figure 1 shows the simulation of monomer conversion (line) along with the experimental conversion data (points). At low initiation rates (#126 and #223) the fit with experimental data is reasonable. At higher rates of initiation (#704 and #715) fit with experimental data is not so good.

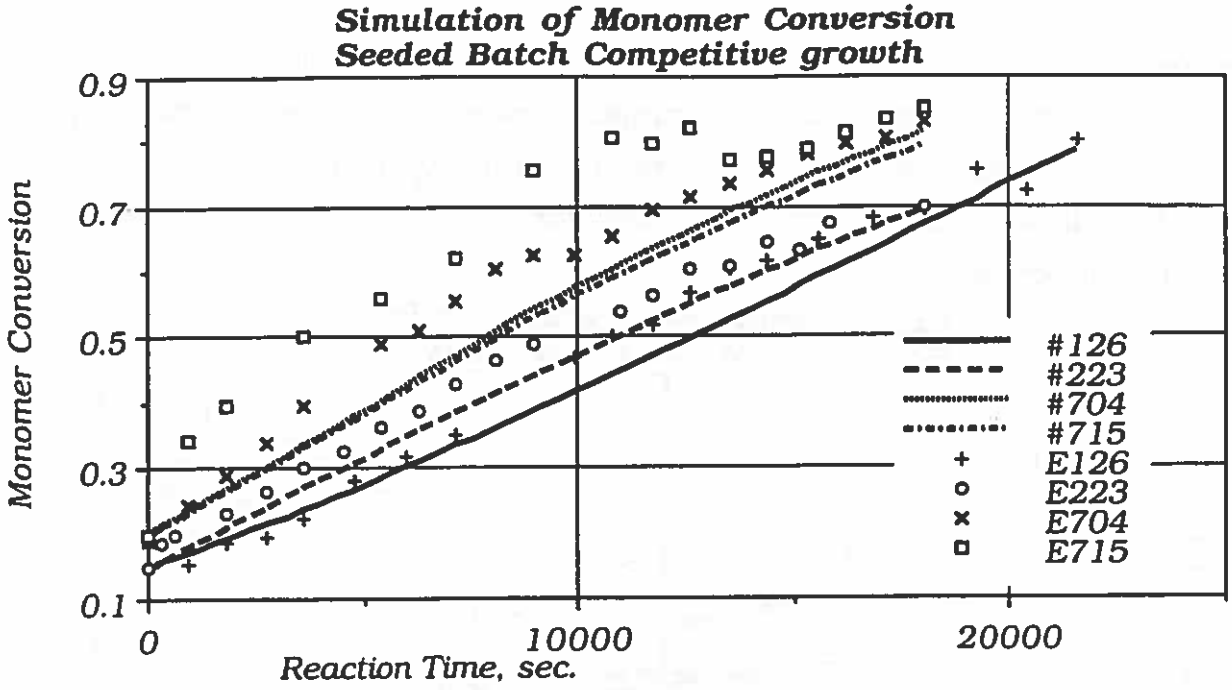

Fig. 1

The size evolution predicted also fits well with experimental observation at low initiation rates as shown in the following table.

SIMULATION RESULT: PARTICLE VOLUME RATIO					
RUN ID	**#126**	**#223**	**#702**	**#704**	**#715**
INITIAL RATIO :	**7.80**	**4.00**	**18.40**	**18.40**	**2.76**
FINAL RATIO :					
Experimental	**2.69**	**2.14**	**6.04**	**6.39**	**2.21**
Model Prediction	**2.85**	**1.94**	**6.02**	**12**	**2.11**

The shape of the rate curves obtained by fitting gravimetric data by a polynomial and then differentiating (Figure 2) illustrates the difference in the polymerization regime at low and high initiation rates. The pronounced maximum in the polymerization rate at low initiation level are not evident at high initiation levels.

Figure 3 shows the calculated contributions from polymerization in the various reaction locus for the case where both the rate and size evolution are reasonably well predicted by the model. At low conversion levels, the rate of

polymerization in the continuous phase is found to be significant. Figure 4 shows the same parameters at high initiation rates. The shape of the overall rate curve is found to differ significantly from the experimental curve. This probably indicates that the rate coefficient for radical transport processes are not well represented in the model.

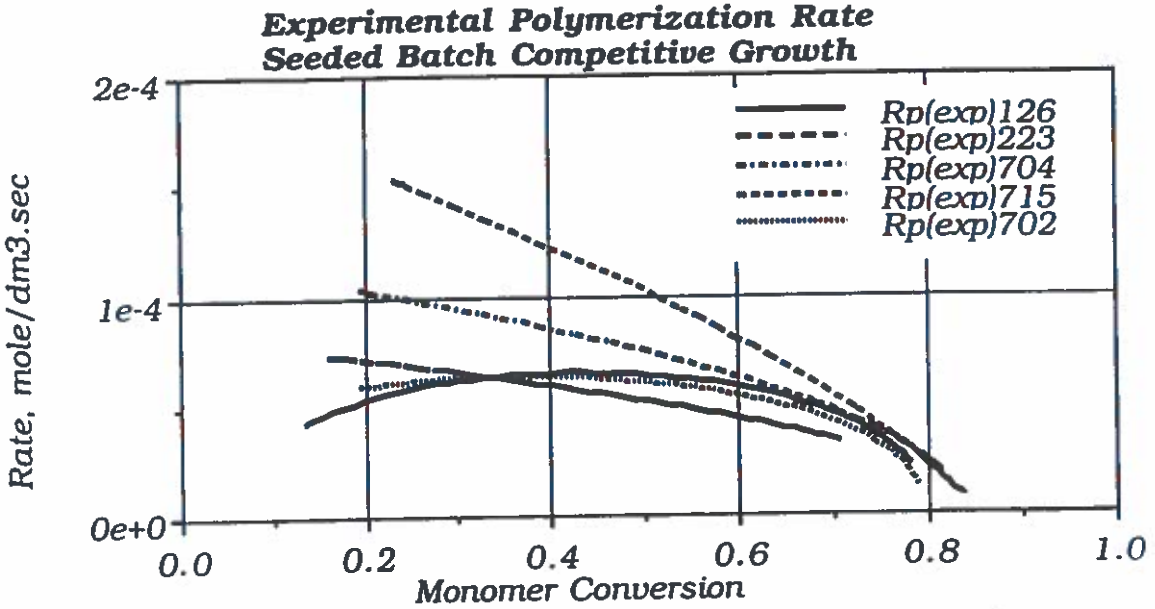

Fig. 2

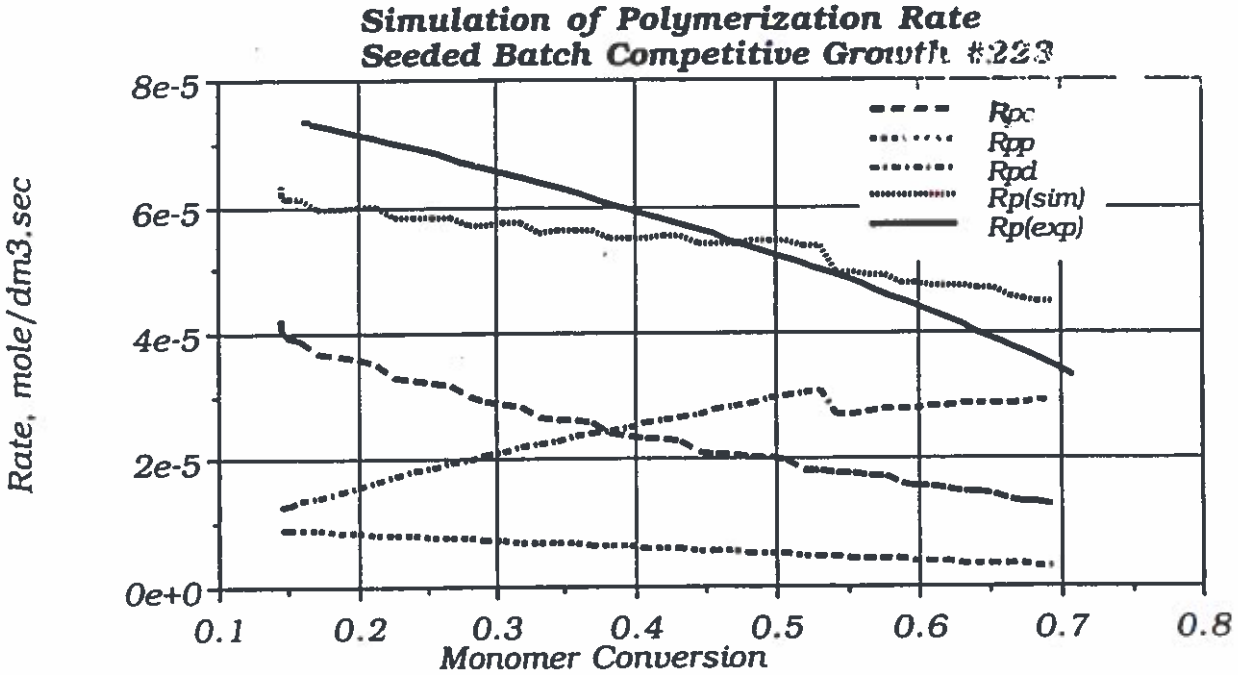

Fig. 3

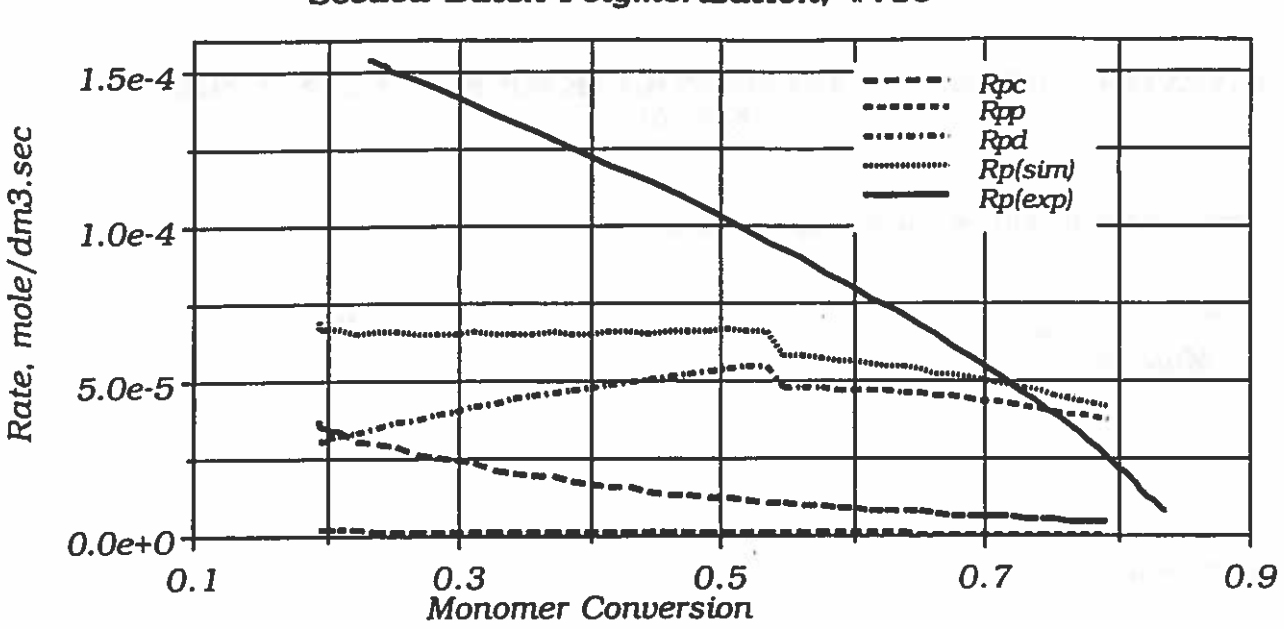

Fig.4

REFERENCES

1) Tseng, C. M. et al, *J. Polym. Sci. Polym. Chem.*, **24**, 2995, (1986).

2) A. J. Paine, *J. Colloid Interface Sci.*, **138** (1), 157, (1990).

3) Lok, K. P. and C. K. Ober, *Can J. Chem.*, **63**, 209, (1985).

4) Williamson, B. et al, *J. Colloid Interface Sci.*, **119** (2), 559, (1987).

5) Vanderhoff, J. W. et al; *J. Polym. Sci.*, **20** , 225, (1956).

6) Degraff, A. W. and G. W. Poehlein, *J. Polym. Sci.*, part A2, **9**, 1955, (1971).

7) Poehlein, G. W. et al, *Br. Polym. J.*, **14** (4), 143, (1982).

8) Lee, H. C. and G. W. Poehlein, *Polym. Proc. Engg.*, **5** (1), 37, (1987).

9) Lu, Y. Y., Phd Dissertation, Lehigh University, (1988).

10) Lu, Y. Y., M. S. El-Aasser and j. W. Vanderhoff, *J. Polym. Sci., Polym. Physics*, **26**, 1187, (1988).

11) Buback, M et al, *J. Polym. Sci., Polym. Letters*, **26**, 293, (1988).

12) Buback, M et al, *J. Polym. Sci., Polym. Chemistry*, 30, 851, (1992).

13) Vivaldo-Lima, E., A. E. Hamielec and P. E. Wood, *Polym. Reaction Eng.* **2**, 17, (1994).

INVESTIGATION OF POLYELECTROLYTE MICELLES IN AQUEOUS MEDIUM.

Frédéric Caldérara, Gilles Vallernaud and Gérard Riess

Ecole Nationale Supérieure de Chimie de Mulhouse, 3 rue Alfred Werner, 68093 Mulhouse Cedex, France

Introduction

When dissolved in selective solvents, block copolymers associate and form micelles which consist of a core composed of the insoluble blocks and a protective shell formed by the soluble blocks [1,2].

Similar to low molecular weight surfactants, the micellization of block copolymers can be described by the model of closed association [3]. This model is characterized by an equilibrium between molecularly dissolved copolymer (unimer) and spherical micelles with narrow molecular weight and size distribution [4-6]. The micellization process as well as the structural parameters of the micelles (micellar size, structure and aggregation number) are controlled by many factors including chemical nature and the lengths of the copolymer blocks, interactions between the solvent and the copolymer blocks, copolymer concentration, temperature and preparation methods.

The vast majority of the studies on block copolymer micelles were done with hydrophobic copolymers in organic solvents [1,2,7,8].

Micellization of amphiphilic nonionic block copolymers (poly(propylene oxide)-b-poly(ethylene oxide) and poly(styrene)-b-poly(ethylene oxide)) in aqueous solutions has been intensively investigated only recently [9-13].

Only little is known however about the micellization of block copolymers possessing a polyelectrolyte block in aqueous medium. These polyelectrolyte block copolymers may form micelles with a hydrophobic core and a ionic shell when dissolved in aqueous medium.

Polyelectrolyte micelles were first examined by Selb and Gallot [14,15]. The system investigated was of poly(styrene)-b-poly(4-vinyl-N-ethylpyridinium bromide) block copolymers in water/methanol/LiBr mixtures. The effect of the molecular characteristics of the block copolymers, solvent composition, salt concentration and temperature on micelle properties was examined using light scattering and sedimentation velocity measurements.

More recently, the poly(styrene)-b-poly(methacrylic acid) block copolymer micelles in various aqueous solvents have received considerable attention. The micellar solutions were examined by different techniques including static and quasielastic light scattering, sedimentation velocity, viscosity measurements and fluorescence [16-22].

In order to contribute to a better understanding of polyelectrolyte micellar systems, micelles formed by poly(styrene)-b-poly(4-vinyl-N-methylpyrididium iodide) diblock copolymers (PS-b-P4VP$^+$I$^-$) were studied in aqueous solutions (pure water and KI aqueous solution) by quasielastic light scattering and viscosity measurements.

Experimental

Block copolymer synthesis

The Poly(styrene)-b-poly(4-vinylpyridine) block copolymers (PS-b-P4VP) were synthesized by sequential anionic polymerization in THF using sec-butyllithium as the initiator, according to previous studies [23,24]. In a typical synthesis, styrene is polymerized first. The "living" polystyryl anion thus obtained is then end-capped with 1,1-diphenylethylene to reduce its reactivity toward the 4-vinylpyridine. The second monomer is subsequently polymerized and the polymerization is terminated by the addition of methanol. The resulting copolymer is recovered by precipitation into heptane and vacuum dried at ambiant temperature for several days.

The block copolymers prepared according to this technique have predetermined molecular weights and relatively narrow molecular weight distributions. The molecular characteristics of the block copolymers under study are presented in table 1.

Table 1. Molecular characteristics of the PS-b-P4VP block copolymers.

Sample	$M_{n,PS}$ (g/mol) a)	$(M_w/M_n)_{PS}$ a)	PS weight % b)	$M_{n,cop}$ (g/mol) c)	$(M_w/M_n)_{cop}$ d)
FC6	16000	1,13	28,5	56000	1,35
FC8	24500	1,11	43,5	56500	1,30
FC10	14000	1,08	38,0	37000	1,25

a) PS precursor number-average molecular weight ($M_{n,PS}$) and polydispersity index ($(M_w/M_n)_{PS}$) based on GPC analysis using PS standards
b) PS weight % based on ^1H NMR analysis
c) Calculation of the block copolymer number-average molecular weight ($M_{n,cop}$) is based on both GPC analysis of PS precursor and ^1H NMR analysis
d) Calculation of the block copolymer polydispersity index ($(M_w/M_n)_{cop}$) is based on GPC analysis using PS standards

Quaternization of P4VP blocks

The quaternization of the P4VP block of the block copolymers was carried out in chloroform with methyl iodide (50% excess) at 50°C for 24 hours. Excess methyl iodide was removed under reduced pressure. The quaternized block copolymers were purified by precipitation into heptane and dried under vacuum at ambiant temperature for several days.

The extend of quaternization was found to be around 95% as determined by elemental analysis. The molecular characteristics of the quaternized block copolymers are presented in table 2.

Table 2. Molecular characteristics of the PS-b-P4VP$^+I^-$ quaternized block copolymers.

Sample	Degree of quaternization (%) a)	$M_{n,PS}$ b)	PS weight % c)	$M_{n,qcop}$ (g/mol) c)
qFC6	94,5	16000	15,0	107000
qFC8	93,0	24500	25,0	97000
qFC10	95,0	14000	21,0	66500

a) Degree of quaternization calculated according to the I/N ratio determined by elemental analysis
b) PS precursor number-average molecular weight ($M_{n,PS}$) based on GPC analysis using PS standards
c) Calculation of the quaternized block copolymer PS content and number-average molecular weight ($M_{n,qcop}$) is based on the extend of quaternization

Micellar solutions preparation

None of the samples investigated was directly soluble in water. Uniform micellar solutions were prepared by the stepwise dialysis technique. Typically, the copolymers are dissolved in a THF/water 50/50 v/v mixture which is a good solvent for both blocks. THF is subsequently replaced by water by a stepwise dialysis at 20°C using a thermostated dializer bath and Spectrapor membrane tubings.

The micellar KI containing aqueous solutions were prepared by addition of the desired amount of salt to the micellar water solutions obtained by the dialysis technique described above. All further dilutions were made at constant concentration of salt.

In order to obtain dust free solutions, the THF/water solvent mixtures containing the block copolymers were filtered through Dynagard 0,45 µm filters just before dialysis.

Quasielastic light scattering (QELS)

The intensity fluctuations of the scattered light at 90° were measured at 20°C using a Coultronics N4 apparatus with a 32-channel correlator and a He-Ne laser light source.

The characteristic decay rate (Γ) was obtained from the first moment of the line width distribution according to the cumulant method [25]. The translational diffusion coefficient (D_T) was calculated from:

$$D_T = \Gamma / q^2$$

where $q = (4\pi n/\lambda_o)\sin(\theta/2)$ is the scattering vector (with n the refractive index of the solvent, λ_o the wavelength in vacuum and θ the scattering angle).

Micellar hydrodynamic radii (R_h) were calculated using the Stokes-Einstein relation:

$$R_h = k_B T / 6\pi\eta D_o$$

where k_B is the Boltzmann constant, T the absolute temperature, η the viscosity of the solvent and D_o the translational diffusion coefficient at infinite micellar dilution.

The micellar solution concentration was in the range 1.10^{-3} - 5.10^{-3} g/ml.

Viscosity measurements

The viscosity measurements were made in a Ubbelohde type Schott automatic viscometer (model CT050) with a photoelectric detection of flow times and a thermostatically controlled bath. The measurements were carry out at 20°C within the concentration range $2{,}5.10^{-3}$ - 30.10^{-3} g/ml.

Results and discussion

Figure 1 shows a typical viscometric behavior of a PS-b-P4VP$^+$I$^-$ sample in pure water. As expected for polyelectrolyte micellar systems, the reduced viscosity (η_{sp} / c) of our micellar solutions increases with dilution in pure water. This unique concentration dependence of the reduced viscosity is attributed to specific interactions (repulsion forces) between the shell forming blocks causing them to expand. These specific interactions which increase with dilution, result from an extraction process of mobile ions from the micellar shell to the solution.

An empirical viscosity-concentration relationship has been proposed by Fuoss [26] for polyelectrolyte homopolymer solutions:

$$\eta_{sp} / c = A / (1 + B.c^{1/2})$$

where A is the extrapolated η_{sp} / c value at c = 0 and represents thus the intrinsic viscosity $(\eta_{sp} / c)_{c\to 0}$ and B is a constant.

All samples investigated yield polyelectrolyte micellar solutions which viscometric behavior in pure water follows the Fuoss relation, as it can be seen from figure 2. Straight lines are obtained when c / η_{sp} is plotted against $c^{1/2}$.

The intrinsic viscosities ([η]) determined according to the Fuoss extrapolation as well as the micellar hydrodynamic radii (R_h) measured by QELS are compiled in table 3.

Figure 1. Viscometric behavior of sample qFC6 in pure water.

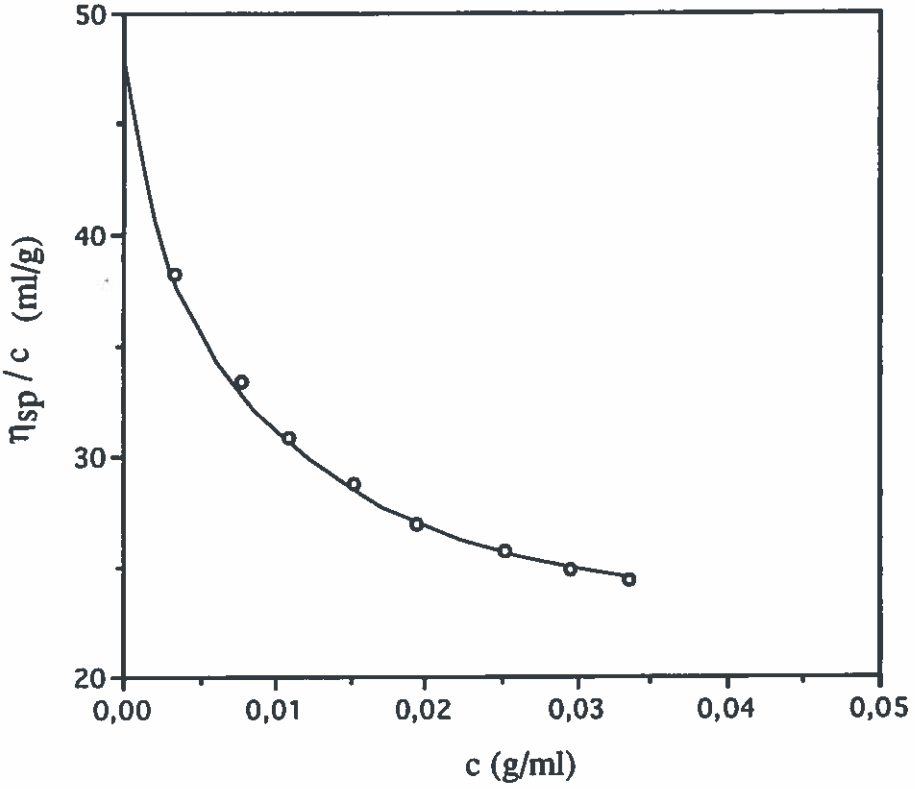

Figure 2. Viscometric behavior of samples qFC6, qFC8 and qFC10 in pure water.

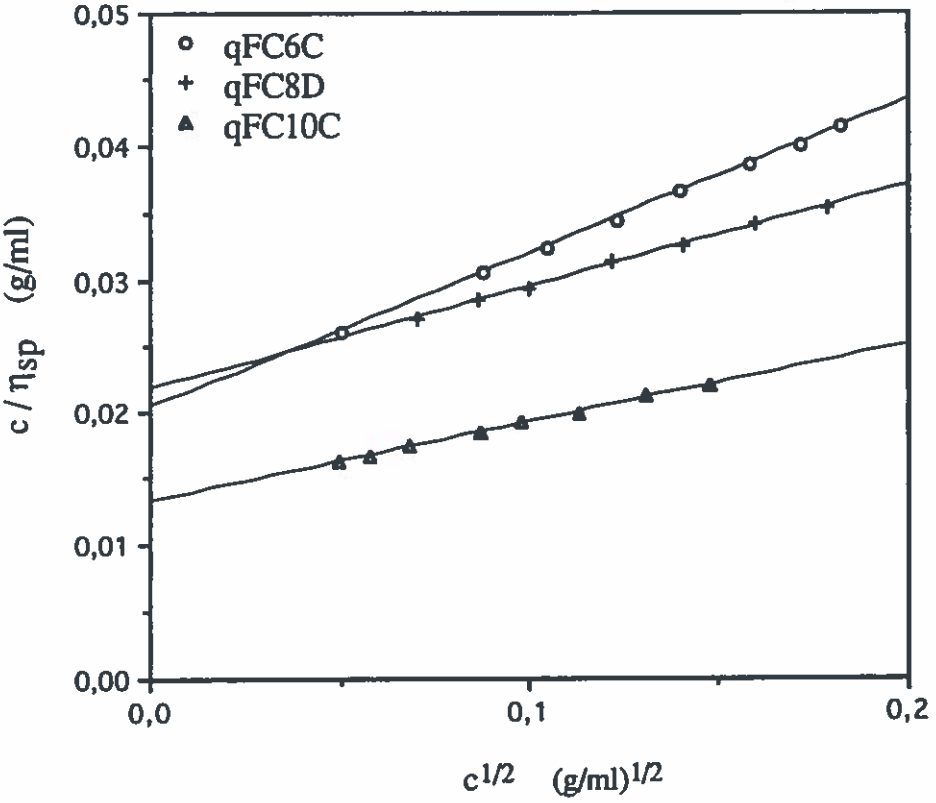

Assuming that the studied polyelectrolyte micelles can be approximated by the model of the hydrodynamically equivalent spheres, the intrinsic viscosity can be related to the density of the micelles (ρ) according to the Einstein relation:

$$[\eta] = 2{,}5/\rho = 2{,}5(4\pi N_A R_h^3) / (3M_m)$$

where N_A is the Avogadro number, R_h the micellar hydrodynamic radius and M_m the micellar average molecular weight.

The values of the micellar average molecular weights (M_m), aggregation numbers ($N_{Agg} = M_m / M_{cop}$ where M_{cop} is the average molecular weight of one quaternized copolymer unimer) and micellar densities calculated according to the Einstein relation are compiled in table 3.

The aggregation numbers range between 20 - 30 which corresponds to values usually observed with conventional block copolymer micelles [1,2].

Table 3. Micellar characteristics of the PS-b-P4VP$^+$I$^-$ polyelectrolyte block copolymers in pure water and in aqueous KI ([KI] = 0,03M) solution.

Sample	Solvent	R_h (nm) a)	[η] (ml/g) b)	$M_m x10^6$ (g/mol) c)	N_{Agg} d)	ρ (g/cm^3) e)
qFC6	H_2O	26,0	48,7	2,3	21	0,05
qFC8	H_2O	24,2	45,5	2,0	21	0,05
qFC10	H_2O	29,4	75,3	2,1	32	0,03
qFC6	H_2O + KI	18,4	17,2	2,3	21	0,14
qFC8	H_2O + KI	18,6	18,3	2,2	23	0,14
qFC10	H_2O + KI	24,3	42,2	2,1	32	0,06

a) R_h: hydrodynamic radius obtained from QELS measurements
b) [η]: intrinsic viscosity determined by viscosity measurements according to the Fuoss extrapolation (pure water solutions) or to the Huggins extrapolation (KI aqueous solutions)
c) M_m: micellar average molecular weight calculated according to the model of the hydrodynamically equivalent spheres
d) N_{Agg}: aggregation number (ratio of micellar molecular weight to unimer molecular weight)
e) ρ: micellar density calculated according to the Einstein relation ([η] = 2,5 / ρ)

In the presence of salt (KI), the polyelectrolyte effect is suppressed as it can be seen from figure 3. The addition of salt leads to an increase of the ionic strength of the aqueous medium and consequently a suppression of the extraction of mobile ions from the micellar shell. As a result, there is no more repulsion between the shell forming blocks and the rise in η_{sp} / c at low concentration is supressed.

Figure 3. Viscometric behavior of samples qFC6, qFC8 and qFC10 in aqueous KI ([KI] = 0,03M) solution.

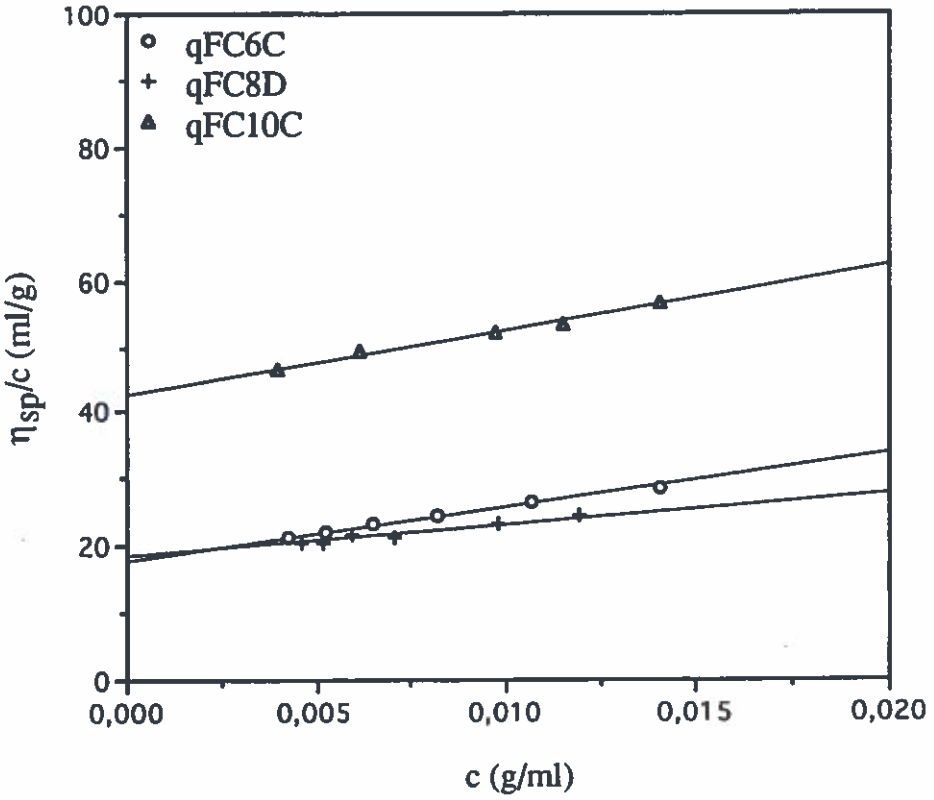

All samples investigated exhibit a linear concentration dependence of η_{sp} / c in the presence of salt and within the concentration range employed, as expected for conventional block copolymer micelles.

The intrinsic viscosities determined according to the well known Huggins extrapolation as well as the micellar hydrodynamic radii measured by QELS in the presence of salt are listed in table 3.

In order to determine the micellar average molecular weight (M_m), aggregation number (N_{Agg}) and density (ρ), we applied the model of the hydrodynamically equivalent spheres to our polyelectrolyte micelles in aqueous salt solution. The corresponding values are listed in table 3.

The comparison between the polyelectrolyte micelles in pure water and in aqueous KI solution (table 3), shows that the micellar molecular weight and the aggregation number remain unchanged in the presence of salt, within the experimental error and under the assumption that the model of the hydrodynamically equivalent spheres can be applied to polyelectrolyte type micelles.

In pure water, the high values of the micellar hydrodynamic radii (R_h) and intrinsic viscosities ([η]) as well as the low values of the micellar densities (ρ), when compared to the corresponding values obtained in aqueous KI solution, can be explained by the fully stretched configuration of the shell forming blocks resulting from the polyelectrolyte effect as already mentioned before.

A schematic representation of the effect of salt addition on the micellar structure is depicted in figure 4.

The suppression of the polyelectrolyte specific interactions in the presence of salt, leads to a decrease of both the micellar hydrodynalic radius (R_h) and intrinsic viscosity ([η]) and consequently an increase of the micellar density (ρ). Furthermore, the density values found in the presence of salt, are in the range of densities usually observed with conventional block copolymer micelles.

Figure 4. Schematic representation of the effect of salt on micellar structure in water.

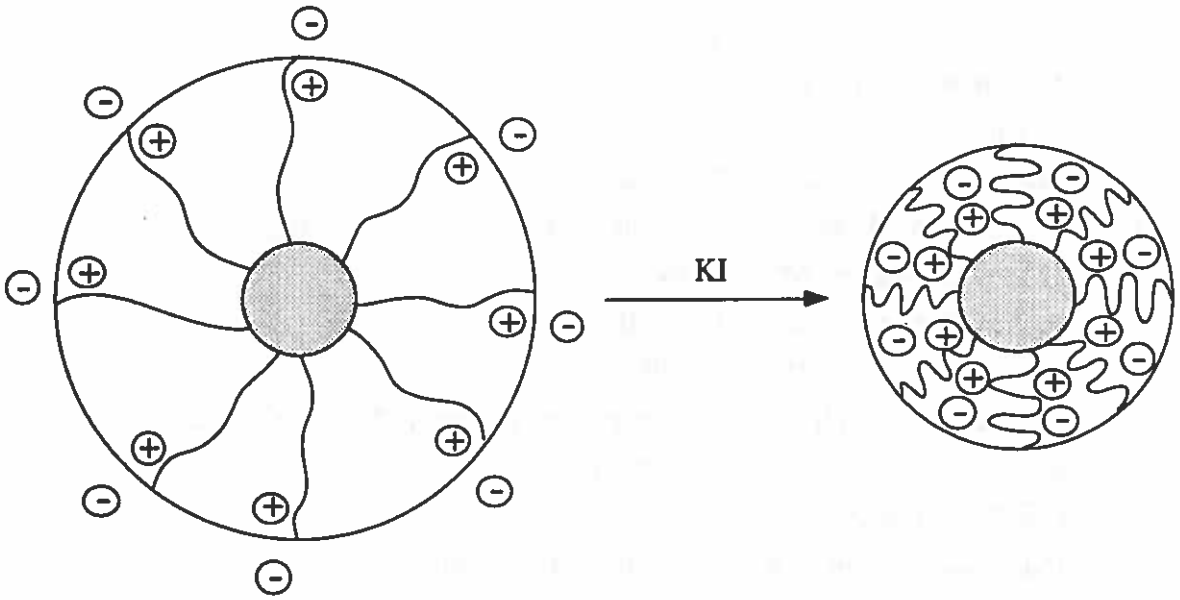

Finally, we hope that further studies on polyelectrolyte micelles in aqueous medium will give us a more detailed analysis and thus a better understanding of the solution properties of such complex systems.

References

1. Z. Tuzar, P. Kratochvil
In *Surface and Colloid Science*; E. Matijevic Ed.;
Plenum Press: New York, Vol. 15 (1993)

2. G. Riess, P. Bahadur, G. Hurtrez
In *Encyclopedia of Polymer Science and Engineering*; 2nd ed.; Wiley: New York, Vol. 2, p 324 (1985)
3. H.G. Elias, R. Bareiss
Chimia, **21**, 53 (1967)
4. Z. Tuzar, V. Petrus, P. Kratochvil
Makromol. Chem., **175**, 3181 (1974)
5. R. Nagarajan, K. Ganesh
J. Chem. Phys., **90**, 5843 (1989)
6. Z. Tuzar, J. Plestil, C. Kohak, D. Hlavata, A. Sikora
Makromol. Chem., **184**, 2111 (1983)
7. J.R. Quintana, M. Villacampa, I.A. Katime
Makromol. Chem., **194**, 983 (1993)
8. J.R. Quintana, M. Villacampa, I.A. Katime
Macromolecules, **26**, 606 (1993)
9. M. Ikemi, N. Ogadiri, S. Tanaka, I. Shinohara, A. Chiba
Macromolecules, **14**, 34 (1981)
10. Z. Zhou, B. Chu
Macromolecules, **21**, 2548 (1988)
11. R. Xu, M.A. Winnik, F.R. Hallett, G. Riess, M.D. Croucher
Macromolecules, **24**, 87 (1991)
12. R. Xu, M.A. Winnik, G. Riess, B. Chu, M.D. Croucher
Macromolecules, **25**, 644 (1992)
13. F. Caldérara, Z. Hruska, G. Hurtrez, J.P. Lerch, T. Nugay, G. Riess
Macromolecules, **27**, 1210 (1994)
14. J. Selb, Y. Gallot
Makromol. Chem., **181**, 809 (1980); **181**, 2605 (1980)
15. J. Selb, Y. Gallot
Makromol. Chem., **182**, 1491 (1981); **182**, 1513 (1981)
16. Z. Tuzar, S.E. Webber, C. Ramireddy, P. Munk
Polym. Prepr. Am. Chem. Soc., **32**(1), 525 (1991)
17. T. Cao, P. Munk, C. Ramireddy, Z. Tuzar, S.E. Webber
Macromolecules, **24**, 6300 (1991)
18. P. Munk, C. Ramireddy, M. Tian, S.E. Webber, K. Prochazka, Z. Tuzar
Makromol. Chem., Makromol. Symp., **58**, 195 (1992)

19. K. Prochazka, D. Kiserow, C. Ramireddy, Z. Tuzar, P. Munk, S.E. Webber
Macromolecules, **25**, 454 (1992)
20. D. Kiserow, K. Prochazka, C. Ramireddy, Z. Tuzar, P. Munk, S.E. Webber
Macromolecules, **25**, 461 (1992)
21. I. Astafieva, X.F. Zhong, A. Eisenberg
Macromolecules, **26**, 7339 (1993)
22. A. Qin, M. Tian, C. Ramireddy, S.E. Webber, P. Munk, Z. Tuzar
Macromolecules, **27**, 120 (1994)
23. P. Grosius, Y. Gallot, A. Skoulios
Makromol. Chem., **132**, 35 (1970)
24. K. Ishizu, Y. Kashi, T. Fukutomi, T. Kakurai
Makromol. Chem., **183**, 3099 (1982)
25. D.E. Koppel
J. Chem. Phys., **57**, 4814 (1972)
26. R.M. Fuoss, U.P. Strauss
J. Polym. Sci., **3**, 246 (1948)

POLYMER COLLOIDS AT PRINCETON

William B. Russel
Department of Chemical Engineering
Princeton University
Princeton NJ 08544-5263

recent publications

C.Shen, W.B. Russel, and F.M. Auzerais, "Colloidal gel filtration: experiment and theory" *AIChE Journal* **40** 1876-91 (1994).

R.A. Lionberger and W.B. Russel, "High frequency modulus of hard sphere colloids" *J. Rheol.* **38** 1885-1908.

Adsorbed Diblock Copolymer Layers: Effect of Curvature and Electrostatic Forces

Ramesh Hariharan and Dr. Claudine Biver (Elf Atochem)

Diblock copolymers adsorb onto latex particles from a selective solvent to form a relative homogeneous layer of the soluble block attached by a thin molecularly adsorbed or melt layer of the insoluble block. The adsorbed amount and the total thickness of the layer depend on a number of factors, including excluded volume interactions among the segments of the soluble blocks. In this work we characterize the hydrodynamic layer thickness δ via photon correlation spectroscopy for poly(tert-butyl styrene)/polystyrene sulfonate on polystyrene latices in water at a range of salt concentrations c_s. The latter block is soluble in water only because of the sulfonate groups, which impart a profound sensitivity to ionic strength.

A series of experiments with latices of different sizes and ionic strengths of 10^{-4}-1 M NaCl illustrate the significant effects of particle radius a and electrostatic excluded volume v. Interpretation is complicated, however, by significant, uncorrelated variations in adsorbed amount σ, apparently depending on uncontrolled aspects of the surface chemistry. Hence, we adopted the Daoud-Cotton model, which views each chain as a string of swollen blobs with sizes determined geometrically by the adsorbed amount and radial position. This theory yields

$$\left(1+\frac{\delta}{a}\right)^{5/3} = 1+\frac{N\sigma^{1/3}\ell}{a}\left(\frac{v}{\ell^3}\right)^{1/3}$$

where N and ℓ are the length and number of Kuhn segments per chain. As illustrated in the figure, this model correlates remarkably well our measurements for four different particle sizes at a fixed molecular weight and ionic strength, data from the literature for triblocks exhibiting less curvature (Li, et al. *Langmuir* **10** 4475 1994), and two measurements (our own and collaborators) for micelles with much higher curvature. The excluded volume parameter was extracted via standard theories from measured second virial coefficients for the soluble polymers in solution.

For a polyelectrolyte the electrostatic excluded varies varies with salt concentration c_s as

$$v \approx \frac{\ell^2}{\kappa} \approx c_s^{-1/2}.$$

Thus, for relatively flat layers the theory predicts

$$\delta \approx c_s^{-1/6},$$

which is very close to the dependence seen in our experiments. We are now in the process of assembling this data with that from diblock micelles and star polyelectrolytes, and adsorbed layers to test the approach over a broad range of δ/a and excluded volume conditions.

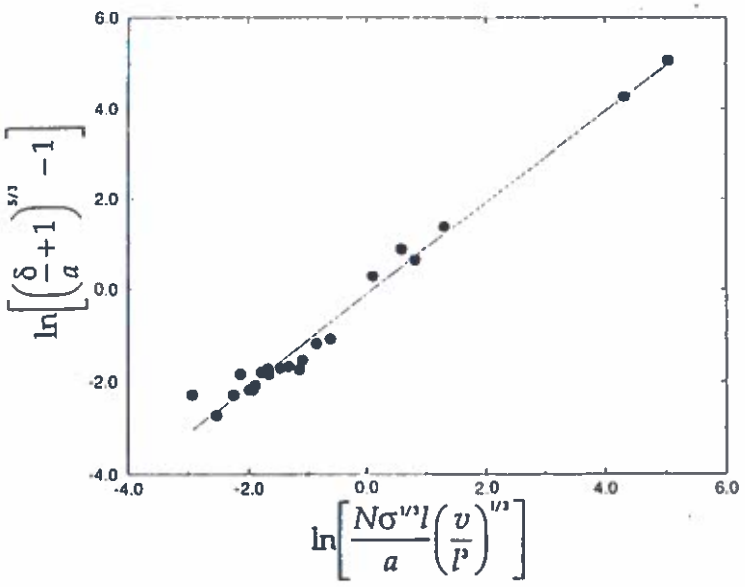

International Polymer Colloids Group Newsletter
Spring 1995 Contribution
Polymer Research Group
University of New Hampshire
Durham, NH 03824 USA
Donald C. Sundberg

LATEX MORPHOLOGY

Extension of UNHLATEX_EQMORPH to semi-continuous feed

Yvon Durant

We previously reported different advances in the development of our software, *UNHLATEX_EQMORPH*, aimed at modeling the structure of particles in emulsion polymerization. Following a discussion with Alfred Rudin we agreed that the extension of our model to the case of semi-continuous feed would be of significant benefit. Because most of the required knowledge for this improvement was previously known, it was rather simple to implement this process change. It is important to understand that this extension of the model remains under the assumption of "thermodynamic equilibrium" where the polymerization kinetics are significantly slower than the kinetics of phase separation. The modification implied by the semi-continuous process are of two folds:

- increasing particle volume as a function of conversion
- control the monomer concentration as a function of conversion

We primarily studied a linear feed of monomer over time. The conversion at the end of the feed depend on the monomer addition speed, and this experimental parameter is the only supplemental parameter required. The relation between instantaneous and global conversion can be semi empirically fit. The instantaneous conversion governs the interfacial properties, such as the interfacial tensions, while the global conversion governs the volumetric properties, such as the monomer distribution between the different phases. The instantaneous conversion is always higher than the global conversion, with a large differential at low overall conversion, and a "plateau" behavior at the end of the feed, as shown in the following figure for different feed rates.

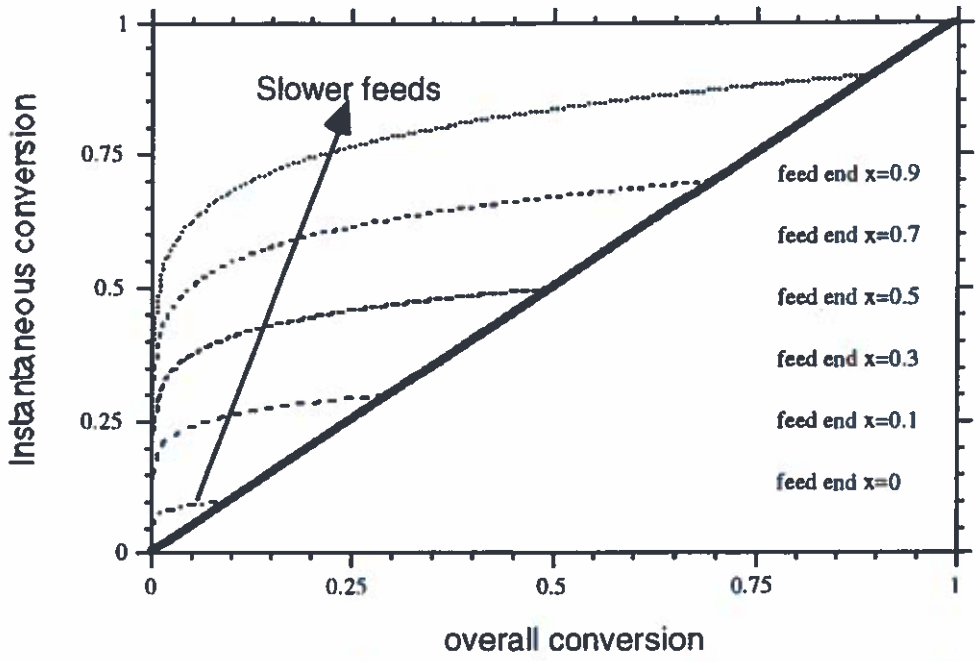

During the feed these two conversions are used to recalculate the overall monomer distribution, and the instantaneous interfacial tensions. At the end of the feed, the reaction is typical of a batch process.

We observed that all the interfacial tensions are significantly increased during the feed as compared to batch conditions, allowing a control of the morphology development early in the polymerization process. On average the possibility of creating a totally engulfed structure, such as a core shell or an inverted core shell is more likely. Because of the higher instantaneous conversion and the smaller surfaces (smaller volume), increased interfacial tension contrast (between the two polymers-water interfaces) appears at lower global conversion. While for a batch case totally engulfed structures are not likely to appear until 60-80% conversion (if at all), for a semi batch this may be the case at conversion as low as 10%, for slow feed rates (feed end x>0.7). This simple extension of our modeling efforts gives us a better understanding of morphology control, and a tool better matching industrial process conditions.

INTERFACIAL TENSION STUDIES

Measurement of interfacial tensions

Yvon Durant

Our research program in interfacial science has lead us to the fundamental need of accurately measuring the interfacial tension of various polymeric systems. As reported earlier, we have been studying the effect of monomer and surfactant on the interfacial tension between water and a polymer. For that work we developed an instrument based on the pendant drop method to measure interfacial tensions at atmospherique pressure and temperatures lower than 90°C. The pendant drop method allows us to accurately measure interfacial tensions between two liquids under true equilibrium conditions, without any macroscopic dynamics of the interface.

Later, we modified the same instrument to include the capability of measuring contact angles.

A new research program requires the measurement of the interfacial tension between pure polymers and water. Here it is necessary to keep the sample at a temperature higher than the Tg of the polymer to achieve reasonable polymer viscosities. For a polymer such as polystyrene, temperatures of 130 to 150°C are necessary, thereby causing elevated pressure due to the water. Thus we have built a second version of the interfacial tension meter which can operate at such temperatures and pressures and which allows multiple techniques to be run on the same instrument. We have also improved our analysis time, and increased our range of experimental conditions. The following capabilities are offered by the new instrument :

- analysis of pendant drops for liquid/liquid systems
- pendant drop volumes from 1 µl to 3ml.
- analysis liquid lens for liquid/liquid systems of high viscosity
- analysis contact angles for solid/liquid systems
- measurement of advancing and receding contact angles by expansion or tilting techniques
- temperature from 30°C to 190°C
- pressures from 0.01 to 13 Bars
- time dependence of interfacial or surface tensions
- time resolution between measurement of 30 seconds

A simplified description of the instrument is shown below, where an environmental chamber is used to keep the sample (lens, drop, or pendant drop) under required temperature and pressure via two PID process controllers. On the top of this chamber a syringe is connected to control the size of the drop, through a magnetically coupled steping motor. We use a high quality homogeneous parallel light beam to illuminate the contents of the environmental chamber, and a high resolution CCD camera to collect the image. A frame grabber transfers the image to a PC, which performs the shape analysis, and all the further calculations. Because of the required knowledge of the magnification power of the optical setup, a parallel light pathway is used to maintain calibration during a measurement. The following graph is the front view of this instrument.

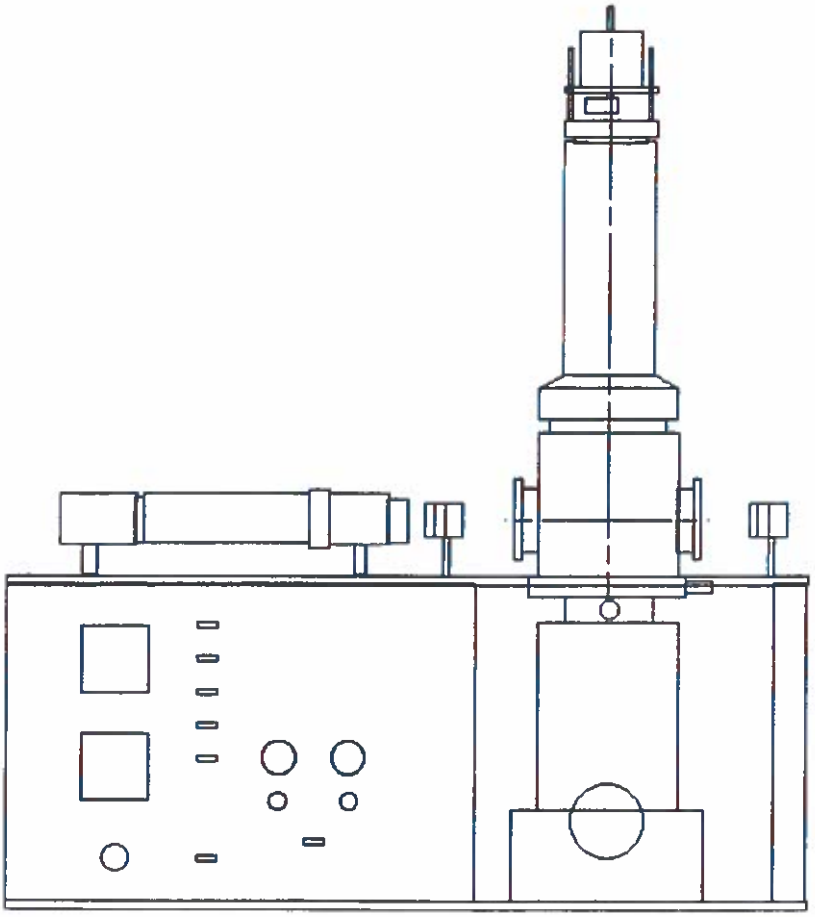

Competitive Adsorption of Surfactants at Water/Polymer Interfaces

John Learson

As reported in the Spring 1994 IPCG Newsletter, we have been investigating the interfacial energies at water/polymer interfaces when there is more than a single surfactant present. In particular, we have been studying the binary surfactant system comprised of SDS and one of several nonyl phenyl ethylene oxides (NP-X, where X indicates the number of moles of ethylene oxide). When the polymer phase is comprised of pure polymer, both surfactants compete for the interface in particular ways and the nature of the competition depends greatly upon the value of X. As the ratio between the SDS and NP-X changes, the interfacial tension varies in a highly non-linear manner. When monomer is present in the polymer phase, as it is during a polymerization process, the NP-X has a tendency to partition into the organic phase and thereby distort the previous ratio of the surfactants in the water phase. This has an important effect upon the interfacial tension and complicates the understanding of the competitive adsorption process. Given this state of affairs, we have begun to investigate the partitioning of several NP-X's between water and polymer phases with monomer present.

A number of our previous interfacial studies have used poly(dimethyl siloxane), PDMS, as a model polymer having very low polarity. It is also a liquid at room temperature even at significant molecular weights, thereby making it conducive to the

use of the pendant drop method for the measurement of interfacial tensions. In the present study we have used toluene to simulate the presence of monomer and performed a series of experiments in which organic phases composed of various ratios of PDMS and toluene were brought to equilibrium with aqueous phases containing various concentrations of NP-X. The partitioning of the NP-X was experimentally determined by measuring the NP-X concentration in the aqueous phase by HPLC. The data shown below are for NP-30. Here one can see that the addition of PDMS (MW=3900) to pure toluene changes the partitioning of the NP-30 in a dramatic fashion. At polymer:toluene ratios characteristic of emulsion polymerization, the response to changes in solvent (monomer) content is much less pronounced. Nonetheless, the partitioning of this surfactant into the organic phase is significant and it would appear that it needs to be taken into account when attempting to account for the interfacial tension generated from mixed surfactant systems, especially when the NP-X content is low (small amounts can make large changes in interfacial tensions). The solid lines in the figure presented below have been drawn on to emphasize the approximate behavior of the data. The linear nature of the lines is our choice and should not interfer scientific meaning at this point.

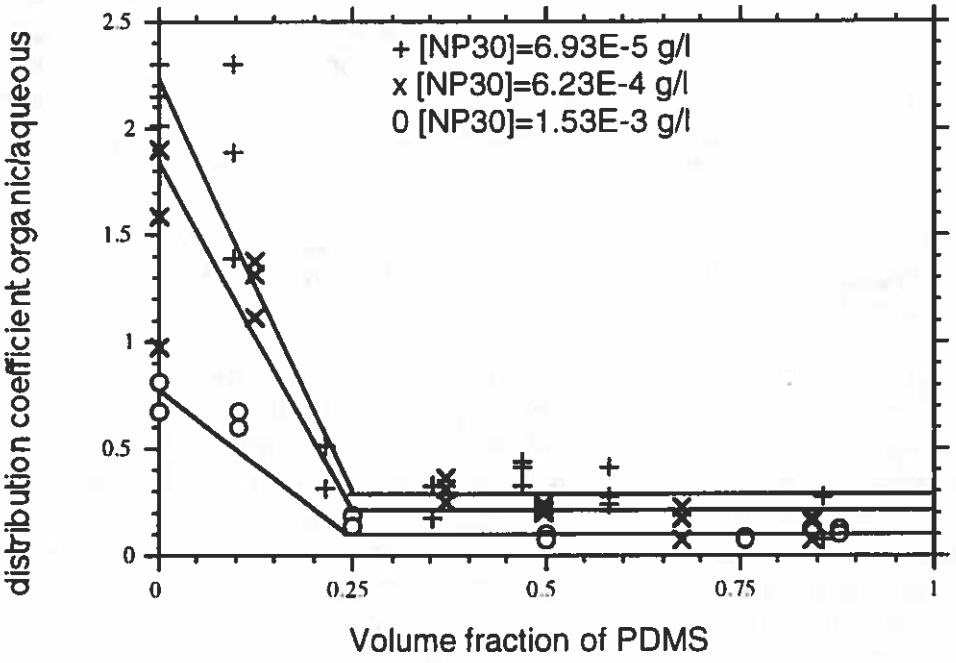

GRAFT COPOLYMERIZATION STUDIES

The two abstracts presented below are attached to papers which are under review by the Journal of Polymer Science and have to do with the mechanism and kinetics of grafting a variety of vinyl monomers onto polybutadiene backbone polymer.

Grafting of Styrene, Acrylate and Methacrylate Monomers onto cis-Polybutadiene Using Benzoyl Peroxide Initiator in Solution Polymerization

Nai-Jen Huang

Benzoyl peroxide (BPO), due to its high radical activity as compared to AIBN, is known to promote grafting onto cis-polybutadiene. Switching from AIBN to BPO initiator made a dramatic difference in the extent of grafting for styrene and methacrylate monomers, but only a modest difference for acrylate monomer. For styrene and methacrylate monomers, graft site formation is due to BPO initiator radical attack onto the backbone via allylic hydrogen abstraction. Significant levels of grafting are achieved and depend upon the relative concentrations of monomer and backbone polymer but not upon the initiator level.

For acrylic monomer, graft site formation was found to be due to polymer radical attack at the double bond in the backbone. Abstraction of allylic hydrogen also occurs but results in the retardation of the overall reaction rate. Graft level was dependent upon initiator and backbone polymer concentrations but not upon monomer concentration. The effective role of the initiator is only to produce polymer radicals; the BPO has no direct role in the formation of effective graft sites.

Grafting of Styrene, Acrylic and Methacrylic Monomers onto vinyl-Polybutadiene Using Benzoyl Peroxide and AIBN Initiators in Solution Polymerization

Nai-Jen Huang

Vinyl-1,2 polybutadiene (vinyl-PBD) was used as the backbone polymer for the grafting of styrene, methacrylate and acrylate monomers using both BPO and AIBN initiators. Radical attack on the backbone can occur through the pendant vinyl group or at the tertiary allylic hydrogen site. Effective graft sites are formed via double bond addition of either primary (initiator) or polymer radicals. The production of tertiary allylic radicals on the backbone chain also occurs and results in moderate to dramatic reaction rate retardation in every monomer system. The type of initiator is only important when the polymer radicals are not very active, as in the case of styrene, and to a lesser extent for methacrylate monomer. Graft efficiencies are generally higher when using vinyl-PBD than when using cis-PBD.

Contribution to the International Polymer Colloids Group Newsletter

MPI Colloid and Interface Research

Kantsraße 55, D 14513 Teltow-Seehof, Germany

Reporter: Klaus Tauer

Modelling Particle Formation in Emulsion Polymerization - An Approach by Means of the Classical Nucleation Theory

K. Tauer*, I. Kühn

Abstract A framework for modelling particle nucleation in emulsion polymerization has been developed based on a combination of classical nucleation theory with radical polymerization kinetics and the Flory-Huggins theory of polymer solutions. The basic assumption is that water born oligomers form stable nuclei under critical conditions. The only adjustable model parameter is the activation energy of nucleation. The model allows to calculate the chain length of the nucleating oligomers, the number of chains forming one nucleus, the diameter of the nucleus, the total number of nuclei formed, and the rate of nucleation.

Model Development

It is well established in CNT /1/ that, if no foreign phase is present, the formation of a new phase starts with the formation of small clusters. These clusters may redissociate or grow by accretion to become nuclei of the new phase. For emulsion polymerization this process may be described as follows

$$m \cdot P_j \rightarrow \left(P_j\right)_m$$

where m is the number of oligomeric chains P_j of chain length j forming one cluster. Additionally, the surface energy, $\sigma \cdot a_n$, of the clusters impedes the nucleation. Thus, the free energy of formation of a cluster may be written as (1)

$$\Delta G = -m \cdot kT \cdot \ln S + \sigma \cdot a_n \qquad (1)$$

where S is the supersaturation of the P_j's in water (ratio of concentration to solubility), a_n is the surface of a nucleus, and σ is the interfacial tension nucleus to water. Substituting a_n by m and j one gets equation (2) describing the energy difference between m molecules in solution and the solid nucleus consisting of m molecules with chain length j.

$$\Delta G = -c_1 \cdot m \cdot \ln S + c_2 \cdot (m \cdot j)^{2/3} \cdot \sigma \qquad (2)$$

$$c_1 = 4{,}1868 \cdot 10^7 \, R \cdot T / N_A \quad (erg)$$

$$c_2 = (4 \cdot \pi)^{1/3} \cdot \left(\frac{3 \cdot MG_{mon}}{d_p \cdot N_A} \right)^{2/3} \quad (cm^2)$$

Here N_A is Avogadro's number, R is the gas constant, T is the absolute temperature, d_p is the polymer density, and MG_{mon} is the molecular weight of the monomer, respectively.

The curve ΔG versus m goes through a maximum, however for small values of m, ΔG is always positive. As the second derivative of ΔG with respect to m is always negative the equilibrium is not stable, e.g. the system shows no tendency to go back to the equilibrium state if once moved a little bit apart from it. This means, that nuclei with m smaller a critical value M_c will dissolve, whereas nuclei with $m > M_c$ will grow indefinitely. M_c is the critical value of m corresponding to the maximum in the ΔG versus m curve. Furthermore, one obtains from equation (2) the equations (3) to (5) for ΔG_{max} and the critical values M_c and D_c (critical nucleus size), respectively.

$$\Delta G_{max} = \frac{4}{27} \cdot \frac{c_2^3}{c_1^2} \cdot \frac{j^2 \cdot \sigma^3}{(\ln S)^2} \qquad (3)$$

$$M_C = \left(\frac{2}{3} \cdot \frac{c_2}{c_1} \cdot \frac{j^{2/3} \cdot \sigma}{\ln S} \right)^3 \qquad (4)$$

$$D_C = 10^7 \cdot \frac{2}{3} \cdot \left(\frac{6}{\pi} \right)^{1/3} \cdot \frac{C_1}{C_2} \cdot \left(\frac{MG_{mon}}{d_p \cdot N_A} \right)^{1/3} \cdot \frac{j \cdot \sigma}{\ln S} \qquad (5)$$

ΔG_{max} corresponds to an activation energy of nucleation. Therefore the number of nuclei formed, N_c, and the rate of nucleation, R_n, can be expressed according to Nielsen /2/ as

follows leading to equations (6), (7). k_n is the nucleation rate constant /2/, v_w the molar volume of water, and d the diffusion coefficient of the oligomers in water.

$$N_C = \frac{1}{v_W} \cdot \exp(-\Delta G_{max} / kT) \qquad (6)$$

$$R_n = k_n \cdot N_C \qquad (7)$$

$$k_n = \frac{2d}{\left(\frac{6}{\pi} \cdot \frac{MG_w}{d_w} \cdot \frac{1}{N_A}\right)^{2/3}}$$

To calculate the supersaturation, S, relations are needed for the concentration of oligomers, C(j,t), and for their solubility $C_o(j)$.

Equation (9) should be valid for the solubility of the oligomers in dependence on their chain length if an approximation is used to calculate ϕ_2 (ϕ_2 - volume fraction of oligomers in diluent phase, χ - Flory-Huggins interaction parameter) proposed by Barrett /3/ equation (8) .

$$\ln \phi_2 = j \cdot (1 - \chi - 1/j) \qquad (8)$$

$$C_0(j) = \frac{\phi_2}{\frac{j \cdot MG_{mon}}{d_p} \cdot (1 - \phi_2)} \qquad (9)$$

The current total (cumulative) concentration of oligomers, C(j,t) depending on polymerization time and chain length can be calculated using well known equations from radical polymerization kinetics /4/ (10) - (12). In these equations I_o is the initial initiator concentration, I the current initiator concentration at time t, k_d is the initiator decomposition rate constant, $2fk_d$ the radical flux, f the radical efficiency factor, k_t the termination rate constant, k_p the propagation rate constant, and M_w the monomer concentration in the water phase.

$$C(t,j) = \frac{1}{2} \cdot \frac{\beta}{(1+\beta)^j} \cdot I_0 \cdot \left(1 - \exp(-k_d \cdot t)\right) \qquad (10)$$

$$\beta = \frac{\left(2 \cdot f \cdot k_d \cdot I \cdot k_t\right)^{1/2}}{k_p \cdot M_w} \qquad (11)$$

$$I = I_0 \cdot \exp(-k_d \cdot t) \qquad (12)$$

With the equations (3) - (12) it might be possible to estimate the nucleation behaviour in emulsion polymerization starting with a total homogeneous system consisting of water, monomer and initiator solved in water, respectively.

The equations are easy to solve numerically, and the solutions may be considered as matrices with the variables t and j. To solve the equations, that means to calculate for which values of j and t nucleation occurs the following algorithm was applied:

(a) nucleation occurs if $\Delta G_{max} >> v \cdot kT$ (nucleation condition, v is a simple parameter to modify activation energy),

(b) nucleation occurs only if $M_c(j,t)$, $D_c(j,t)$, $N_c(j,t)$, and $R_n(j,t)$, are positive (physical meaningful),

(c) for negative values $M_c(j,t)$, $D_c(j,t)$, $N_c(j,t)$, and $R_n(j,t)$ were set equal to zero,

(d) a nucleation surface plot was constructed by multiplying the matrices $M_c(j,t)$, $D_c(j,t)$, $N_c(j,t)$ and $R_n(j,t)$ element by element whereby a value greater than zero for the resulting matrix indicates that nucleation can take place for the corresponding j and t values, that means in the j-t plane spikes occur indicating nucleation.

Table 1 summarises the values of the rate parameters and model constants used for the calculations. All kinetic values needed as well as values for j_{crit} for styrene and methyl methacrylate have been found in a paper of Morrison and Gilbert /5/. The propagation rate constant for vinyl acetate was taken from /6/ and the monomer solubility in water from /7/. Values concerning j_{crit} for vinyl acetate have been found in /8/. In the calculations for styrene and methyl methacrylate we also included the dependence of k_p on the degree of oligomerisation as it is proposed by Gilbert /5/. However, the calculations showed that there is only a very weak influence on the calculated nucleation behaviour whether or not one considers a k_p dependence on j.

The calculations were carried out using the Mathcad 5.0 PLUS software package.

Tab.1 Kinetic constants and model parameters STY - styrene, MMA - methyl methacrylate VAC - vinyl acetate

Symbol	STY	MMA	VAC	Comment
d, cm^2s^{-1}	$1 \cdot 10^{-5}$	$1 \cdot 10^{-5}$	$1 \cdot 10^{-5}$	Oligomer diffusion in water
f	0.5	0.5	0.5	Radical efficiency factor
k_d, s^{-1}	$1 \cdot 10^{-6}$	$1 \cdot 10^{-6}$	$1 \cdot 10^{-6}$	Initiator decomposition
k_{p1}, $cm^3mol^{-1}s^{-1}$	$7 \cdot 10^5$	$3.3 \cdot 10^6$	$2 \cdot 10^6$	Monomer addition to primary radical, initiation
k_{p2}, $cm^3mol^{-1}s^{-1}$	$4.5 \cdot 10^5$	$3.3 \cdot 10^6$	$6.5 \cdot 10^5$	First monomer addition after initiation
k_p, $cm^3mol^{-1}s^{-1}$	$2.6 \cdot 10^5$	$3.3 \cdot 10^6$	$6.5 \cdot 10^5$	Monomer addition if $j \geq 2$
k_t, $cm^3mol^{-1}s^{-1}$	$3 \cdot 10^{12}$	$3 \cdot 10^{12}$	$3 \cdot 10^{12}$	Radical termination
d_p, g cm^{-3}	1.054	1.17	1.18	Density polymer
d_w, g cm^{-3}	1.0	1.0	1.0	Density water
I_o, mol cm^{-3}	$6 \cdot 10^{-6}$	$6 \cdot 10^{-6}$	$6 \cdot 10^{-6}$	Initial initiator concentration
MG_m, g mol^{-1}	104.15	86.09	100.12	Molecular weight of monomer
MG_w, g mol^{-1}	18.0	18.0	18.0	Molecular weight of water
M_w, mol cm^{-3}	$4.3 \cdot 10^{-6}$	$1.5 \cdot 10^{-4}$	$2.9 \cdot 10^{-4}$	Monomer concentration in water
v	10	10	10	Nucleation criteria: $\Delta G_{max} > v \cdot kT$
T, K	323.15	323.15	323.15	Polymerization temperature
χ	4.8	2.4	2.0	Flory-Huggins interaction parameter
σ, mN m^{-1}	1.5	0.8	0.75	Interfacial tension nucleus to water

Figure 1 shows the results for the three monomers in form of the j-t or "nucleation" plane. Table 2 summarises the numerical results with respect to the time gap of particle appearance after starting the polymerization (t_c), the degree of oligomerisation at which nucleation occurs (j_{crit}), the diameter of the nuclei (D_c), and the number of chains per nucleus (M_c). It is to note, that this results are obtained for v = 10 corresponding to a fairly high activation energy of 10 times kT to satisfy the nucleation condition $\Delta G_{max} >> kT$. In principal, v might be accessible if one will really be able to investigate the particle nucleation in emulsion polymerization experimentally. Until today this is alas not possible, and hence v is an adjustable parameter.

For different monomers nucleation occurs at quite different times and j-values. Thus, the influence of the monomer properties, especially of the different water solubilities is clearly to

be seen. The higher the water solubility the higher j_{crit} and the longer time it takes until particles are occurring.

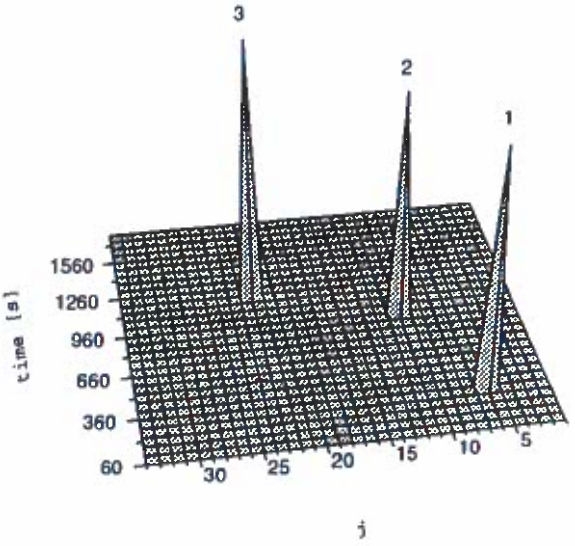

Fig. 1 Calculated "nucleation" plane (j-t plane) for styrene (1), methyl methacrylate (2), and vinyl acetate (3) emulsion polymerization (parameters for calculation see Table 1)

Tab.2 Numerical results characterising particle nucleation (for an explanation of abbreviations see the text), experimental data for critical chain length: $j_{crit,exp.}$

Monomer	j_{crit}	$j_{crit,exp.}$	t_c (min)	D_c (nm)	M_c
STY	6	5	6	11.8	887
MMA	11	10	16	8.7	223
VAC	22	18-20	20	8.0	110

Especially, the results with respect to j_{crit} correspond well with experimental values for the three monomers. The agreement of calculated and measured values of j_{crit} is amazing in particular, as no special fits have been made to get this results.

References

/1/ A. W. Adamson, *Physical Chemistry of Surfaces* (J. Wiley&Sons, Inc., New York, 1990).
/2/ A. E. Nielsen, *Kinetics of Precipitation* (Pergamon Press, Oxford, 1964).
/3/ K. E. J. Barrett, *Dispersion polymerization in organic media*, (Wiley-Interscience, Bristol, 1975).
/4/ H. G. Elias, *Makromoleküle* (Hüthig & Wepf Verlag, Basel, Heidelberg, 1972).
/5/ B.R. Morrison, R.G. Gilbert, *Macromol. Chem. Phys., Macromol. Symp., in Press*
/6/ F.K. Hansen, J. Ugelstad, *Makromol. Chem.* **180**, 2423 (1979)
/7/ B.R. Vijayendran, *J. Appl. Pol. Sci.* **23**, 733 (1979)
/8/ K. Schmutzler, R. Kakusche, W.-D. Hergeth, *Acta Polymerica* **40**, 238 (1989)

This paper will be published in Macromolecules in April 1995

CONTRIBUTION TO IPCG FROM THE TRONDHEIM GROUP.

John Ugelstad

We have continued research in the areas described in previous reports, and also extended the areas in different directions.

1. RESEARCH IN EMULSION POLYMERIZATION OF VINYL CHLORIDE.

1.1 Latexes with a broad particle size distribution.

The methods we have studied are mostly different variations of the miniemulsion method where the stable monomer emulsions are prepared by diffusion of monomer into stable aqueous dispersions of the Y compounds. An aspect of this method which is of great practical importance is the ability to regulate the size and the size distribution of the preemulsion of the Y compound and that this is combined with a sufficient stability of the emulsion over time.

In practice one has to consider that one has limitations in the homogenization procedure. Preferably one wants a process where one keeps the homogenization procedure constant on a reasonable level and regulate the size of the Y droplets with the type of Y compounds. We have found a close correspondance between the size and size distribution of the Y droplets in the original Y dispersion, the size and the size distribution of the swollen Y droplets (with ethylene dichloride as a model for VC), and the particle size of the latexes after swelling and polymerization with VC.

We have in order to achieve a simple, easily performed method, where the droplet size and thereby the particle size could be varied at constant homogenization conditions, applied a number of systems with various mixture of Y compounds. The essential point is that Y compounds which are easily homogenized give preemulsions which are too unstable for the long time storage which is necessarry in practice. On the other hand the high molecular weight Y compounds which give sufficient stability are so viscous that the homogenization procedures will not allow the production of small sized preemulsions. The solution to this problem is illustrated in Table 1 below where. We apply a mixture of two Y compounds and regulate the size of the droplets by the relative amount of the Y compounds.

2

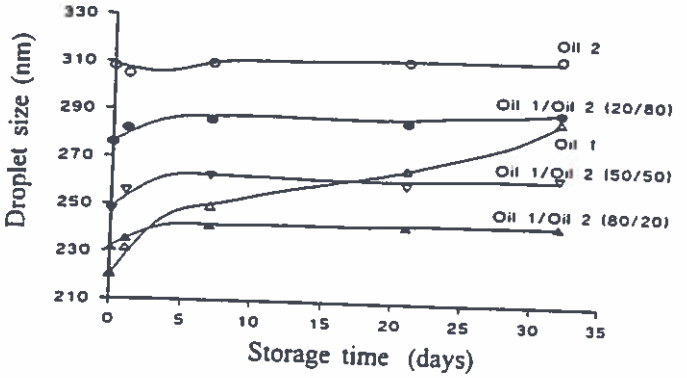

Diagram 4.1 Droplet diameters versus storage time for preemulsions with different viscosity of the oil.

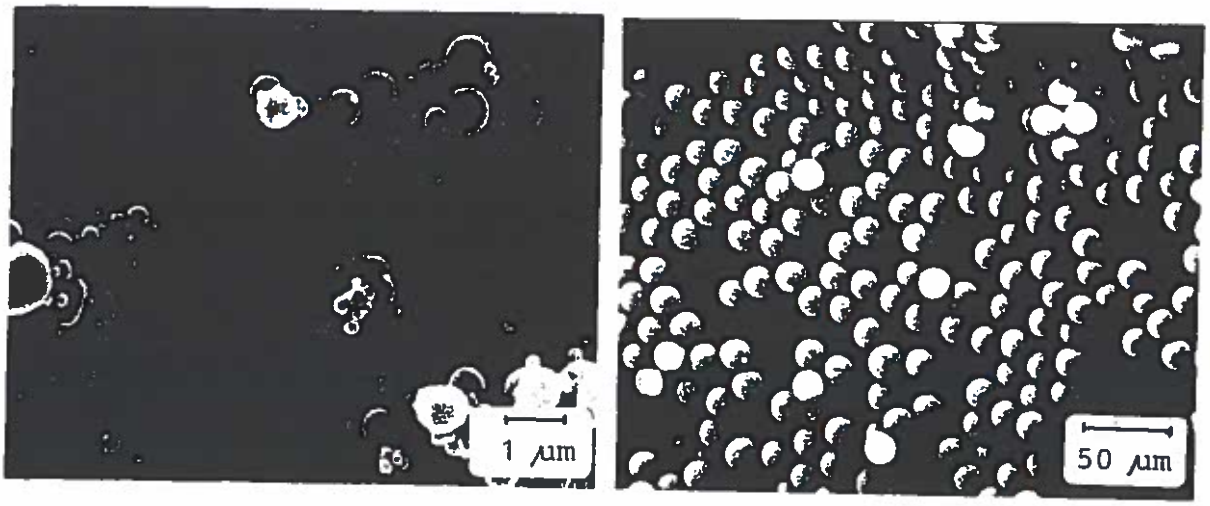

It appears that the Y compound with the lowest viscosity (oil 1) gives a too low stability and is useless alone where a storage stability of 3-4 weeks is required. Oil 2 gives a very high stability towards degradation by diffusion, but on the other hand when used alone, limits droplet size to relatively large droplets. A mixture of two Y compounds allows you to regulate the size of the preemulsion at will, maintaining the long time stability of the preemulsion.
Fig 2a shows results of PVC latexes by the miniemulsion method: A broad particle size distribution as wanted.

1.2 Monodisperse particles of PVC
Fig. 2b shows monodisperse PVC particles prepared by the "activated swelling method".

2. RESEARCH IN MONODISPERSE PARTICLES.

2.1 Particles for chromatographic separation of large sized carbohydrates.

Monodisperse extremely hydrophilic particles with large pores for separation of very large carbohydrates are made.These particles are made with styren- divinyl benzene (80% divinyl benzene) and with various amount and type of porogens. The particles are afterwards provided with a hydrohilic surface by introduction of hydrophilic oligomeric ether chains.
We have prepared a series of such particles where we have varied the type of porgen with the amount of porogen constant, corresponding to about 70%. We have obtained especially good results with linear carboxylic acids as porogen. These particles are able to give an effective separation of molecules with hydrdynamic volumes up to about 10^8. This is better than any other paricles on the market. Such particles are in great demand. The monodispersity of the particles ensures an easy packing of the column and at the same time a very good combination of flow and separation. (See paper of B. Christensen et al. below.)

2.2. Immunofluorometric assays by help of flowcytometry.

New developments within this section, which we have described in several paers, imply that we use at the same time porous particles of different size which are very monodisperse and where we have different monodclonal antibodies on each particle type. We have with this method been able to determine simultanously different types of antigens connected with cancer in serum. The method is very rapid and has aroused great interest from several international companies within the field of biochemicals and equipment in medicin and biochemistry.

3. MAGNETIC PARTICLES.

We continue our work in production and application of magnetic particles.Two students are working with their doctor degrees within these fields.

3.1 Hydrophilic magnetic particles with large capacity for use in immunoprecipitation (immunopurification) of IgG antibodies.

We have previously described that we with magnetic particles with large pores are able to increase the capacity of the binding IgG and subsequently the corresponding antigen ,a factor of ca. 20 times, compared to the same weight of compact particles of the same size. Similar results were obtained with binding of streptavidin which subsequently bind biotinized antibody.
We have continued this work with Protein A covalently coupled to the surface and prepared a particle which efficiently extract IgG_1 antibodies from serum, shows very low nonspecific binding, and where we by acid treatment set free 100% of the attached IgG. Again these particles show a capacity which is 20 times higher per unit weight of particles than the compact ones. This means that particles with a size of about 3000 nm have a capacity per unit weight which is equal to particles of about 150 nm. Advantages are ease of handling and rapid separation in a magnetic field combined with slow settling.

3.2 Positive cell separation.
This work has continued in different directions.
The principle of this procedure is that we, after isolation of the target cells by help of magnetic beads with appropriate monoclonal antibodies attached to the surface, have a method which allow the particles to be detached from the cells, giving free target cells in good yield and with high purity. Especially we have worked with use of particles with bor-hydroxy groups covalently coupled to the surface of the beads.The principle is illustrated below.
Magnetic particles with borhydoxy groups on the surface will bind to the carbohydrate (galactose) units in the Fc part of the monoclonal antibody. After isolation of the cells with magnetic particles attached to them by help of a magnet and washing, sorbitol is added. Sorbitol forms much stronger bonds to the to the boric hydroxy groups and will break the binding to galactose groups which in turn will set free the cells. The method has been shown to be very efficent for all cell types investigated up to now, T_4, T_8, B, N.K.(natural killer) cells.We now have:An efficient isolation of cells up to 90-95%, liberation by sorbitol treatment of 90 to 95 %, giving a yield of target cells of 80 to 90 % . The purity is 95-99%

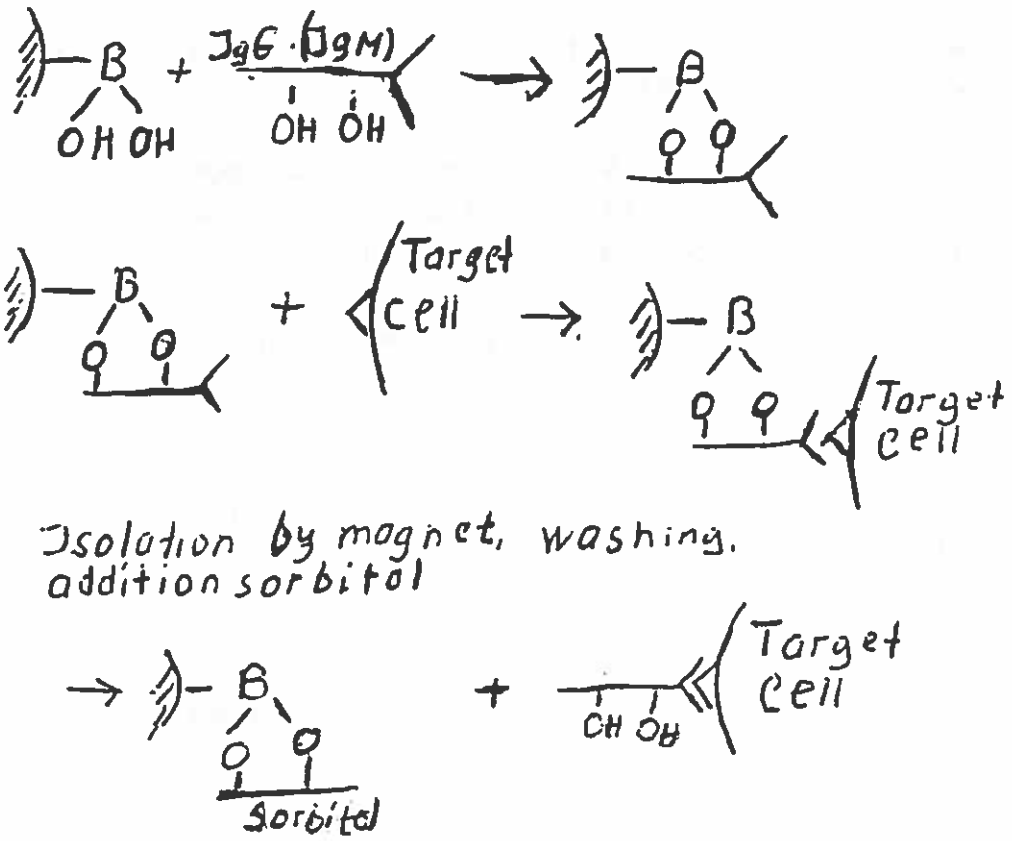

New publications

Bård Sæthre: "Mechanismms and kinetics of miniemulsion polymerisation of vinyl chloride" Thesis 1994

P.C. Mørk, B. Sæthre and J. Ugelstad. "Minisuspension polymerization of vinyl chloride", *Polymer Encyclopedia, In press*

P.C. Mørk, J. Ugelstad and J. O. Aasen: "Compartimentalizes polymerization by oil soluble initiators. Average number of radicals per particle", *J. Polym. Sci. (1995) In press*

P. C. Mørk: "Kinetics of competitive polymerizxation in bidisperdse seed systems using oil soluble initiators" *J. Poym. Sci. (1995) In press*

J. Ugelstad, P. Stenstad, L. Kilaas et al.: "Biochemical and biomedical application of monodisperse particles: *"Macromol. Symp. (December 1994) In press*

A. Rian, L. Kilaas, K. Nustad, P. Stenstad and J. Ugelstad:

biomedical application of monodisperse particles: *"Macromol. Symp. (December 1994) In press*

A. Rian, L. Kilaas, K. Nustad, P. Stenstad and J. Ugelstad: "Immobilation and activity of Protein A on macroporous magnetic particles", *J. Molecular Recogn. Submitted*

J. Ugelstad, R. Schmid, A. Berge et al.: "Monodisperse polymer particles, Preparation and application", *Polymer Encyclopedia In press*

B. Christensen, M. Myhr, O. Aune, S. Hagen, A. Berge and J. Ugelstad: "Macroporous, monodisperse particles in aqueous exclusion chromatogrphy of high molecular weight polysaaccharides", *J. of Polysaccharides, submitted*

J. Frengen, R. Schmid and K. Nustad T. Lindmo,: "A seqential binding assay with a working range extending beyond seven orders of magnitude", *J. Immunolog. Meth.* 178, 131, (1995)

J. Frengen, T. Lindmo, E. Paus, R. Schmid and K. Nustad: " Dual analyte assay based on particle types of different size measured by flow cytometry, *J.Immunolog.Meth.*,178. 141 (1995)

A. VRIJ

Contribution of the Van 't Hoff Laboratory for the Polymer Group Newsletter

MODEL PARTICLES FOR COLLOIDAL DISPERSIONS: FROM HARD SPHERES TO SOFT RODS.

Fifteen Years of Particle Synthesis and Physico-Chemical Research in Utrecht

A. VRIJ AND A.P. PHILIPSE

Van 't Hoff Laboratory for Physical and Colloid Chemistry, Utrecht University

Padualaan 8,, 3584 CH Utrecht, The Netherlands

Abstract

In Utrecht we study 'fine' particles in the colloidal size range in connection with (concentrated) dispersions of such particles in a liquid carrier. Originally the particles were spherical in shape (e.g. silica spheres) but more recently also elongated particles (e.g. boehmite rods) are synthesized and studied. It is very important that the particles are non-clustered during the synthesis and thereafter. The particles are coated with a surface layer of chain molecules or silane coupling agents to make them soluble and stable against coagulation in organic solvents. In that case the particles/solvent system behaves as a 'Complex Fluid' in which the particles show 'hard' or 'soft' repulsion forces as revealed by (light) or (neutron small angle) scattering and other techniques like sedimentation, diffusion, rheology and colloidal filtration.
In more recent studies 'compound' particles were synthesized and studied, consisting e.g. of silica spheres labeled with a fluorescent core, silica spheres with a magnetic core, and silica rods with a core of boehmite, all in aqueous and organic solvents.
Spheres with a fluorescent core are used as labels in optical studies like Confocal Scanning Laser Microscopy. The particles with a magnetic core show very interesting behaviour in an external magnetic field and the elongated particles show double refraction e.g. in a shear field. More over, also phase transitions from isotropic to liquid-crystal like suspensions have been observed.

A brief overview will be given of the synthesis and physical experimentation and will be augmented by references, allowing the interested reader to pursue a particular topic in more detail.

NATO Advanced Research Workshop on 'Fine Particles Science and Technology from Micro to Nanoparticles', (Ed. E. Pelizetti), Maratea, Italy, July 15-21, 1995

A. VRIJ

Contribution of the Van 't Hoff Laboratory for the Polymer Group Newsletter

SYNTHESIS OF PLATINUM NANO-PARTICLES IN AQUEOUS HOST DISPERSIONS OF INORGANIC (IMOGOLITE) RODS

LUIS LIZ MARZÁN AND ALBERT P. PHILIPSE

Van 't Hoff Laboratory for Physical and Colloid Chemistry, Utrecht University

Padualaan 8,, 3584 CH Utrecht, The Netherlands

Abstract

A method is presented to prepare platinum particles (radius 1-3 nm) by reduction of H_2PtCl_6 with $NaBH_4$ in an acid, aqueous host dispersion of high aspect ratio inorganic (imogolite) fibers. The fibers appear to be effective stabilizers for the Pt particles, which settle in absence of imogolite as large aggregates. This influence of the fibers is examined and explained, details of the synthesis of imogolite and platinum are discussed, and possible applications of the imogolite-platinum dispersions for catalysis are indicated.

Colloid and Surfaces A **90** (1994) 95.